Winter 12-15-2017

Roles of Peroxisomes and Peroxisome-Derived Products in Controlling Plant Growth and Stress Responses

Elizabeth May Frick
Washington University in St. Louis

WASHINGTON UNIVERSITY IN ST. LOUIS

Division of Biology and Biomedical Sciences
Plant Biology

Dissertation Examination Committee:
Lucia Strader, Chair
Arpita Bose
Elizabeth Haswell
Joseph Jez
Dmitri Nusinow
Bethany Zolman

Roles of Peroxisomes and Peroxisome-Derived Products in Controlling Plant Growth and Stress Responses

by

Elizabeth M. Frick

A dissertation presented to
The Graduate School
of Washington University in
partial fulfillment of the
requirements for the degree
of Doctor of Philosophy

December 2017
St. Louis, Missouri

Table of Contents

List of Figures

List of Tables

Acknowledgments

The work described in this dissertation was funded by the United States Department of Agriculture- National Institute for Food and Agriculture Fellowship Program (2016-67011-25096 to Elizabeth Frick), the National Institutes of Health (1R01GM112898 to Lucia Strader), and the National Science Foundation (IOS-1453750 to Lucia Strader).

We also gratefully acknowledge Dr. Hagai Yasuor and Dr. Kamil Tyagi from the Agricultural Research Organization in Gilat, Israel, who provided some of the data shown in Chapter 4.

Elizabeth Frick

Washington University in St. Louis

December 2017

Dedicated to my parents, Dr. Theodore Frick and Mrs. Lisa Faller Frick

Abstract of the Dissertation

Roles of peroxisomes and peroxisome-derived products in controlling plant growth and stress responses

by

Elizabeth Frick

Doctor of Philosophy in Biology and Biomedical Sciences

Plant Biology

Washington University in St. Louis, 2017

Professor Lucia Strader, Chair

The peroxisome is a vital organelle conserved through the entire eukaryotic lineage. In all examined species, peroxisomes are responsible for such essential processes as fatty acid beta-oxidation and metabolism of reactive oxygen species (ROS). In plants, peroxisomes have taken on additional specialized roles, such as production of some plant hormones and vitamins. In this work, I have uncovered novel factors regulating peroxisome number in model species *Arabidopsis thaliana*, and novel mechanisms governing how peroxisomes respond to salt stress. I discovered a role for *Arabidopsis* MAP KINASE17 (MPK17) as a negative regulator of peroxisome division that acts in the salt-stress response pathway of peroxisome division. Additionally, I uncovered a novel role for the known peroxisome division factor PEROXISOME AND MITOCHONDRIAL DIVISION FACTOR 1 (PMD1) as another regulator of salt-induced peroxisome division and as the first known plant peroxisome division factor to bind to actin. A forward genetics approach was undertaken to attempt to isolate peroxisome-deficient mutants in

the genetically tractable crop species *Solanum lycopersicum*, screening mutagenized tomato seeds on the auxin precursor indole-3-butyric acid (IBA). Although no peroxisome mutants were isolated by this method, several mutants impaired in various other aspects of auxin homeostasis were isolated and used to make new discoveries regarding the contributions of IBA to vegetative and reproductive tomato development.

Chapter 1: Peroxisome Roles in Growth, Development, and Stress Responses

1.1 Peroxisomes are required for normal plant growth and development

1.1.1 Peroxisome functions

Peroxisomes are small conserved organelles that carry out a variety of critical functions. Specific biochemical functions are conferred by the matrix proteins and enzymes, which are contained within a single cell membrane. In all eukaryotes, peroxisomes perform fatty acid beta-oxidation and metabolism of reactive oxygen species (ROS) (reviewed in Islinger et al., 2012a). In humans, peroxisome functioning is so crucial that defects in peroxisome biogenesis lead to a wide range of disorders with symptoms including retinal dystrophy, liver cysts, bone stippling, hypotonia, seizures and other defects (Steinberg et al., 1993). Infants with the most severe form, Zellweger syndrome, rarely survive past their first year of life (Steinberg et al., 1993). In plants, peroxisomes have acquired a number of additional, specialized roles beyond those conserved through all eukaryotes. Plant-specific functions include synthesis of biotin, branched chain amino acids, vitamins, and processing some hormone precursors into their active forms (reviewed in Islinger et al., 2012a). Before peroxisomes can perform any synthesis or catabolism reactions, they must be specialized through the import of matrix proteins. Matrix proteins are synthesized in the cytosol with a peroxisome targeting sequence (PTS), which allows the cargo receptors to bind (Hu et al., 2012, Fig. 1). After docking to peroxisome membrane proteins, cargo is imported into the peroxisome matrix, and the receptors recycled to perform additional rounds of import (Hu et al., 2012).

Failure to perform any of these steps leads to peroxisome malfunction, the severity of which is amply demonstrated by defects in plant development many peroxisome-deficient mutants exhibit, as described below.

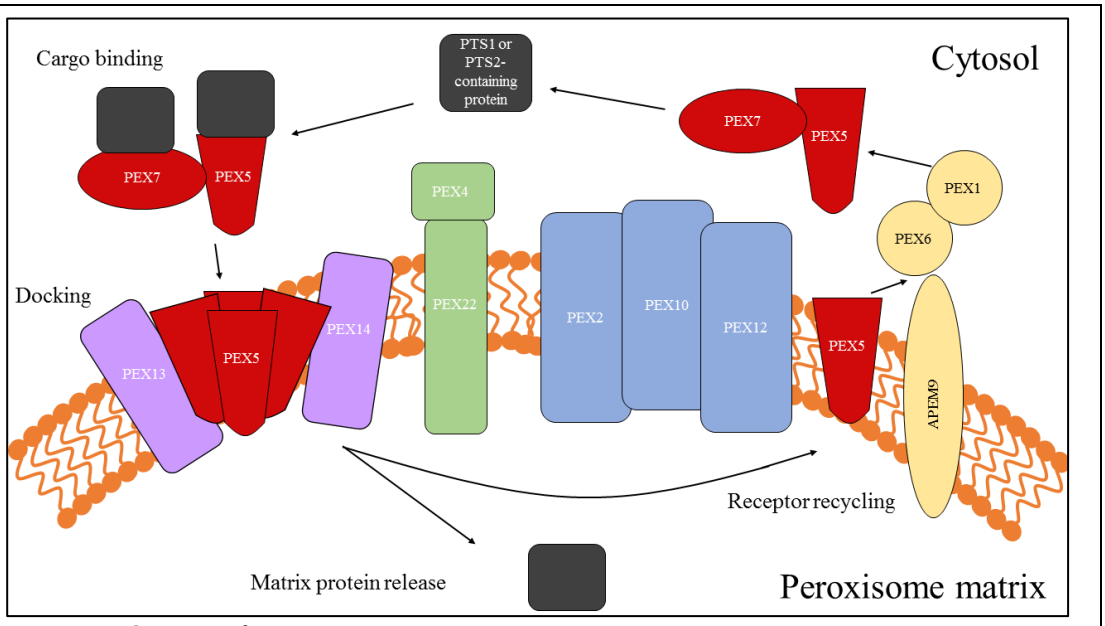

Figure 1: Schematic of peroxisome matrix protein import.

1.1.2 Peroxisomes in plant development

The most dramatic examples that peroxisomes are critical for early plant survival come from the many embryo-lethal peroxisome mutants. Null mutants of *PEX2*, *PEX10*, or *PEX12* a are all embryo lethal (Hu et al., 2002, Sparkes et al., 2003, Fan et al., 2005). All three of these *PEXs* encode zinc RING-finger proteins required for matrix protein import due to their role in receptor recycling (Prestele et al., 2010). The importance of proper import of matrix proteins into maturing peroxisomes is further supported by the severe defects exhibited by the *pex5-10* (Zolman et al., 2005) and *pex7-2* (Ramón and Bartel, 2010) single mutants, which encode the receptors that import PTS2 cargo, and the sharp fertility decrease in *pex5-1 pex7-1* double mutant offspring (Woodward and Bartel, 2005a). The *acx3 acx4* double mutant, defective in early steps of fatty acid beta-oxidation, are also embryo lethal (Rylott et al., 2003). Another

embryo-lethal double mutant is *pex19a pex19b*, which encode the chaperone protein that guides peroxisome membrane proteins through the cytosol (McDonnell et al., 2016). Loss of PEX16, which is required for both peroxisome and oil body formation (Lin et al., 2004), is also embryo lethal (Lin et al., 1999). Many *pex* mutations that are not embryo lethal still cannot germinate without an exogenous sucrose source, because peroxisomes are the site of lipid breakdown and thus energy prior to photosynthesis (Zolman et al., 2000). Beyond the clear importance of *PEX* gene products in early seedling development, defects from decreased peroxisomal function are also apparent later in the plant lifecycle.

Peroxisomes are also required later in the lifecycle of Arabidopsis. Mutants lacking PEX13, APEM9, or PEX16 cannot form viable male and female gametophytes (Boisson-Dernier et al., 2008), (Li et al., 2014), a defect that can be partially rescued by application of plant hormone jasmonic acid (JA) (Li et al., 2014), which is processed inside peroxisomes into its active form (Islinger et al., 2012b). Pea leaves undergoing senescence displayed increase peroxisome activity and number (Pastori and Del Rio, 1997), and transcripts of numerous *Pex11* isoforms are upregulated during the transition to senescence in Arabidopsis (Orth et al., 2007). These phenotypes, although with those displayed in early embryo and seedling development, demonstrate that peroxisomes are required at all stages of the plant lifecycle.

The many ways that disrupting peroxisome function aborts plant development makes the essential role of peroxisomes obvious. Beyond these lethal mutants, other *peroxin* mutants with less severe phenotypes have been instrumental to understanding how peroxisomes function, not just their importance.

1.1.3 Insights from other peroxisome-deficient mutants

Many peroxisome biogenesis mutants identified in plants were isolated in screens for indole-3-butyric acid (IBA) resistance (Zolman et al., 2000). IBA is both a precursor and storage form of the active from of auxin, indole-3-acetic acid (IAA), and undergoes conversion into IAA inside the peroxisome through a process similar to fatty acid beta oxidation ((Zolman and Bartel, 2004), Fig. 2).

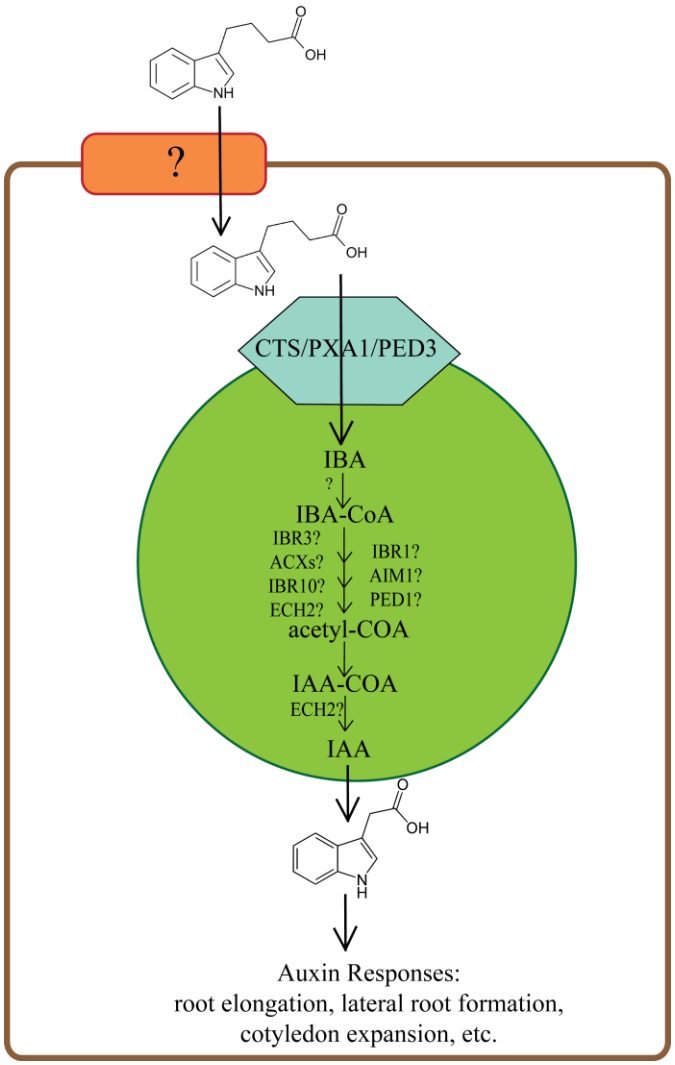

Figure 2: Peroxisomes in auxin homeostasis. IBA is transported into plant cells (brown) through an unknown transporter, then into peroxisomes (green) through CTS/PXA1/PED3. Inside the peroxisome, IBA is converted into IAA, which stimulates numerous responses. Inability to convert IBA into IAA through alterations to peroxisome number, matrix proteins, or import efficiency causes IBA resistance, but does not affect ability to respond to IAA.

Some of the best characterized peroxisome-associated proteins isolated from these IBA resistance screens are also PEX proteins, and are involved in all aspects of peroxisome biology (Table 1).

PEX	Function	Reference
PEX1	Peroxisome protein import, required for biogenesis	(Nito et al., 2007)
PEX4	Receptor recycling	(Zolman et al., 2005)
PEX5	Receptor responsible for transporting PTS1 and 2-containing cargo	(Ramón and Bartel, 2010)
PEX6	Receptor recycling	(Zolman and Bartel, 2004)
PEX7	Receptor responsible for transporting PTS1 and 2-containing cargo	(Ramón and Bartel, 2010)
PEX11s	Peroxisome division	(Orth et al., 2007)
PEX13	Member of docking complex responsible for importing PTS1 and 2-containing cargo into peroxisome	(Monroe-Augustus et al., 2011)
PEX14	Member of docking complex responsible for importing PTS1 and 2-containing cargo into peroxisome	(Monroe-Augustus et al., 2011)
PEX22	Matrix protein import	(Zolman et al., 2005)

Table 1: List of PEX proteins discovered in loss-of-function studies in Arabidopsis and their functions.

PEX4, PEX11, PEX22 are required for peroxisome biogenesis or division (reviewed in Hu et al. 2012). PEX5 (Ramón and Bartel, 2010), PEX7 (Ramón and Bartel, 2010), PEX13 (Monroe-Augustus et al., 2011), and PEX14 (Monroe-Augustus et al., 2011) are peroxisome receptors responsible for transporting in proteins containing a peroxisome targeting sequence 1 or 2 (PTS1, PTS2). PEX4 (Zolman et al., 2005) and PEX6 (Zolman and Bartel, 2004)recycle the peroxisome receptors. Beyond these universally required PEXs, plants can further control peroxisome activity by specializing peroxisome contents. In peas leaves treated with cadmium, peroxisomal glyoxylate cycle enzymes increase in abundance and activity (Sandalio et al., 2001). When *Arabidopsis* is starved, expression of thiolase is upregulated, but other glyoxylate cycle enzymes remain unchanged (Charlton et al., 2005a). Under non-stressed development, peroxisomes in

young seedlings express genes required for lipid breakdown, then decrease or shut off expression of these genes as the plant ages and needs less energy from lipid stores (Charlton et al., 2005a). Beyond changing the contents of peroxisomes, plants can also alter peroxisome activity by regulating the amount and timing of peroxisome divisions. Peroxisome division is one of the most important ways plants increase their peroxisome numbers, and hence is tightly controlled.

1.1.4 Peroxisome division

Peroxisomes arise via two different pathways: through *de novo* biogenesis from the endoplasmic reticulum (ER) and by growth and division of mature peroxisomes (Agrawal et al., 2016). Both pathways exist in all examined species to date, but the predominant method varies by organism. For example, yeast cells only undergo *de novo* biogenesis from the ER if no mature peroxisomes are available to undergo division (Motley and Hettema, 2007), whereas mammalian cells preferentially undergo *de novo* synthesis even when mature peroxisomes are present (Kim et al., 2006). In plants, numerous lines of evidence demonstrate that peroxisomes are derived from the ER, although the exact mechanism remains unclear. Several peroxisomal membrane proteins, including PEX16, PEX10, and APX are found in both the ER and peroxisomes in Arabidopsis (Karnik and Trelease, 2005; Karnik and Trelease, 2007; Lisenbee et al., 2003). In contrast, the process of mature peroxisome division in Arabidopsis is much better understood.

Mature peroxisome division requires three distinct steps; growth and elongation, constriction, and fission (Schrader, 2006).

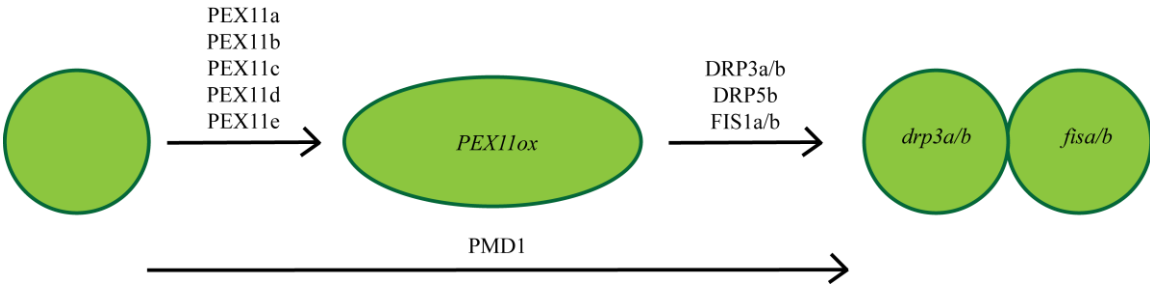

Figure 3. Model of mature plant peroxisome division. Peroxisomes are represented in green, which protein factors participating in each step listed above the arrows. Mutants whose disruption or overexpression alters peroxisome phenotypes are indicated in italics in peroxisomes resembling their mutant phenotype.

The Pex11 family of proteins may be master regulators of peroxisome division, working at all three steps in combination with additional factors. Peroxisome elongation in yeast, mammals, and plants is dependent on Pex11 proteins (Abe and Fujiki, 1998; Li and Gould, 2002; Lingard and Trelease, 2006). Yeast and mammalian Pex11 proteins are also involved in peroxisome fission through interaction with dynamin-like proteins, and also participate in constriction (Williams et al., 2015; Yoshida et al., 2015). Whether other, undiscovered protein factors also participate in constriction is currently unknown. In *Arabidopsis thaliana*, peroxisome elongation is dependent on Pex11 (Koch et al., 2010; Lingard and Trelease, 2006; Orth et al., 2007), and fission is dependent on members of the DYNAMIN RELATED PROTEIN (DRP) and FISSION1 (FIS1) protein families (Mano et al., 2004; Zhang and Hu, 2008). A role for constriction with the Arabidopsis Pex11 family has not yet been shown, nor are there any other constriction-related proteins known (reviewed in Kaur and Hu, 2009). At least one plant-specific division factor, PEROXISOME AND MITOCHONDRIAL DIVISION FACTOR1 (PMD1), also participates in plant peroxisome division in a DRP/FIS-independent manner (Aung and Hu, 2011). The mechanism of PMD1 action on peroxisomes has not yet been elucidated. Clearly, our

understanding of the machinery, timing, and roles of peroxisome division factors remains incomplete.

1.2 Peroxisome Responses to Stress

Peroxisomes in Arabidopsis proliferate in response to a variety of both biotic and abiotic stresses, including salt (Fahy et al., 2017; Mitsuya et al., 2010), pathogens (Koh et al., 2005), high light (Desai and Hu, 2008), cadmium (Rodriguez-Serrano et al., 2016; Rodriguez-Serrano et al., 2009), and general ROS stress (Lopez-Huertas et al., 2000). However, multiple lines of evidence suggest that stress induction of peroxisome proliferation is differentially triggered by each stress. First, plants do not upregulate peroxisome biogenesis gene expression uniformly in response to all of the stresses which result in increased peroxisome division. *PEX1* transcripts increase in response to light, pathogen, and salt stresses, but remains unchanged in response to osmotic stress (Charlton et al., 2005a). In contrast, *PEX10* transcripts increase in response to both salt stress and to osmotic stress (Charlton et al., 2005b). Second, while the number of peroxisomes is reported to increase in response to all the above stresses, the larger peroxisome populations do not behave the same way after division. Pathogen attack not only increases the number of peroxisomes but also reorients peroxisomes to the site of pathogen attack (Koh et al., 2005; Lipka et al., 2005). Under high light stress, plants proliferate peroxisomes and also extend peroxules from these peroxisomes, which associate with mitochondria (Delfosse et al., 2015). Peroxules also form under cadmium stress (Rodriguez-Serrano et al., 2016), but haven't been reported under high salt conditions or pathogen attacks. Together, these data suggest plants can distinguish among these stresses and trigger different peroxisome responses for each of them.

Beyond the “how” of stress-induced peroxisome division, questions about the “why” also remain.

An adaptive benefit from peroxisome proliferation remains elusive for most stresses, with the exception of pathogen attack, during which peroxisomes directly produce anti-fungal compounds (Lipka et al., 2005). Additionally, the rice PEX5 peroxisome receptor is an active anti-fungal protein (Lee et al., 2007). Direct benefit to the plant from increasing peroxisome division during salt stress is less readily apparent. Artificially increasing peroxisome number by overexpressing peroxisome division factors fails to appreciably increase abiotic stress tolerance in Arabidopsis (Koh et al., 2005; Mitsuya et al., 2010). Conversely, salt hypersensitive *fry1-6* and *sos1* mutants fail to proliferate peroxisomes in response to NaCl stress (Fahy et al., 2017). Notably, it has not been shown that overexpressing peroxisome division factors in otherwise salt-hypersensitive backgrounds can rescue the salt hypersensitivity. Before altering peroxisome number could be considered as a means to alter abiotic tolerance, it is crucial to understand why and how plants are undertaking this stress response.

1.3 Questions Addressed in Thesis

Because many aspects of plant peroxisome biology are poorly understood, I have investigated a few in particular during my thesis research. As described Chapter 1.1.4, we do not yet fully understand what protein factors are acting in all steps of peroxisome division. As evidenced by the recent discovery of PMD1, and the absence of division factors acting primarily at the step of constriction, we likely do not yet know the full complement of division factors in plants, nor do we understand the mechanism of action for each known division factors that result in aberrant morphology in these division factors’ absence. This thesis identified a novel regulator

of peroxisome division and discovered mechanistic details about the known division factor PMD1.

Second, the importance of peroxisome division to plant stress responses has not been determined. As explained in Chapter 1.1.2 and 1.1.4, the process of dividing mature peroxisomes, importing the correct matrix components, and monitoring the quality of these organelles requires dozens of protein factors and significant investment of plant resources. In short, increasing peroxisome number is energetically non-trivial, yet for most stresses during which division increases, no benefit to the plant resulting from increased peroxisomes can be observed. If the increase in peroxisome number is truly unnecessary for stress response and survival, discovering the signaling cascade used by Arabidopsis and/or other species that leads to peroxisome division could allow us to alter the peroxisome-specific response and decrease or increase it, whichever would result in better energy use efficiency and increased stress survival. This thesis identified two new protein factors required for salt-responsive division, and part of their mechanism of action, and confirmed existing reports that plants suffer no negative effects to whole under salt stress when this pathway is disrupted.

Last, nearly all of our understanding of plant peroxisomes and peroxisome metabolic contributions comes from studies in the model species *Arabidopsis thaliana*. Its small size, early dependence on lipid metabolism, and ease of genetic manipulation have been powerful research tools. However, out of the top ten produce crops in the United States, only soybean is an oilseed (Walls, 2017), meaning we cannot necessarily extrapolate all peroxisome functions from Arabidopsis to most agronomically important crops, especially our understanding of peroxisome roles in early embryogenesis and development. This thesis generated a screening population

suitable for forward genetics in *S. lycopersicum*, and successfully employed a screening method to identify novel auxin-resistant mutants in tomato.

In this thesis, the impact of peroxisomes and peroxisome-produced products were explored in both the model organism *Arabidopsis thaliana*, as well as the genetically tractable crop *Solanum lycopersicum.* In Arabidopsis, MAP KINASE17 (MPK17) was identified as a novel participant in peroxisome division, and new roles for the known peroxisome division factor PEROXISOME AND MITOCHONDRIAL DIVISION FACTOR1 (PMD1) were identified. The involvement of both MPK17 and PMD1 in stress-responsive peroxisome division was also explored. In *S. lycopersicum*, an IBA-resistance screening approach was employed to expand the collection and characterization of auxin-resistant mutants, especially ones involved in fruit production. This screen led to the identification and preliminary characterization of four novel auxin resistant mutants, greatly expanding the resources available for studying peroxisome-dependent processes such as IBA-to-IAA conversion in non-model organisms.

Chapter 2: MPK17 is a Novel Regulator of Peroxisome Number

This work has been accepted for publication in *Plant Physiology* as

"Kinase MPK17 and the peroxisome division factor PMD1 influence salt-induced peroxisome proliferation."

Elizabeth M. Frick and Lucia C. Strader

Department of Biology, Washington University in St. Louis, St. Louis, Missouri 63130, USA

2.1 MPK17 negatively regulates peroxisome number

MPK17 was first identified in a preliminary screen for altered auxin sensitivity in all the T-DNA insertion lines in Arabidopsis MAP kinases. Analysis of MPK auxin resistance was undertaken after the identification of auxin-resistant mutant *ibr5* as a dual-specificity protein phosphatase predicted to target MAP kinases (Monroe-Augustus et al., 2003). Many T-DNA single insertion lines in Arabidopsis MAP kinases display auxin hypersensitivity (Fig. 4). Because *mpk17* showed a strong degree of hypersensitivity, it was selected for further characterization of its auxin responsiveness.

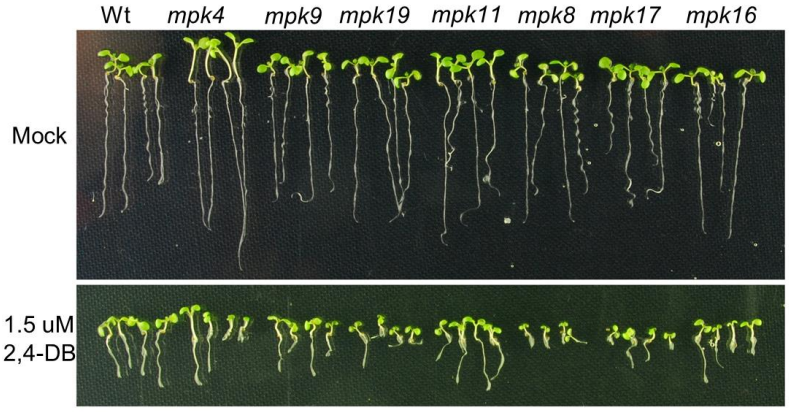

Figure 4: Many Arabidopsis MAP kinases display auxin hypersensitivity. Representative plants grown on mock plates or PN supplemented with indicated auxin. Wild type grown on high concentrations of auxin displays shorter roots and smaller cotyledons than on mock. The *mpk* mutants have significantly shorter roots and smaller cotyledons on auxin than wild type, indicative of auxin hypersensitivity.

An insertional allele defective in *MPK17* (At2g01450; Fig. 5A) displayed increased sensitivity to IBA in root elongation assays (Fig. 5, B and C) and lateral root induction assays (Fig. 5D). I named this allele *mpk17-1* (SALK_020801). Expressing *MPK17* behind its native upstream regulatory region in the *mpk17-1* mutant rescued the IBA hypersensitivity phenotype (Fig. 5C), confirming that the lesion in MPK17 caused the observed IBA hypersensitivity. *mpk17-1* carries a T-DNA insertion in between the fourth and fifth exons of the MPK17 gene and displays nearly undetectable *MPK17* transcript accumulation (Fig. 5, A and E), suggesting that *mpk17-1* is likely a null mutant.

Converse to its IBA hypersensitivity, *mpk17-1* displays wild type sensitivity to the short-chain synthetic auxin 2-4-dichlorophenoxyacetic acid (2,4-D) in root elongation assays (Fig. 5B) and the short-chain synthetic auxin NAA in lateral root induction assays (Fig. 5D). Because this pattern of differential sensitivity to short-chain versus long-chain auxins is characteristic of mutants with peroxisome defects (Hayashi et al. 1998, Zolman et al. 2000), we examined the peroxisomes in wild type and *mpk17-1* backgrounds using the 35S:GFP-PTS1 reporter (Zolman

and Bartel 2004). We found that *mpk17-1* displayed more peroxisomes than wild type (Fig. 5, F, G, and H). In addition, we observed that more peroxisomes in *mpk17-1* were more likely to be clustered together than those from wild type (Fig. 5F). Because *mpk17* displays hypersensitivity to the protoauxins IBA and 2,4-DB (Fig. 5B), which require functional peroxisomes for conversion to active auxins (Zolman et al. 2000), it seems likely that these additional peroxisomes are functional.

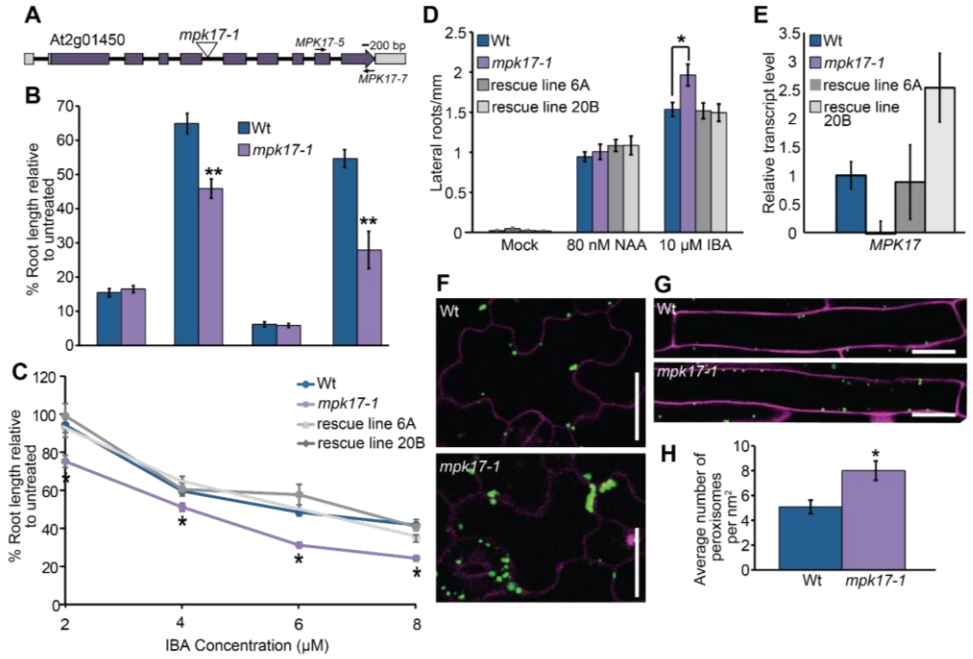

Figure 5: *mpk17-1* phenotypes. *mpk17-1* is hypersensitive to long-chain auxin precursor IBA in root elongation (**A)** and displays wild-type sensitivity to short-chain auxin 2,4-D **(B)** in root elongation assay and lateral root formation (**C)**. Significance was tested by ANOVA, * indicates $p<0.05$. **D)** *mpk17-1* has decreased transcript of *MPK17*, while rescue lines driving *MPK17* behind its native promoter show restored *MPK17* transcription. **E)** *mpk17-1* displays increased peroxisome numbers compared to wild type. Plants expressing a GFP-PTS1 peroxisome marker were grown for 4 days on unsupplemented media, then stained with propidium iodine (magenta) and imaged by confocal. Scale bars= 20 µm

2.2 MPK17 acts through PMD1

Overexpressing the peroxisome division factor PEROXISOME AND MITOCHONDRIAL DIVISION FACTOR1 *PMD1* results in increased peroxisome numbers, with many of these peroxisomes present in clusters (Aung and Hu, 2011). Because this peroxisome phenotype was similar to our observations of *mpk17-1* (Fig. 5F), we examined whether MPK17 acted through this peroxisome division factor. Although *pmd1-1* does not display resistance to the auxin precursor IBA (Fig. 6A,B) (Aung and Hu, 2011), we found that *pmd1-1* suppressed the IBA hypersensitivity displayed by *mpk17-1*; the *mpk17-1 pmd1-1* double mutant displayed wild-type sensitivity to the auxin precursor IBA in root elongation (Fig. 6A) and lateral root induction (Fig.

6B) assays. Additionally, *pmd1-1* suppressed the increased peroxisome numbers found in *mpk17-1* (Fig. 6C).

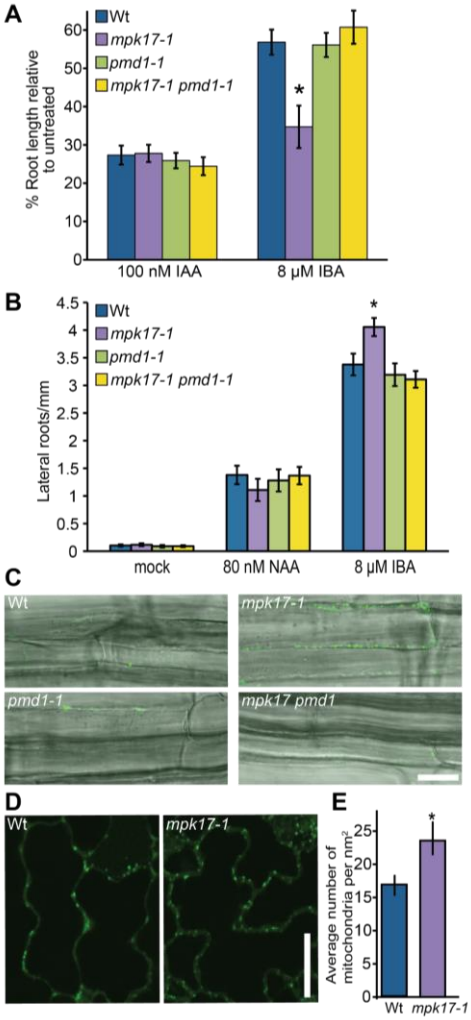

Figure 6: *mpk17* mutant phenotypes are suppressed by loss of *PMD1*. A, Normalized primary root lengths of 8-day old Wt (Col-0), *pmd1-1*, *mpk17-1*, and *mpk17-1 pmd1-1* grown on media supplemented with ethanol (mock) or 8 µM IBA (*=p ≤ 0.05, ANOVA). B, Emerged lateral roots of Wt (Col-0), *pmd1-1*, *mpk17-1*, and *mpk17-1 pmd1-1* were counted four days after transfer of 4-day-old seedlings to medium supplemented with indicated hormones. Error bars indicate standard error of the mean. C, Fluorescence images of Wt, *mpk17-1*, *pmd1-1*, and *mpk17-1 pmd1-1* seedling roots stained with BODIPY. Scale bar = 25 µm. D, Confocal images of Wt and *mpk17*-carrying the *COX4-YFP* (Aung and Hu 2011, Nelson et al. 2007) mitochondrial marker. Scale bar = 20 µm. E, Mean number (± SE) of mitochondria in Wt and *mpk17-1 COX4-YFP* lines. *mpk17-1* displays significantly more mitochondria than wild type (* = p ≤ 0.05, two-tailed unpaired t-test).

In addition to regulating peroxisome proliferation, PMD1 regulates mitochondria proliferation (Aung and Hu, 2011). Therefore, if MPK17 acts upstream of PMD1, we expect the *mpk17-1* mutant to display increased mitochondria numbers, in addition to the observed increase in peroxisome numbers. We therefore crossed *mpk17-1* to the mitochondria reporter line COX4-YFP (Aung and Hu, 2011; Nelson et al., 2007) and found that *mpk17-1* displays increased mitochondrial numbers compared to wild type (Fig. 6, D and E). Because PMD1 and MPK17 appear to act in both peroxisome and mitochondria

division and because *pmd1-1* suppresses *mpk17-1*, it is possible that MPK17 and PMD1 act in the same pathway to regulate the proliferation of these organelles, with PMD1 acting downstream of MPK17. However, we do not yet know the phosphorylation targets of MPK17 or any signaling or transcriptional machinery upstream of PMD1, and therefore cannot directly link MPK17 to PMD1. Thus, it remains a possibility that these proteins act in independent pathways that affect these processes.

2.3 MPK17 and PMD1 regulate peroxisome division under NaCl stress

Because peroxisomes divide in response to a variety of stressful conditions (Charlton et al., 2005b; Desai and Hu, 2008; Koh et al., 2005; Lipka et al., 2005; Mitsuya et al., 2010), and because both *mpk17-1* (Fig. 2G) and *pmd1-1* (Aung and Hu, 2011) display clearly aberrant peroxisome division, we examined stress-induced peroxisome proliferation in *mpk17-1* and *pmd1-1*. If MPK17 and PMD1 are not involved in peroxisome division upon salt stress, we would expect the same increase in peroxisome number in the mutants as wild type when salt-stressed. If both MPK17 and PMD1 increase peroxisome division during salt stress, we would expect to see no difference in peroxisome number between the mutants grown in the presence or absence of salt. Neither mutant proliferates peroxisomes in response to NaCl stress (Fig. 7, A and D). This is consistent with both MPK17 and PMD1 acting in a salt-responsive peroxisome division pathway. Indeed, although *mpk17-1* has significantly more peroxisomes than wild type when grown on unsupplemented media, *mpk17-1* has fewer peroxisomes than wild type when grown on media supplemented with NaCl (Fig. 7B). Further, expression of wild type MPK17 under its native promoter in the *mpk17-1* background restores peroxisome proliferation on NaCl (Fig. 7D). In addition, *PMD1* transcript trends towards a mild elevation in both the *mpk17*

mutant and in response to NaCl in wild type, although these differences are not statistically significant (Fig. 7C). The tested KCl and mannitol concentrations failed to stimulate peroxisome proliferation in wild type (Fig. 7D), despite the high KCl affecting seedling physiology, suggesting that peroxisome proliferation in response to NaCl is not caused by osmotic changes and is specific to Na+ ions.

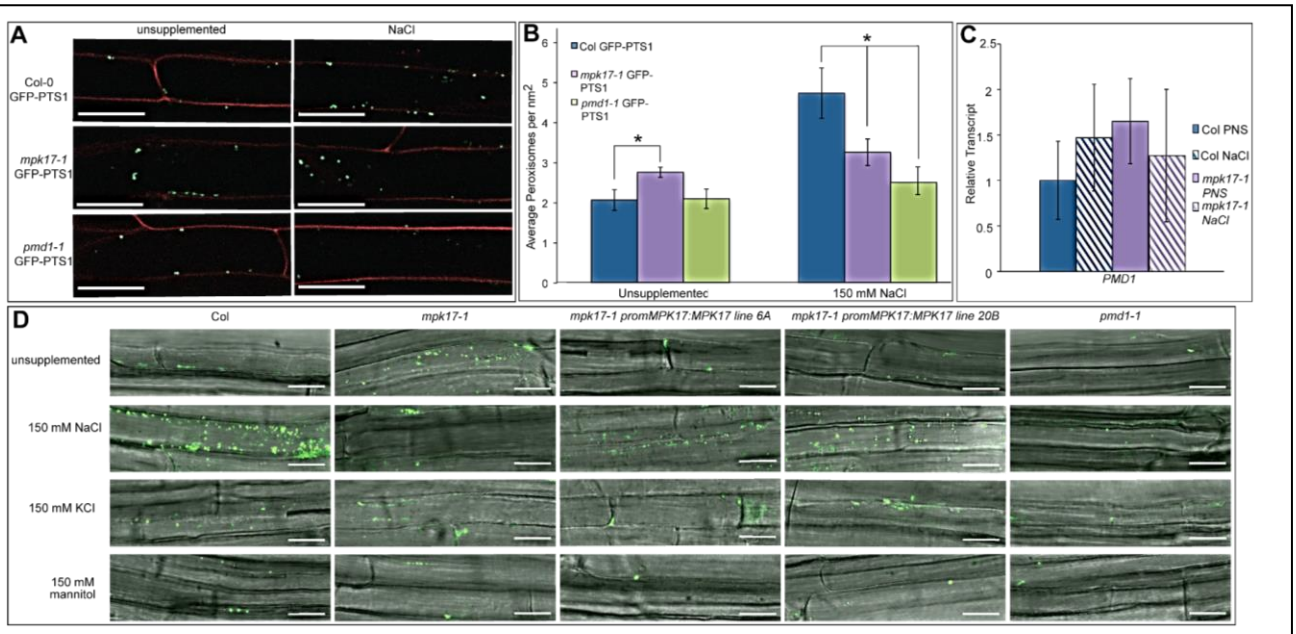

Figure 7: *mpk17-1* and *pmd1-1* fail to proliferate peroxisomes in response to NaCl treatment. A, Seedlings carrying the GFP-PTS1 peroxisome marker (Zolman and Bartel, 2004) were grown on unsupplemented media for 3 days, then transferred to indicated treatments overnight prior to counterstaining with propidium iodide and imaging by confocal microscopy. GFP-PTS1 signal has been false-colored green and propidium iodide signal has been false-colored red. B, Mean number (± SE) of peroxisomes in Wt (Col-0), *mpk17-1*, and *pmd1-1* when grown in the absence (unsupplemented) or presence of 150 mM NaCl. *mpk17-1* displays significantly more peroxisomes (* indicates $p \leq 0.05$, two-tailed unpaired t-test) than wild type on unsupplemented media, but significantly fewer peroxisomes than wild type when treated with NaCl. *pmd1-1* is statistically indistinguishable from wild type on unsupplemented media, and displays significantly fewer peroxisomes than wild type when treated with NaCl ($p < 0.05$, two-tailed unpaired t-test). C, Mean relative *PMD1* transcript accumulation in 7-day-old Wild type (Wt) and *mpk17-1* grown under continuous white light at 22 °C on unsupplemented media or media supplemented with 150 mM NaCl, determined by qPCR. D, Seedlings of Wt (Col-0), *mpk17-1*, *pmd1-1*, and two independent *mpk17* rescue lines were grown for 3 days on unsupplemented media, then transferred to indicated treatments overnight. Seedlings were stained with BODIPY to visualize peroxisomes (Landrum et al., 2010) and imaged by confocal microscopy. Scale bar = 25 µm.

I then investigated whether the inability to proliferate peroxisomes in response to NaCl without *MPK17* or *PMD1* affects the whole plant tolerance to NaCl. I examined the sensitivity of *mpk17-1* and *pmd1-1* to NaCl using multiple salt tolerance assays, including examination of germination in the presence of salt (Fig. 8A), seedling root elongation inhibition by salt (Fig. 8B), and final adult plant height in response to salt watering (Fig. 8C).

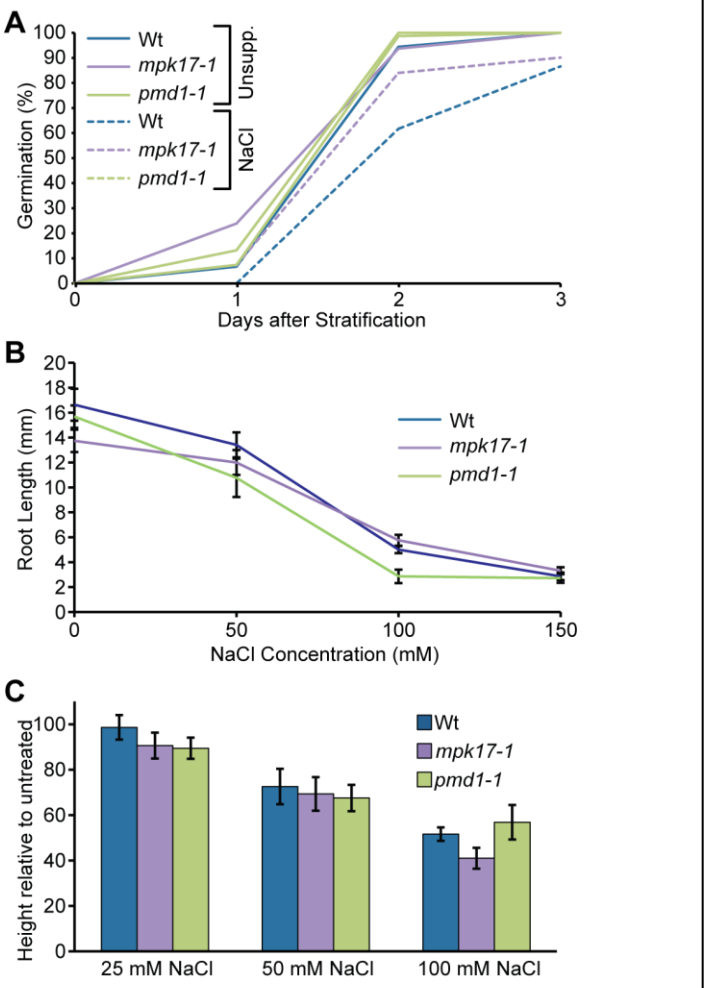

Figure 8: Neither *mpk17-1* nor *pmd1-1* display detectable tolerance to NaCl. A, Percent seed germination of Wt (Col-0), *mpk17-1*, and *pmd1-1* when grown on unsupplemented PNS media or PNS supplemented with 150 mM NaCl. B, Mean primary root lengths (± SE; $n \geq 10$) of Wt (Col-0), *mpk17-1*, and *pmd1-1* seedlings when grown on PNS media supplemented with the indicated concentration of NaCl. C, Mean (± SE; $n \geq 5$) final relative adult plant height of Wt (Col-0), *mpk17-1*, and *pmd1-1* when watered with the indicated concentration of NaCl during growth.

These assays cover a range of NaCl stress conditions, from a short-term acute stress in root elongation to low-level, persistent stress over the majority of the plant's lifespan, through continuous watering with NaCl from 3 weeks old until senescence. We were unable to detect any consistent, significant differences between wild type, *mpk17-1*, or *pmd1-1* in any of these assays; however, it may be possible that peroxisome proliferation confers an advantage under salt stress under non-lab conditions.

2.4 MPK17 and PMD1 proliferate peroxisomes normally to other stresses

As detailed in Chapter 1.2, NaCl is far from the only stress to induce peroxisome-division. To determine if MPK17 and PMD1 acted to induce peroxisome division specifically for NaCl stress, or whether MPK17 and PMD1 increase peroxisome division after any general stress, the ability of *mpk17-1* and *pmd1-1* to proliferate peroxisomes on a variety of other stresses was tested. In all tested stresses, *mpk17-1* and *pmd1-1* are indistinguishable from wild type, showing that MPK17 and PMD1 are acting in an NaCl-specific response pathway.

2.4.1 *mpk17-1* and *pmd1-1* respond normally to cadmium stress

Peroxisomes are reported to divide rapidly when grown on high levels of cadmium (Rodríguez-Serrano et al., 2016). To test whether peroxisomes in *mpk17-1* and *pmd1-1* are capable of dividing in response to heavy metals, seedlings were exposed to a short term $CdCl_2$ stress, then imaged. Wild type did not display a statistically significant increase in peroxisome division (Fig. 9A), contrary to published reports which reported a 3-fold increase in peroxisome number after three hours (Rodriguez-Serrano et al., 2016). Under short term treatment, both *mpk17-1* and *pmd1-1* also formed peroxules as both seen during these experiments and

previously described in wild type under cadmium stress (Figure 9C, (Rodriguez-Serrano et al., 2016).

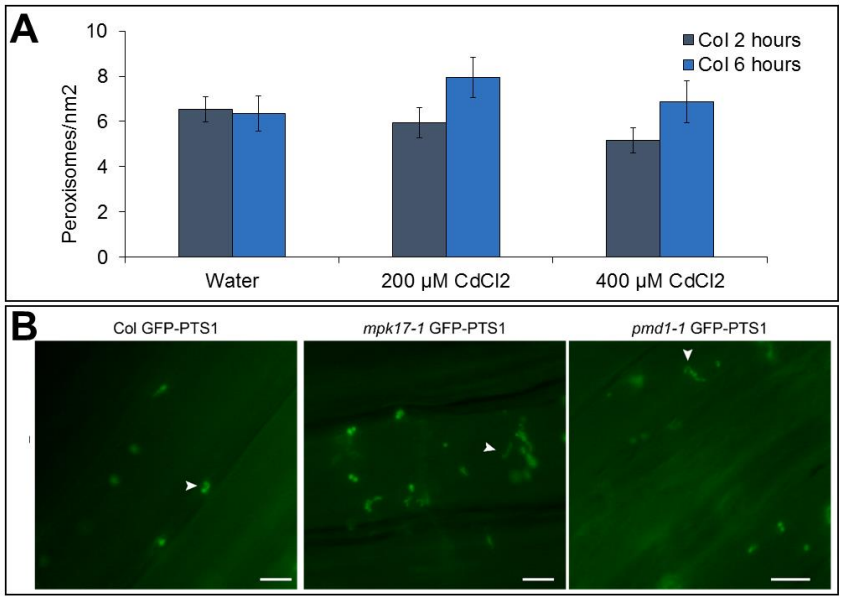

Figure 9: Peroxisomes under cadmium stress **A)** Peroxisomes in wild type do not increase significantly under short term cadmium stress. **B)** *mpk17-1* and *pmd1-1* respond normally to growth on cadmium by forming peroxules, marked with white arrowheads. Scale bars= 5 µm

2.4.2 *mpk17-1* and *pmd1-1* respond normally to high light

Sudden light exposure has also been reported to induce peroxisome division (Orth et al., 2007), likely by increasing transcription of Pex11b (Desai and Hu, 2008). To determine whether the PMD1 division factor might also be acting in this pathway, I examined the ability of peroxisomes in *mpk17-1* and *pmd1-1* to respond to sudden light exposure. Findings in wild type support those previously reported, that sudden light exposure of dark-grown seedlings will rapidly and transiently increase peroxisome number (Fig. 10; Orth et al., 2007; Desai and Hu, 2008). Peroxisomes in dark-grown *mpk17-1* and *pmd1-1* hypocotyls behave the same as wild type, showing a statistically significant increase in peroxisome number within 4 hours of light exposure, with peroxisome numbers decreasing back towards initial dark grown levels after 8 hours of light exposure (Fig. 10).

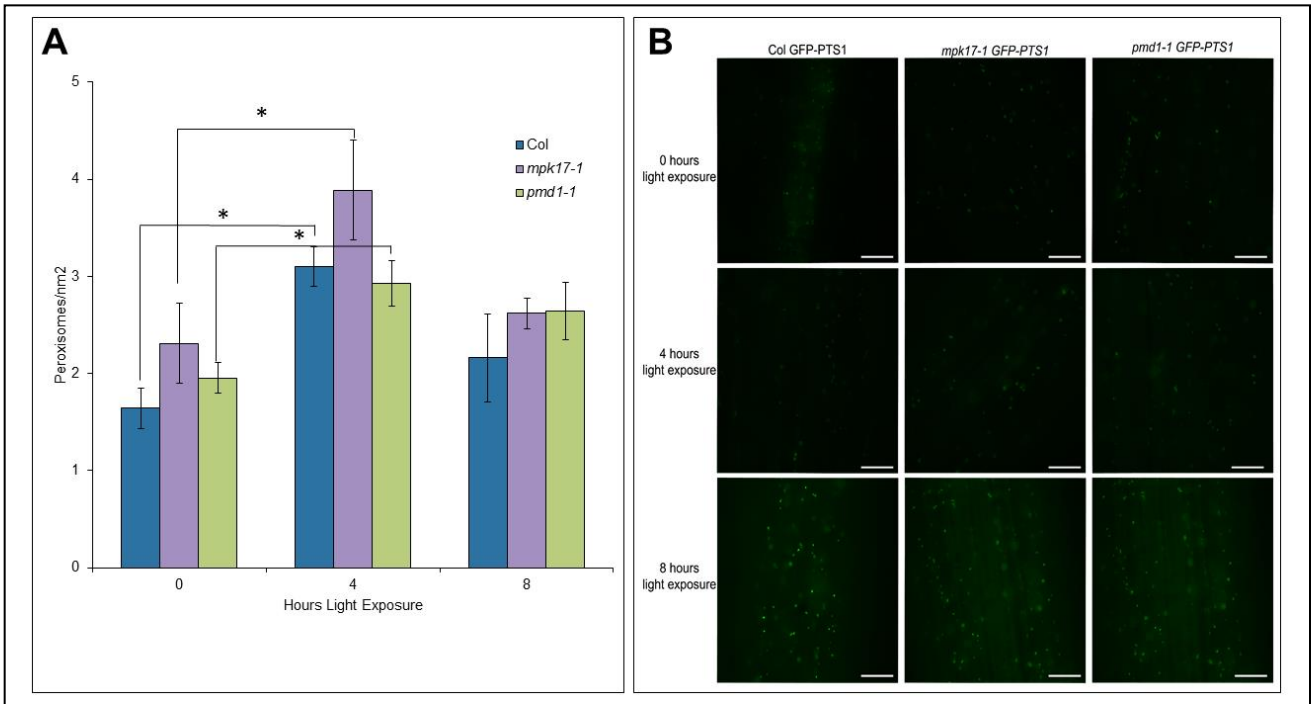

Figure 10: Peroxisomes in *mpk17-1* and *pmd1-1* respond normally to sudden light exposure. **A)** Number of peroxisomes in dark grown hypocotyls after indicated length of light exposure. * indicates p value < 0.05. **B)** Representative images of the set used to quantify peroxisome number.

2.4.3 *mpk17-1* and *pmd1-1* are not impaired in ROS responses

One hypothesis to explain stress induced peroxisome division in Arabidopsis is that all the division-inducing stresses also increase intracellular ROS, so the division is a result of increased ROS, not from the stress itself. Peroxisomes break down many species of ROS, so a quick increase in peroxisome number could be necessary to remove ROS after the stress signal has been perceived, but before ROS can damage cellular components. If this hypothesis is true, mutants that do not respond divide peroxisomes during stress should have increased ROS during the stress. Additionally, any mutant that does not display peroxisome division in response to one stress would be expected to have altered responses to all division-inducing stresses, including chemicals known to increase intracellular ROS. As shown in Chapter 2.4.1-2.4.3, *mpk17-1* and *pmd1-1* respond normally to cadmium and light stress, and only fail to divide peroxisomes in response in NaCl stress. *mpk17-1* was also evaluated on ROS-producing chemical clofibrate, which increases peroxisome division in mammalian cells (Hess et al., 1965). *mpk17-1* is capable of responding to clofibrate and proliferates peroxisomes like wild type, strongly suggesting that

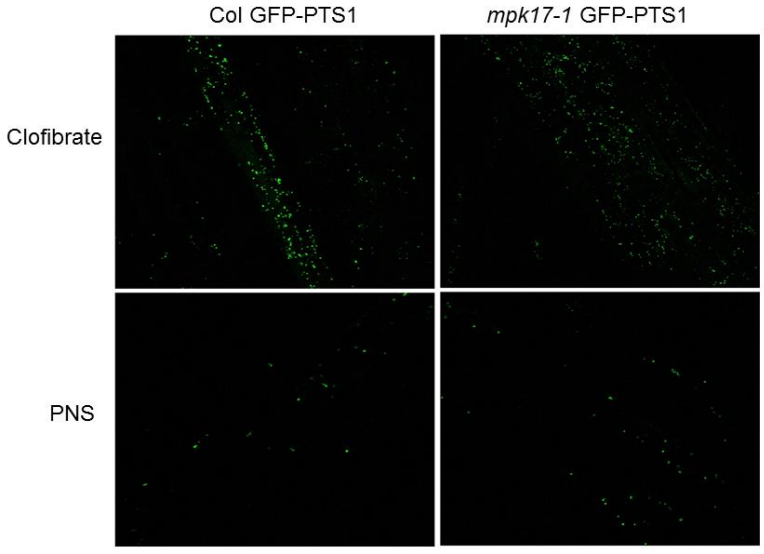

Figure 11: *mpk17-1* responds to ROS-generating chemical clofibrate.

ROS signaling is not impaired (Fig. 11).

To assess whether the decrease in peroxisome numbers in *mpk17-1* and *pmd1-1* on NaCl resulted in abnormal levels of ROS species, 3,3-diaminobenzidine (DAB) staining was used to qualitatively compare the amount of ROS in wild type, *mpk17-1*, and *pmd1-1*. DAB is monomeric until exposure to H_2O_2, at which point it polymerizes and can be visualized as a dark aggregate in cleared plant tissue (Hans Thordal-Christensen; Ziguo Zhang; Yangdou Wei, 1997). All genotypes were examined after growth on regular PN media or media supplemented with 150 mM NaCl. Neither *mpk17-1* nor *pmd1-1* display obvious alterations in the amount of H_2O_2 on either condition when compared to wild type (Fig. 12).

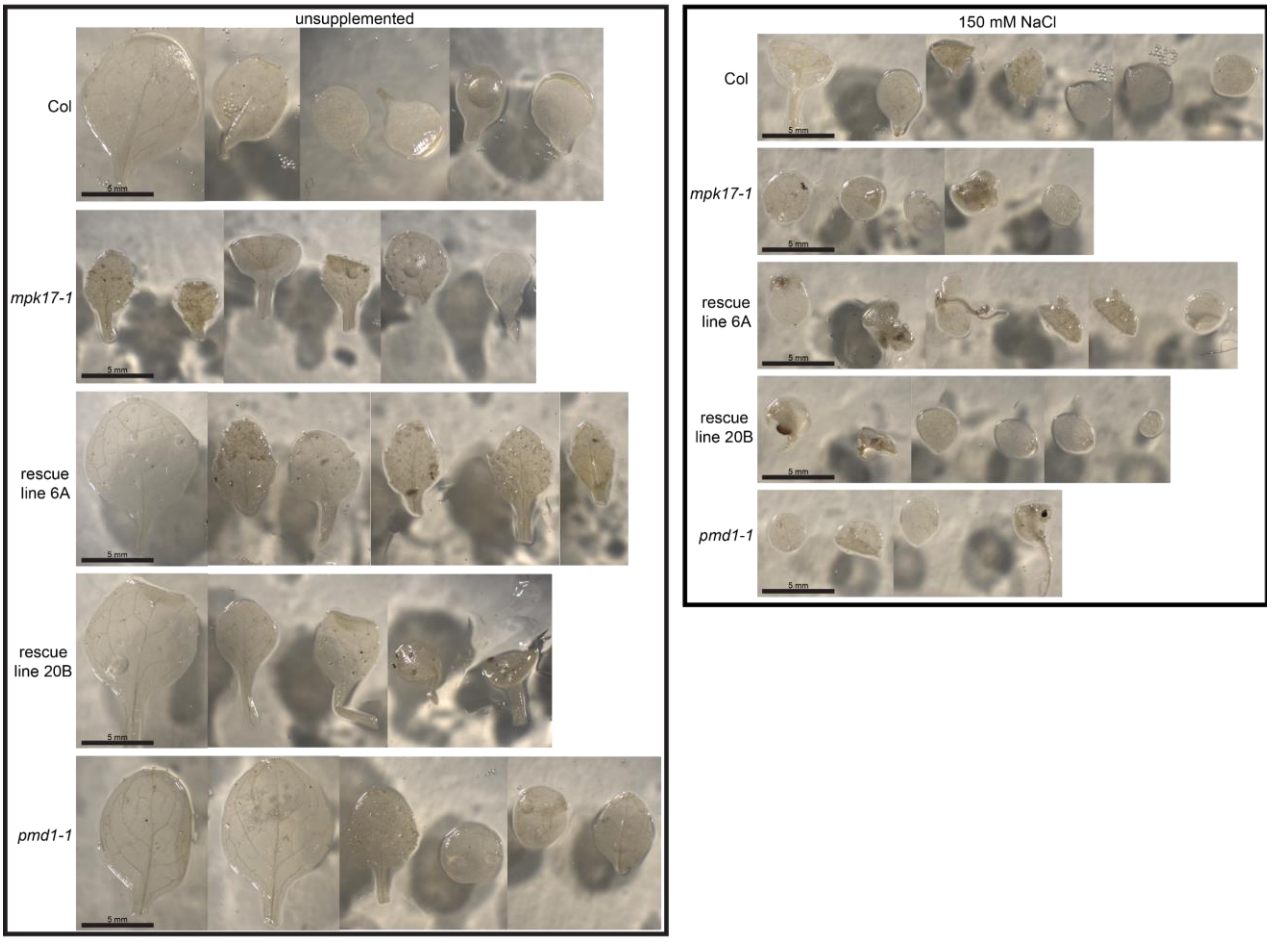

Figure 12: Neither *mpk17-1* nor *pmd1-1* display an obvious differences when compared to wild type in the amount of H_2O_2 produced under normal growth conditions or salt stress.

2.5 PMD1 binds actin

To further elucidate the function of the recently discovered PMD1 protein, I used the online protein structure prediction program Phyre2 to model secondary protein structure (Kelley et al. 2015). Phyre2 created a homology model of PMD1 (Fig. 13A) and predicted the PMD1 protein structure to have similarity to the heavy chains of dynein and myosin proteins. The PMD1 model suggests that, similar to dynein and myosin, the N-terminal portion of PMD1 (from residues 1-303) possess a heavy chain comprised of the coil-coil protein structure (Fig. 13A). However, unlike dynein and myosin, PMD1 is not predicted to have a region conferring ATPase activity

(Fig. 13A), and therefore is unlikely to facilitate movement in the absence of motor proteins. This Phyre2-generated model suggests the possibility that PMD1 roles in peroxisome biogenesis might rely on the plant cytoskeleton.

The cytoskeleton consists of microtubules and actin filaments. Peroxisomes travel along the

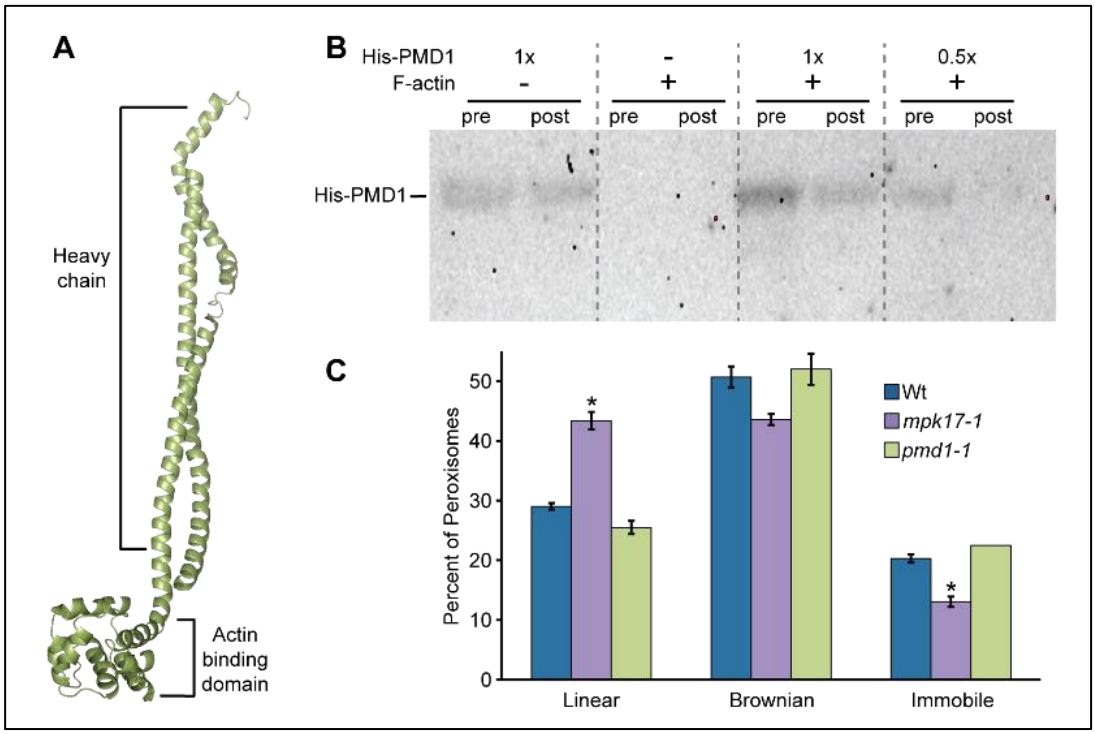

Figure 13: PMD1 is an actin-binding protein. **A**) Phyre2.0 predicted structure of PMD1 resembles dynein and myosin heavy chain proteins. The top portion has high similarity the coil-coil portion of a heavy chain, and the bottom domain is highly similar to the actin binding domain, but without a catalytic domain**. B)** Peroxisomes in the *mpk17-1* background move in a linear fashion more than peroxisomes in Col or *pmd1-1*. Additionally, fewer peroxisomes were immobile in *mpk17-1* than in Col or *pmd1-1*. 4 day old roots were imaged in the maturation zone on the Leica LSM at a rate of 13 frames/sec, for 29 seconds, then peroxisomes were tracked and primary type of movement was logged for each peroxisome. At least 5 individuals of each genotype were imaged, with 3 images per individual, totaling more than 400 peroxisomes per genotype. An ANOVA was done on each movement type, and showed that *mpk17-1* displays significantly more linear peroxisome movement than either wild type or *pmd1-1*, and a significantly smaller percentage of immobile peroxisomes ($p < 0.05$) **C)** PMD1 binds to actin. An actin cosedimentation assay was performed with His-tagged PMD1 protein. Full-strength His-PMD1 and a one-half dilution of PMD1 were both used, and both showed depletion from the supernatant after spinning with polymerized F-actin, indicating actin binding and

cytoskeleton, but which cytoskeleton varies by kingdom. In animals, peroxisomes travel along the microtubule cytoskeleton (Rapp et al., 1996; Schrader et al., 1996; Wiemer et al., 1997) In

plants and yeast, peroxisome travel along the actin cytoskeleton (Hoepfner et al., 2001; Mathur et al., 2002). DRP peroxisome division factors interact with actin-associated proteins in yeast (Yu and Cai, 2004). However, direct interaction of a plant peroxisome division factor with actin filaments has not been reported.

The PMD1 homology model is consistent with the possibility that PMD1 interacts with either microtubules or actin. Because peroxisomes travel along the actin cytoskeleton in plants (Mathur et al., 2002) and PMD1 localizes to peroxisomes (Aung and Hu, 2011), we tested whether PMD1 could directly interact with the actin cytoskeleton using an actin-cosedimentation assay with heterologously-expressed His-PMD1$^{1-303}$ protein and purified G-actin (Schafer et al., 1998). In this assay, proteins are incubated in the presence of G-actin and polymerization of G-actin to F-actin is induced. Afterwards, the reaction is subjected to high-speed centrifugation and proteins that bind F-actin are depleted from the supernatant as the polymerized F-actin pellets to the bottom of the tube. Proteins remaining in the supernatant are separated by SDS-PAGE and immunoblot analysis used to examine protein levels. His-PMD1$^{1-303}$ protein is depleted from the supernatant in this assay (Fig. 13B), indicating that PMD1 can directly bind actin *in vitro*.

Because PMD1 associates with actin (Fig. 13B), along which peroxisomes move (Mathur et al., 2002), we examined *in planta* peroxisome movement in the *pmd1-1* and *mpk17-1* mutants. In wild type, peroxisomes display various movement types when examined over a 30-second period. Approximately half the peroxisomes in wild type exhibit Brownian movement, approximately 20% are immobile, and approximately 30% display linear movement (Fig. 13C). Although peroxisomes in *pmd1-1* display a slight decrease in linear movement, this difference is not statistically significant (p=0.10; Fig. 13C). However, a significantly smaller percentage of peroxisomes in *mpk17-1* were immobile compared to either wild type or *pmd1-1* (Fig. 13C), and

a significantly higher percentage of peroxisomes in *mpk17-1* moved in a linear fashion (Fig. 13C). These results suggest increased peroxisome movement along actin filaments in *mpk17-1*, despite the increased clustering of peroxisomes observed in this mutant (Fig. 5). These data are consistent with the possibility that PMD1 directly tethers peroxisomes to actin; however, because PMD1 lacks a region conferring ATPase activity, it is unlikely to act as a motor and provide the energy for peroxisome movement along the actin filament.

2.6 Discussion

Based on the phenotype of *mpk17-1* as IBA hypersensitivity with increased peroxisome numbers, and the known role of *PMD1* increasing peroxisome division (Aung and Hu 2011), we suggest a genetic model in which MPK17 inhibits PMD1, a factor promoting peroxisome division (Fig. 14). Because *pmd1-1* suppresses the *mpk17-1* increased peroxisome number phenotype, PMD1 acts downstream of MPK17 (Fig. 7). We do not yet know the phosphorylation targets of MPK17. We were unable to detect an interaction between MPK17 and PMD1 using a yeast two-hybrid assay, consistent with the possibility that PMD1 is not a direct target of putative MPK17 kinase activity. Therefore, there are likely additional components missing from this model. Additionally, we cannot exclude the possibility that MPK17 inhibits peroxisome biogenesis generally, not only division through one specific factor. Further work will need to be done to determine precisely how broad or narrow an effect *MPK17* has on peroxisome division.

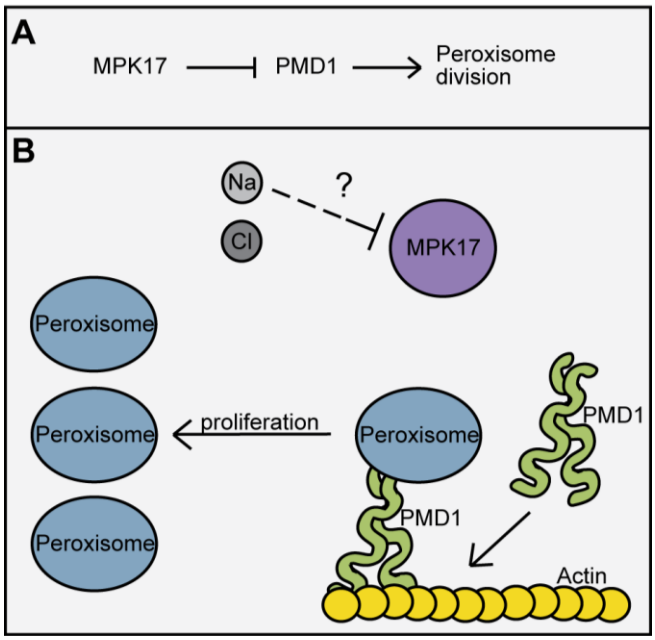

Figure 14: Proposed model of NaCl-regulated peroxisome division mediated through PMD1. Under low-NaCl conditions, MPK17 actively represses transcription and activity of PMD1. Under high NaCl conditions, MPK17 is inactivated and transcription of PMD1 increases, leading to increased numbers of peroxisomes and increased connections between peroxisomes and the actin cytoskeleton.

In this work, we have demonstrated a novel function for Arabidopsis MPK17 that affects peroxisome and mitochondrial division. These effects by MPK17 depend on PMD1, a peroxisome and mitochondrial division factor. Although Arabidopsis MPK17 is essentially uncharacterized compared to its well-understood relatives MPK3 and MPK6 (reviewed in Mishra et al., 2006), studies on MPK17 homologs from other plants suggest it plays roles in stress response. For example, cotton *GhMPK17* salinity stress tolerance and ABA treatment, and overexpression of *GhMPK17* in Arabidopsis led to increased tolerance of both salinity and ABA (Zhang et al., 2014). Similarly, in *Setaria italica*, *SiMPK17* transcript is upregulated in response to dehydration stress (Lata et al., 2010). Transcript of the maize homolog, *ZmMPK17*, increases upon cold, ROS, or osmotic stresses and during treatments with abscisic acid, salicylic acid,

jasmonic acid, and ethylene (Pan et al., 2012). Further, the two closest rice *MPK17* homologs, *OsMPK13* and *OsMPK14*, are induced upon inoculation with a rice fungal pathogen (Reyna and Yang, 2006). Clearly, MPK17 and its homologs respond to stress transcriptionally and, at least in some cases, mediates tolerance to various stress conditions.

Disruption of either *MPK17* or *PMD1* results in decreased salt-induced peroxisome proliferation, thus both MPK17 and PMD1 are necessary for this dynamic salt response. Because the peroxisome numbers in non salt-stressed *mpk17-1* are not as high as wild type grown on NaCl, division through the actions of *MPK17* and*PMD1* cannot be the sole salt-responsive peroxisome division pathway(s). The ability to divide peroxisomes in response to NaCl does not substantially impact survival or growth of these mutants under high-NaCl conditions (Fig. 4), which suggests that peroxisome proliferation may not enhance the fitness of NaCl- stressed plants. This result contrasts with recent results by Fahy et al. (2017), who observed that the salt-hypersensitive mutants *fry1* and *sos1* did not proliferate peroxisomes in response to NaCl, and have very poor survival on high NaCl. Both *mpk17* and *pmd1* display the same nonproliferation molecular phenotype, but no whole plant NaCl phenotype. It remains unclear whether peroxisome proliferation in response to NaCl may provide salt tolerance to the plant under specific conditions, or whether peroxisome proliferation is a side effect caused by regulation of a different pathway.

In this study, we also discovered a novel function for PMD1 as an actin-binding protein (Fig. 13B). PMD1 may act as a mechanical input to the peroxisome (and mitochondrial) division process, an idea that is supported by the peroxisome clustering phenotype seen in *PMD1* overexpression lines (Aung and Hu, 2011). The increased fraction of *mpk17-1* peroxisomes moving in a linear versus Brownian pattern is also consistent with the hypothesis that

connections between PMD1 and the actin cytoskeleton contribute to peroxisome distribution *in planta*, as *mpk17-1* contains more PMD1, and *mpk17-1* peroxisomes show an increased ability to move around the cell than in wild type or *pmd1-1*. Peroxisomes in cells treated with latrunculin B still undergo Brownian movement (Mathur et al., 2002), further supporting the hypothesis by Aung and Hu (2011) that PMD1 might act in peroxisome distribution within the plant cell. Recently, the distribution, not just the number, of peroxisomes was shown to be vital for proper cell division in mice skin cells (Asare et al., 2017). Knocking down Pex11b retained peroxisome attachment to the microtubule cytoskeleton, but peroxisomes were mislocalized. This mislocalization led to improper positioning of the peroxisomes during cell division and mitotic delay, as well as aberrant angles of the mitotic plane of division (Asare et al., 2017). Other findings suggest the ability of plants to traffic actin-dependent contents is important for ordinary growth and development, not just organelle distribution during stress. The speed of myosins was shown to directly affect plant size, with expression of a faster myosin leading to larger plant size, and slower myosin causing smaller plant size (Tominaga et al., 2013). These data further support a role for localization, not just number, in peroxisome function.

These findings illuminate the importance of the actin cytoskeleton in peroxisome division. Future research to determine whether additional peroxisome or mitochondrial division factors associate with actin will be of interest and may provide molecular insight into how actin affects peroxisome division. Many questions remain about how, why, and when plants regulate peroxisome numbers and what adaptive function peroxisome proliferation may provide to plants.

2.6 Materials and Methods

Growth Conditions and Phenotypic Assays

Arabidopsis thaliana mutants were all in the Columbia-0 (Col-0) background, which was used as the wild type in all assays. Seeds were surface sterilized (Last and Fink, 1988) and stratified overnight at 4 °C prior to plating on plant nutrient (PN) medium (Haughn and Somerville, 1986) supplemented with 0.5% w/v sucrose and solidified with 0.6% agar, unless otherwise noted. Seedlings were grown at 22 °C under continuous illumination.

To examine auxin-responsive root elongation, seeds were plated on media supplemented with ethanol (mock), or the indicated concentrations of indole-3-acetic acid (Sigma, St. Louis, MO), indole-3-butyric acid (Sigma, St. Louis, MO), 2,4-dichlorophenoxyacetic acid (Sigma, St. Louis, MO), or 2,4-dichlorophenoxybutyric acid (Sigma, St. Louis, MO). All hormone stocks were dissolved in 100% ethanol. Plates were incubated at 22 °C under yellow-filtered light to prevent indole backbone degradation (Stasinopoulos and Hangarter, 1990). After 8 days of growth, seedlings were removed from the agar and root length measured.

To examine auxin-responsive lateral root formation, seeds were plated on unsupplemented media and grown under continuous white light for 4 days prior to transfer to media supplemented with ethanol (Mock) or the indicated auxin. Seedlings were grown for an additional 4 days under continuous yellow light. Emerged lateral roots were counted under a dissecting scope and root length measured to determine the number of lateral roots formed per mm root length.

To examine inhibition of root elongation on salt, seeds were plated on unsupplemented media and grown under continuous white light for 4 days prior to transfer to plates supplemented with the indicated concentration of NaCl, KCl, or mannitol and solidified with 0.7% agar. Upon transferring, root tips were aligned and marked. Plates were then placed vertically under continuous white light and grown for an additional 4 days before imaging and measurement of post-transfer growth using ImageJ.

To examine seedling bleaching caused by salt, seeds were plated on sterile Whatman filter paper set on top of unsupplemented media and grown under continuous white light for 4 days. Filter papers with seedlings were then transferred to plates supplemented with the indicated concentration of NaCl and grown under continuous white light for an additional 7 days. After 7 days and 14 days, the number of green seedlings (seedlings with at least 1 green cotyledon) and bleached (colorless) were counted.

To examine adult plant growth response to salt watering, seedlings were grown for one week on unsupplemented media, then transferred to individual 9x9cm pots containing soil. Ten individuals of each genotype were used for each treatment. Plants were grown at 21ºC, 50% humidity under continuous light in a growth chamber and were top-watered uniformly for one week with distilled water prior to daily top-watering with 25 mLs of distilled water supplemented with the indicated amount of NaCl. Plant mortality was logged daily. Plant height was measured after 2 weeks of watering treatment, when plants were beginning to senesce.

Vector Construction and Transformation

To create *mpk17-1* rescue lines, the 2 kB region upstream of MPK17 and the full-length MPK17 gene were amplified using Pfx Platinum (Life Technologies) polymerase using MPK17-16 and MPK17-withstop primers listed in Supplemental Table 1. This region was subcloned into pENTR-DTOPO (Life Technologies), then cloned into pMDC123 (Curtis and Grossniklaus, 2003) using LR Clonase II (Life Technologies) to create MPK17promoter:MPK17. MPK17promoter:MPK17 was then transformed into GV3101 *Agrobacterium tumefaciens* strain, which were used for floral dip transformation (Clough and Bent, 1998) of *mpk17-1* plants.

To create the construct for PMD1 protein expression, the portion of *PMD1* cDNA (U83915) encoding PMD1 from amino acids 1-303 and thus lacking the predicted PMD1 transmembrane domain was PCR amplified using PMD1-*Nde*I (5´-CATATGGCGGATGTTGAAGATC-3´) and PMD1-*Xho*I 5´-(CTCGAGCTAAGCAGCTCCAACTGATCC-3´) and the resultant product cloned into pCR4 (Life Technologies). $PMD1^{1-303}$ was then released using restriction enzymes *Nde*I and *Xho*I and subcloned into the protein expression vector pET28A (Novagen) to create pET28-$PMD1^{1-303}$.

Genetic Analyses

Plants were genotyped by PCR using the primer pairs in Supplemental Table 1. Col-0 carrying the GFP-PTS1 reporter (Zolman and Bartel 2004) was crossed to *mpk17-1* and *pmd1-1* and resultant F_2 seedlings genotyped to obtain *mpk17-1 GFP-PTS1* and *pmd1-1 GFP-PTS1*. Col-0 and *pmd1-1* carrying the COX4-YFP mitochondrial reporter (Aung and Hu, 2011; Nelson et al., 2007) were crossed to *mpk17-1* and resultant F_2 seedlings genotyped to obtain *mpk17-1 COX4-YFP*. Fluorescent reporter lines were genotyped with a combination of PCR and by the presence of the fluorescent reporter.

To obtain *mpk17* rescue lines, *mpk17-1* mutants were transformed using the floral dip method (Clough and Bent, 1998). *mpk17-1* seedlings carrying the *MPK17promoter:MPK17* transgene were selected for Basta (phosphinothricin; Gold Biotechnology) resistance in the T_1 generation and lines homozygous for the transgene were selected in subsequent generations. Non-segregating T_3 lines were genotyped for both the *mpk17-1* TDNA insertion and presence of wild type *MPK17* from the transgene. Later generations were genotyped by both PCR and Basta plating.

Imaging and Peroxisome Quantification

To determine the effects of salt treatment and cytoskeleton inhibitors on peroxisome numbers, three-day-old seedlings were transferred to plant growth media supplemented with 150 mM NaCl, 2 µM latrunculin with and without 150 mM NaCl, and 20 µM oryzalin with and without 150 mM NaCl. Plants were grown on salt and cytoskeleton inhibitors overnight at 22°C under continuous white light, then incubated in propidium iodide (Invitrogen) and imaged by confocal, using identical settings for each image. Peroxisomes were quantified in ImageJ by selecting the root area, then using "Find Maxima" with appropriate parameters (thresholding between 6-10, dark background mode).

To determine peroxisome numbers and movement, 7-day-old seedlings were mounted on microscope slides in liquid plant media containing 0.1% agar; slides had a ToughTag™ positioned on either end of the coverslip to provide a cushion between the slide and coverslip. Seedlings were imaged at a rate of 13 frames/sec for 29 seconds on a Leica DM6 B upright fluorescence scope equipped with a Leica DFC 3000 G camera. For each genotype, at least 9 different individuals were imaged, with 3 images/root in the maturation zone taken. Videos were analyzed using ImageJ. The movement type for each peroxisome was categorized as either Linear (indicates rapid, mostly unidirectional movement through the cell), Brownian (refers to back-and-forth movement of a peroxisome), or "Immobile" (the peroxisome exhibited no movement during the 29 seconds recording).

To image and quantify peroxisomes for light-induced proliferation, seeds were grown on plant growth media for 24 hours in white light, then wrapped in foil and grown in darkness for another three days. Plates were then unwrapped and exposed to white light for the indicated amounts of time before imaging on a Leica DM6 B upright fluorescence scope equipped with a

Leica DFC 3000 G camera. Unwrapping of plates was staggered to account for imaging time between genotypes. Peroxisomes were quantified in ImageJ by selecting the root area, then using "Find Maxima" with appropriate parameters (thresholding between 5-9, dark background mode).

To determine the effects of cadmium on peroxisome numbers, four-day-old seedlings were transferred to plant growth media supplemented with water, 200 µM $CdCl_2$, or 400 µM $CdCl_2$ for 2 and 6 hours. Roots were imaged on a Leica DM6 B upright fluorescence scope equipped with a Leica DFC 3000 G camera. Peroxisomes were quantified in ImageJ by selecting the root area, then using "Find Maxima" with appropriate parameters (thresholding between 6-10, dark background mode).

To image and quantify mitochondria, four-day-old seedlings carrying the COX4-YFP were counterstained with propidium iodide and imaged by confocal with a Zeiss LSM510 using identical settings for each image. Images were analyzed in ImageJ using the "Find Maxima" tool as described for peroxisomes above.

Protein Expression and Purification

$PMD1^{1-303}$ was expressed in *Escherichia coli* (DE3) Rosetta cells (Invitrogen) as an N-terminal His-tagged protein. Bacterial cultures were grown at 37 °C to an A_{600nm} = ~0.5. Protein expression was induced with a final concentration of 1 mM isopropyl β-D-1-thiogalactopyranoside, then grown for and additional 18 h at 18 °C. Bacterial cells were pelleted and resuspended in lysis buffer [50 mM Tris pH 8.0, 20 mM imidazole, 500 mM NaCl, 10% (vol/vol) glycerol, 1% Tween-20]. Resuspended cells were lysed by sonication, and cell debris was pelleted by centrifugation. The soluble cell lysate was passed over a Ni^{2+}-nitrilotriacetic acid (NTA) chromatography column. The column was washed with wash buffer [50 mM Tris pH 8.0,

20 mM imidazole, 500 mM NaCl, 10% (vol/vol) glycerol] and bound protein eluted with elution buffer [50 mM Tris pH 8.0, 250 mM imidazole, 500 mM NaCl, 10% (vol/vol) glycerol].

Actin cosedimentation assay

The actin cosedimention assay was performed with purified His-PMD1$^{1-303}$ and G-actin, which was a kind gift from the lab of John Cooper (Washington University in St. Louis). Prior to the assay, the 10 µM G-actin and His-PMD1$^{1-303}$ were independently centrifuged at 200,000xg at 4 ºC for 20 minutes to remove any protein complexes. One X and half X concentrations of His-PMD1$^{1-303}$ were incubated with G-actin, 20X KMEI polymerization buffer [0.2 M imidazole pH 7.0, 1 M KCl, 20 mM $MgCl_2$, 20 mM EGTA,1 mM NaN_3] and G-actin buffer with ATP [2 mM Tris-Cl pH 8.0, 0.1 mM $CaCl_2$, 1 mM NaN_3, 0.2 mM Na-ATP, 0.5 mM DTT]. Samples were rocked at room temperature for one hour. A 50 µL aliquot was removed from each sample prior to centrifugation to create the "pre-spin" sample. The remaining sample was then moved to a tube containing 50 µL of 20% sucrose in G-actin buffer [2.0 mM Tris-Cl pH 8.0, 0.1 mM $CaCl_2$, 1 mM NaN_3] and centrifuged at 100,000xg at 4ºC for 30 minutes. After centrifugation, a 50 µL aliquot from the post-spin supernatant was removed from each sample to new tubes to create the "post-spin" samples. Each sample was mixed with an equal volume of Nu-PAGE sample buffer [141 mM Tris, 2% LDS, 0.51 mM EDTA, 10% glycerol, 0.175 mM phenol red, 0.22 mM Coomassie blue] and boiled for 5 minutes prior to separation by electrophoresis through a 10% Bis-Tris Plus gel (Invitrogen). After separation, proteins were transferred to a nitrocellulose membrane. The membrane was blocked in 8% milk diluted in 1X TBS-T [20 mM Tris, pH 7.5, 150 mM NaCl, 1% Tween] for one hour, then incubated with a 1:200 dilution of α-His (Santa Cruz) in blocking buffer at 4ºC overnight. The membrane was washed three times with 1X TBS-T for 5 minutes per wash prior to a 4 hours incubation with 1:5000 goat α-rabbit

HRP-conjugated antibody dilution (Santa Cruz). After incubation with secondary antibody, the membrane was washed 3 times with 1X TBS-T for 5 minutes per wash. The membrane was immersed in WesternBright ECL HRP (Bioexpress) substrate and imaged using a Biorad ChemiDoc.

Chapter 3: Roles for IBA-derived auxin in plant development

This work has been accepted for publication in the *Journal of Experimental Botany*

Elizabeth M. Frick and Lucia C. Strader

Department of Biology, Washington University in St. Louis, St. Louis, Missouri 63130, USA

NSF Science and Technology Center for Engineering Mechanobiology

The term auxin is derived from the Greek word "auxein", which means "to grow". Because auxin is a potent regulator of cell division, cell expansion, and cell differentiation (reviewed in Enders and Strader, 2015), it is involved in nearly every aspect of plant development. Therefore, regulation of auxin levels and response is critical for normal plant form and function. Plants use a number of cellular mechanisms to regulate auxin levels and response, including transport, *de novo* biosynthesis, and management of inputs from various auxin precursors and storage forms (reviewed in Korasick et al., 2013).

The predominant active auxin, IAA, is transported long distances through plants via the combined action of distinct families of transporters (reviewed in Zažímalová et al., 2010). The AUX1/LAX family of transporters act as IAA uptake carriers, whereas members of the ABCB and PIN family of transporters facilitate IAA efflux. Together, these transporters facilitate long distance, directional transport of IAA through the plant to regulate numerous aspects of plant development.

The main auxin biosynthesis pathway uses the TRYPTOPHAN AMINOTRANSFERASE OF ARABIDOPSIS1 (TAA1) and YUCCA family of enzymes (reviewed in Zhao, 2012). In this pathway, tryptophan is converted to indole-3-pyruvic acid (IPyA) through the activity of the

TAA1 family of aminotransferase enzymes. The YUCCA family of flavin monooxygenase-like enzymes then converts IPyA to IAA. Conversion of IPyA to IAA is the rate-limiting step in this process; ovexpression of YUCCA family members results in elevated auxin levels. Further, tissue-specific expression of various YUCCA family members allows for *de novo* auxin biosynthesis to drive specific aspects of plant development (reviewed in Zhao, 2010).

In addition to biosynthesis of IAA via the IPyA pathway, the pool of active auxin can be modulated by inputs from additional storage forms and precursors, such as IAA conjugates and indole-3-butyric acid (IBA). These auxin inputs can drive distinct aspects of plant development (reviewed in Korasick et al., 2013). In this review, we focus on specific roles for IBA-derived auxin in plant development.

3.1 IBA conversion and transport mechanisms

For decades, IBA was described as a "synthetic auxin" that elicited auxin-like effects such as root initiation, stem bending, and leaf epinasty (Zimmerman and Wilcoxon, 1935). Indeed, IBA is the active ingredient in plant propagation medias, such as Rootone®, used to induce adventitious rooting in stem cuttings. Later studies have demonstrated that IBA is an endogenous compound in a variety of examined plant species (reviewed in Korasick et al., 2013).

The side chain in the 3 position on the indole ring of IBA has four carbons, as opposed to the two carbon side-chain of IAA; this lengthened side chain results in a molecule that is likely unable to adopt a conformation for binding into the TIR1-Aux/IAA co-receptor pocket (Uzunova et al., 2016). Indeed, surface Plasmon resonance analysis suggests that IBA has no measured

binding activity (Uzunova et al., 2016), consistent with the genetic evidence that IBA activity is through its conversion to IAA (reviewed in Strader and Bartel, 2011).

IBA is likely converted to IAA in a process similar to fatty-acid β-oxidation. Many plants convert IBA into IAA (reviewed in Epstein and Ludwig-Müller, 1993), including Arabidopsis (Strader et al., 2010), hazelnut (Kreiser et al., 2016), and elm (Kreiser et al., 2016). In Arabidopsis, this process is peroxisome-dependent (Strader et al., 2010) and multiple mutants defective in peroxisome biogenesis and peroxisomal enzymes have been identified for IBA resistance while retaining sensitivity to the active auxin IAA (reviewed in Hu et al., 2012). The PEROXISOMAL TRANSPORTER1/COMATOSE/ABCD1 (PXA1/CTS/ABCD1) transporter is likely to move IBA into the peroxisome for metabolism into active auxin (reviewed in Michniewicz et al., 2014; Strader and Bartel, 2011). Whereas some peroxisomal enzymes, such as the PED1 3-ketoacyl-CoA thiolase, likely act in both fatty acid (Hayashi et al., 1998) and IBA β-oxidation (Zolman et al., 2000), other peroxisome enzymes appear to be specific to IBA β-oxidation. Specifically, the predicted short-chain dehydrogenase/reductase INDOLE-3-BUTYRIC ACID RESPONSE1 (IBR1) (Zolman et al., 2008), the acyl-CoA dehydrogenase/oxidase-like IBR3 (Zolman et al., 2007), the predicted enoyl-CoA hydratase IBR10 (Zolman et al., 2008), and the predicted enoyl-CoA hydratase ENOYL-COA HYDRATASE2 (ECH2) (Strader et al., 2011) are enzymes that may act solely in the conversion of the auxin precursor IBA to active IAA.

Similar to mechanisms regulating IAA levels (reviewed in Korasick et al., 2013; Zažímalová et al., 2010), mechanisms to regulate IBA levels include formation of IBA conjugates and IBA transport (Fig. 15). IBA exists in both amide- and ester-linked amide forms (reviewed in Bajguz

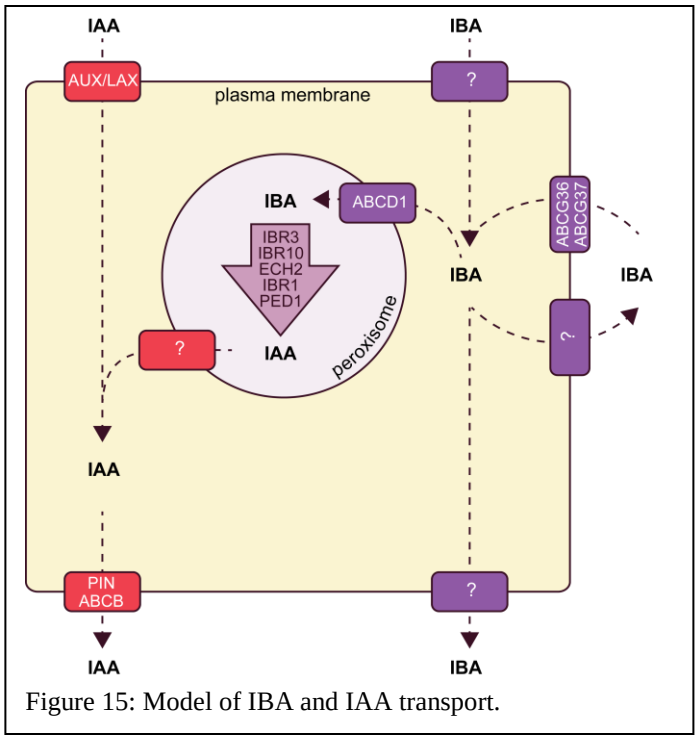

Figure 15: Model of IBA and IAA transport.

and Piotrowska, 2009; Ludwig-Müller, 2011; Woodward and Bartel, 2005b). Beyond some members of the GH3 amino acid synthetase family which are able to conjugate amino acids to IBA as well as to IAA (Staswick et al., 2005), IBA-specific amino acid conjugating enzymes have not yet been reported. The hydrolases TaIAR3 from wheat(Campanella et al., 2004), BrIAR3 (Savić et al., 2009), and BrILL2 from *Brassica rapa* (Savić et al., 2009) display higher affinity for IBA-amino acid conjugates than for IAA-amino acid conjugates, consistent with the possibility that IBA may be stored in amino-acid conjugate form for storage. Additionally, IBA is likely to be stored as conjugates to sugar. The enzymes UGT74E2 (Tognetti et al., 2010) and UGT75D1 (Zhang et al., 2016) promote the formation of IBA-glucose; overexpression of either *UGT74E2* (Tognetti et al., 2010) or UGT75D1 (Zhang et al., 2016) results in elevated IBA-

glucose levels. Identification and characterization of enzymes involved in IBA conjugate synthesis and hydrolysis will be important for understanding roles of these potential storage forms in auxin homeostasis. For example, after identifying GH3.1, GH3.2, GH3.5, and GH3.17 and IAA amido synthetases conjugated amino acids to IAA, the knockout lines could be examined and used to show the importance of IAA-amino acid conjugates in regulating IAA homeostasis *in planta* (Staswick et al., 2005). Similarly, identification of ILR1, IAR3, ILL1, and ILL2 as IAA hydrolases was instrumental in understanding how IAA conjugates are cleaved and contribute to the free IAA pool *in planta* (LeClere et al., 2002). Identification of the IBA-specific synthetases and hydrolases will similarly inform our understanding of how plants regulate their pools of free IBA.

Auxin distribution throughout the body of the plant is mediated by the cellular auxin transport to achieve the long-distance movement of IAA. Similarly, IBA and/or IBA conjugates are thought to move long distances through the plant (reviewed in Michniewicz et al., 2014; Strader and Bartel, 2011). Tracking of radiolabel in plants treated with [^{3}H]IBA allowed for the acropetal and basipetal movement of signal in *Cleopatra mandarin* midrib sections (Epstein and Sagee, 1992), and in various Arabidopsis tissues (Ludwig-Müller et al., 1995b; Rashotte et al., 2003). However, these studies are complicated by IBA metabolism to IAA and to conjugates. Later studies determined that most of the radioactive transported material was not the original [^{3}H]IBA, but rather [^{3}H]IAA derived from [^{3}H]IBA (Růžička et al., 2010), or [$^{13}C_1$]IAA, Ester-[$^{13}C_1$]IBA conjugates, or Amide-[$^{13}C_1$]IBA conjugates derived from [$^{13}C_1$]IBA (Liu et al., 2012a). These studies are consistent with IBA conjugates being the major form of transported IBA. However, IBA uptake is a saturable process (Ludwig-Müller et al., 1995b; Rashotte et al., 2003), which suggests that IBA uptake into plant cells is carrier-mediated. Further, examined

transporters of IAA, including AUX1, PIN2, PIN7, ABCB1, and ABCB19, do not appear to facilitate the transport of IBA (reviewed in Michniewicz et al., 2014), suggesting that other carriers act in the transport of IBA.

Several IBA transporters have been identified, although there likely are additional carriers (reviewed in Michniewicz et al., 2014; Strader and Bartel, 2011). IBA efflux is promoted by ATP-BINDING CASSETTE G36 / PLEIOTROPIC DRUG RESISTANCE 8 / PENETRATION 3 (ABCG36/PDR8/PEN3) (Strader and Bartel, 2009), ABCG37/PDR9/PIS1 (Růžička et al., 2010; Strader et al., 2008), and possibly by additional members of the PDR subclade of the ABCG family (Michniewicz et al., 2014). Mutants defective in ABCG29 (Michniewicz et al., 2014), ABCG33 (Michniewicz et al., 2014), ABCG36 (Strader and Bartel, 2009), or ABCG37 (Růžička et al., 2010; Strader et al., 2008) display increased sensitivity to the auxin precursor IBA and retain wild type sensitivity to the active auxin IAA. Consistent with the IBA hypersensitivity displayed, root tips excised from mutants defective in either ABCG36 (Strader and Bartel, 2009) or ABCG37 (Růžička et al., 2010; Strader et al., 2008) hyperaccumulate [^{3}H]IBA, but not [^{3}H]IAA. The IBA hypersensitivity combined with the hyperaccumulation of [^{3}H]IBA in these mutants is consistent with roles for ABCG36 and ABCG37 in effluxing IBA from the root. Although ABCG36 and ABCG37 appear to transport the auxin precursor IBA, but not active IAA, they likely transport additional substrates, as is common for members of the PLEIOTROPIC DRUG RESISTANCE family of transporters. In particular, ABCG37 likely transports the synthetic auxin 2,4-dichlorophenoxy acetic acid (2,4-D) (Ito and Gray, 2006; Růžička et al., 2010; Strader et al., 2008), the synthetic auxin precursor 2,4-dichlorophenoxy butyric acid (2,4-DB) (Růžička et al., 2010; Strader et al., 2008), 1-N-naphthylphthalamic acid NPA (Ito and Gray, 2006), the auxin breakdown product oxIAA-Hex (Peer et al., 2013),

and non-auxinic phenolic coumarin compounds (Fourcroy et al., 2014). Further, ABCG36 likely transports the synthetic auxin precursor 2,4-DB (Strader and Bartel, 2009), oxIAA-Hex (Peer et al., 2013), cadmium / cadmium conjugates (Kim et al., 2007), coumarin (Fourcroy et al., 2014), and a precursor to 4-O-β-D-glucosyl-indol-3-yl formamide (Lu et al., 2015). Clearly, these transporters have roles outside of their regulation of cellular IBA levels.

Analysis of mutants with altered IBA-to-IAA conversion, altered management of storage forms, and altered transport have revealed roles for IBA-derived auxin in multiple specific developmental processes.

3.2 IBA-derived auxin drives aspects of root development

IBA-derived auxin has strong roles in various aspects of root development, including regulation of root apical meristem size, root hair elongation, lateral root development, and formation of adventitious roots. Mutations disrupting IBA metabolism and chemicals that affect IBA metabolism result in multiple root phenotypes, revealing specific roles for IBA-derived auxin in these processes.

The root apical meristem is a collection of undifferentiated cells at the root tip region that display indeterminate growth. The balanced cell division and differentiation in this tissue gives rise to new root tissue, while maintaining a small group of cells that undergo occasional cell division, called the quiescent center. Maintaining proper auxin levels and establishment of an auxin gradient in these tissues is essential to establish root patterning and meristem formation (reviewed in Iyer-Pascuzzi and Benfey, 2009). The *ech2 ibr10* double mutant, defective in β-oxidation enzymes required for IBA-to-IAA conversion, displays decreased *DR5-GUS* activity in root tips. Further the *ech2 ibr1 ibr3 ibr10* quadruple mutant, defective in multiple IBA

conversion enzymes, has reduced free IAA levels in the root tip and displays a reduced meristem size (Strader et al., 2011), consistent with IBA conversion to IAA acting as a major input into the auxin pool in this tissue.

Root hairs are long tubular outgrowths protruding from the epidermal cell layer of roots that aid in nutrient and water acquisition by increasing root surface area. Auxin affects the positioning of the root hair outgrowth site and promotes root hair elongation (reviewed in Honkanen and Dolan, 2016). Multiple lines of evidence suggest that IBA-derived auxin promotes root hair expansion. First, mutants defective in the ABCG36 or ABCG37 transporters, which likely act to efflux IBA out of the root, display longer root hairs (Růžička et al., 2010; Strader and Bartel, 2009). Further, blocking IBA-to-IAA conversion suppresses the long-root-hair phenotype observed in *abcg36* mutants (Strader et al., 2010), suggesting that elevated IBA-derived IAA levels in the *abcg36* mutant cause the elongated root hair phenotype. In addition, mutants defective in IBA conversion enzymes display root hairs that can be rescued with exogenous auxin (Strader et al., 2010; Strader et al., 2011), consistent with the possibility that blocking IBA conversion can result in decreased auxin levels in root epidermal cells.

Lateral roots are post-embryonic organs originating from the primary root. The number and positioning of lateral roots is critical to establish the ideal root system for adaptation to local environments (reviewed in Rellán-Álvarez et al., 2016). Auxin drives both lateral root initiation and lateral root emergence (reviewed in Laskowski and Ten Tusscher, 2017). Mutants defective in IBA conversion enzymes display greatly decreased production of lateral roots (Strader et al., 2011). Further, treatment of seedlings with the compound naxillin results in increased lateral root production with limited effects on primary root elongation (De Rybel et al., 2012). Naxillin activity requires an intact IBA-to-IAA conversion pathway (De Rybel et al., 2012), consistent

with the possibility that naxillin promotes IBA conversion to active IAA. Furthermore, IBA-to-IAA conversion occurs in the lateral root cap and contributes to the priming of lateral root prebranch sites by setting up the amplitude and frequency of auxin oscillations through the root (De Rybel et al., 2012; Xuan et al., 2015). These oscillations are necessary to establish the lateral root prebranch sites (Xuan et al., 2015), pointing to an important role for IBA-derived auxin in driving lateral root development.

Adventitious roots are similar to lateral roots in many regards, but are defined by their origination from aerial tissues, such as stems or leaves. Adventitious root formation is often a part of adaptive responses to stress and shares both common and distinct regulatory mechanisms to lateral root formation (reviewed in Bellini et al., 2014). Zimmerman and Wilcoxin first reported that IBA could stimulate adventitious rooting in cuttings of several species in 1935 (reviewed in Preece, 2003). Throughout the 1930s, IBA arose as the compound of choice for horticulturalists to induce adventitious roots on stem cuttings for plant propagation and is the active ingredient in many modern rooting compounds, such as Rootone® or Hormodin®. In Arabidopsis, IBA promotion of adventitious rooting requires its conversion to IAA; the *ech2 ibr10* mutant, defective in IBA-to-IAA conversion enzymes, fails to produce adventitious roots in response to IBA (Veloccia et al., 2016). Indeed, cuttings from elm cultivars displaying higher levels of IBA-to-IAA conversion also display relatively high rates of adventitious rooting in response to rooting compounds (Kreiser et al., 2016), suggesting that IBA conversion may be critical for plant propagation in certain species.

3.3 IBA-derived auxin drives aspects of shoot development

In addition to its varied roles in root development, IBA-derived auxin plays distinct roles in shoot development, with particular roles in cotyledon expansion and apical hook formation.

Altering IBA homeostasis or IBA conversion to IAA has striking effects on cotyledon expansion. For example, mutants defective in the ABCG36 transporter displays larger cotyledons than wild type (Strader and Bartel, 2009), consistent with its role in IBA efflux and suggesting that auxin levels are elevated in the cotyledons of this mutant. Combining the *abcg36* mutation with mutations in IBA conversion enzymes suppresses this large cotyledon phenotype (Strader et al., 2010), suggesting that IBA-derived IAA, rather than IBA itself, drives the increased cotyledon expansion observed in the *abcg36* mutant. Further, a strong genetic block in IBA-to-IAA conversion results in dramatically reduced cotyledon expansion, concomitant with decreased cotyledon epidermal cell size (Strader et al., 2011). Likewise, overexpression of the IBA glycosylating enzyme UGT75D1 results in decreased cotyledon size (Zhang et al., 2016), consistent with decreased contributions to the auxin pool in these overexpression lines. IBA-derived auxin also appears to play a role in compensated cell enlargement (CCE), a phenomenon that allows for increased cell expansion to occur when cell numbers are limited to achieve a "normal" organ size in plants. Mutants defective in ECH2, an enzyme required for IBA-to-IAA conversion, are defective in CCE in cotyledons (Katano et al., 2016), suggesting that IBA-derived auxin is important for driving cotyledon cell expansion not only during normal development, but also under conditions where cell numbers are limiting.

Auxin is a critical driver of pavement cell lobing (reviewed in Pan et al., 2015). Auxin-driven intercalary growth results in lobes and indentations among neighboring cotyledon and leaf

epidermal cells. The *ech2 ibr1 ibr3 ibr10* mutant, defective in IBA-to-IAA conversion, displays a strong defect in pavement cell lobing, in addition to decreased cotyledon size (Strader et al., 2011), consistent with IBA-derived auxin contributing to the lobing process. Additionally, overexpressing the IBA glycosylating enzyme UGT75D1 results in small cotyledon pavement cells (Fakhry et al., 2016) that appear to display decreased lobing. Further research will be required to understand how IBA-to-IAA conversion is regulated to affect pavement cell lobing.

Contributions to the auxin pool by IBA in shoot tissues is not limited to the cotyledons. In addition, IBA-derived auxin affects apical hook formation and maintenance (Strader et al., 2011), shoot branching (Tognetti et al., 2010), and vegetative stress responses (Tognetti et al., 2010; Zhang et al., 2016). The strong effects of IBA-derived auxin on multiple aspects of plant growth and development suggest that IBA is an important contributor to the auxin pool.

Considering developmental roles of IBA in both aerial and root tissue over the plant lifecycle, a unifying theme is that IBA acting as an auxin reserve within the plant. Conversion of this auxin reserve pool is crucial for a variety of important developmental events, as enumerated above, but these processes may not represent the totality of IBA-dependent development. Though we understand the importance of IBA-to-IAA conversion in many facets of development, other questions about IBA's role are sure to further refine our understanding of this important auxin. These open questions in IBA biology are expanded upon in the next section.

3.4 Open Questions

Difficulties in detecting IBA. The auxin precursor IBA has been identified as an endogenous compound in numerous plant species, including various monocots and dicots (reviewed in Korasick et al., 2013). However, many labs have reported difficulty identifying

IBA, including a report that questioned its presence when it was undetected by GC mass spectrometry in samples from Arabidopsis, Populus, and wheat (Novák et al., 2012). Further, IBA concentrations are often reported to be at lower levels than IAA concentrations (Liu et al., 2012b; Ludwig-Müller et al., 1997; Ludwig-Müller et al., 1993; Sutter and Cohen, 1992) and detection of IBA in maize kernels varies by variety examined (Epstein et al., 1989; Ludwig-Müller et al., 1997; Ludwig-Müller et al., 1993). However, IBA has been detected in Arabidopsis by mass spectrometry (Liu et al., 2012b; Ludwig-Müller et al., 1993; Strader et al., 2010). Further, mutants defective in enzymes required for IBA-to-IAA conversion display developmental phenotypes consistent with an auxin deficiency and decreased levels of free IAA (Strader et al., 2011), consistent with endogenous IBA contributing to the auxin pool. These differences in detection of IBA in different labs and in different samples may reflect biological differences in IBA accumulation under different growth conditions.

Missing IBA transporters. IBA and IAA appear to use independent transport systems (reviewed in Michniewicz et al., 2014; Strader and Bartel, 2011). Thus far, only a two IBA carriers have been reported, ABCG36 (Strader and Bartel, 2009) and ABCG37 (Růžička et al., 2010; Strader et al., 2008). The *arm2* mutant in rice displays decreased IBA uptake and response and unaltered IAA uptake or response (Chhun et al., 2005), suggesting this mutant is defective in an IBA uptake carrier. Likewise, the *rib1* mutant in Arabidopsis displays IBA resistance and response and unaltered IAA uptake or response (Poupart et al., 2005; Poupart and Waddell, 2000), suggesting this mutant is also defective in an IBA uptake carrier. Because IBA uptake is a saturable process (Ludwig-Müller et al., 1995b; Rashotte et al., 2003), IBA uptake is likely a carrier-mediated process. Perhaps identification of the defective gene in *arm2* or *rib1* could provide insight into the molecular basis of IBA uptake. Identification of additional IBA carriers

will be instrumental in understanding regulation of IBA homeostasis and contributions to the auxin pool.

Regulation of IBA-derived IAA in the auxin pool. Because IBA-derived auxin plays critical roles in plant development, mechanisms likely exist to regulate IBA contributions to the auxin pool. Mechanisms to regulate these contributions could include regulated transport, formation and release from conjugates, and transcriptional control of IBA conversion enzymes. Evidence already suggests that regulation of IBA contributions to the auxin pool is important for stress responses. For example, overexpression of *UGT74E2* results in elevated IBA-glucose levels, increased tolerance to drought and salt stress, and increased shoot branching (Tognetti et al., 2010). Similarly, overexpression of *UGT75D1* results in increased tolerance to osmotic stress (Zhang et al., 2016). Additionally, eFP Browser-annotated (Schmid et al., 2005; Winter et al., 2007) expression of genes encoding the IBA conversion enzymes ECH2, IBR1, IBR3, and IBR10, although seemingly unaffected by treatment with various hormones (Fig. 16a), are upregulated by several biotic (Fig. 16b) and abiotic (Fig. 16c,d) stresses, consistent with the

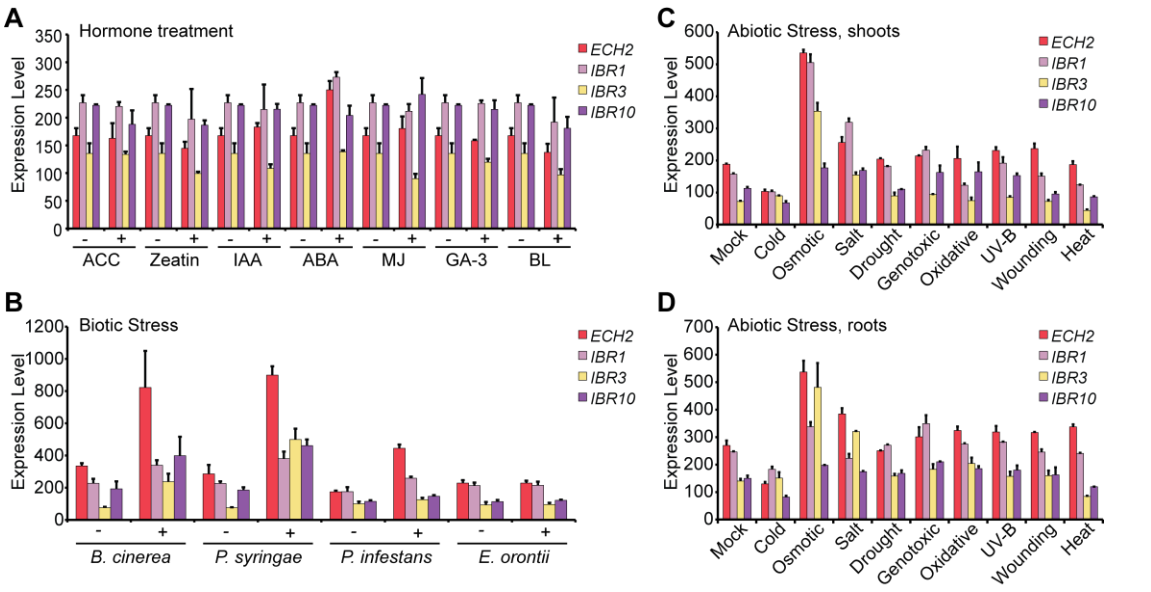

Figure 16: Expression of IBA conversion enzymes. **A**) Expression does not change under hormone treatment. **B)** Expression of IBA conversion enzymes increases under biotic stress and **C,D)** abiotic stress.

possibility that IBA-to-IAA conversion plays roles in stress response. Future research will be needed to elucidate those conditions in which IBA contributions to the auxin pool affect growth and stress responses, as well as the regulatory mechanisms that allow these contributions.

IBA activity outside of conversion to IAA. In the earliest studies of auxinic compounds in rooting and propagation assays, IBA was reported to be more effective than IAA (reviewed in Preece, 2003), causing speculation that IBA itself can act as a signaling molecule (reviewed in Ludwig-Müller, 2000). In addition, IBA is more effective than IAA at inducing crown roots in maize (Martínez-de la Cruz et al., 2015). The *lrt1* mutant in rice displays decreased lateral rooting and decreased gravitropism. Application of IAA rescues the lateral root phenotypes of *lrt1*, but not agravitropic growth, whereas IBA application rescues both the lateral root and gravitropism phenotypes (Chhun et al., 2003), consistent with the possibility that IBA plays some roles that IAA cannot. Additionally, some stress conditions caused increased accumulation of IBA, but no detectable increase in IAA (Ludwig-Müller et al., 1995c). Further, arbuscular

mycorrhizal fungi inoculation of maize roots results in elevated IBA, but not IAA levels (Ludwig-Müller et al., 1997). These conditions under which IBA levels are elevated, combined with the potency of IBA in rooting assays, provide some measure of support for roles in which IBA, rather than IBA-derived IAA, might act as a signaling molecule. However, genetic data in Arabidopsis suggest that IBA has no discernable activity outside of its conversion to IAA (Strader et al., 2010; Strader et al., 2011; Zolman et al., 2008; Zolman et al., 2007; Zolman et al., 2000). Potential explanations for the effectiveness of IBA in promoting rooting include the stability of IBA against degradation (Nordström et al., 1991) and effects of nitric oxide produced during the IBA-to-IAA conversion process (Schlicht et al., 2013), which contribute to lateral root formation. Although data in Arabidopsis are consistent with IBA activity caused by IBA-derived IAA, it remains a formal possibility that IBA could act as a signaling molecule.

IBA Synthesis. We do not currently know the molecular mechanism of IBA synthesis. IBA synthesis from IAA has been demonstrated in microsomal membrane preparations from maize (Ludwig-Müller et al., 1995a) or Arabidopsis (Ludwig-Müller, 2007) seedlings when provided with acetyl-CoA and ATP. Identifying the enzymes required for IBA synthesis will be an important step in understanding IBA biosynthesis. Further, generating mutants defective in IBA synthesis will allow for experiments to understand roles for IBA-derived auxin, and perhaps IBA itself, in plant development.

Chapter 4: IBA Resistance Screening in *Solanum lycopersicum*

Portions of this chapter were contributed by Dr. Hagai Yasuor and Dr. Kamal Tyagi from the Agricultural Research Organization in Gilat, Israel. All data from collaborators in marked as such in text and figures.

While the advent of cheap and easy sequencing technologies paired with powerful bioinformatics tools has recently increased the utility of reverse genetics, the importance of forward genetic approaches in elucidating signaling pathways cannot be overstated. Plant genetic screens have historically been mostly utilized in Arabidopsis due to its small stature, compact genome size, and availability of genetic manipulation tools. However, the ever-decreasing price of sequencing and the advent of cheap genome editing technologies makes forward genetics screens feasible in larger, more agriculturally-relevant species as well. In this chapter, I report the rationale, design, and results of a forward genetics screen for IBA resistance in *Solanum lycopersicum*.

4.1 IBA resistance screens in Arabidopsis

Levels of active auxin, IAA, are tightly regulated within plants through a variety of mechanisms including synthesis, degradation, and conjugation to amino acids (Korasick et al., 2013). Synthesis occurs through multiple pathways *in planta*. The best-understood biosynthetic pathways derive from tryptophan and use indole-3-acetonitrile, indole-3-pyruvic acid (IPA), indole-3-acetaldehyde, and indoleacetamide as direct precursors to IAA (Korasick et al., 2013). In Arabidopsis, the IPA-to-IAA pathway is a major contributor to the free auxin pool, evidenced by decreased IAA levels in mutants unable to convert IPA to IAA and defects in floral development, gravitropism, hypocotyl elongation, and other classic auxin responses (Stepanova

et al., 2008; Tao et al., 2008; Mashiguchi et al., 2011; Yamada et al., 2009). The clear auxin deficient phenotypes in mutants that cannot convert IPA to IAA demonstrates that plants cannot always compensate for the loss of one IAA synthesis pathways by increasing flux through another. A similar response, but with different auxin deficient phenotypes, is observed when the ability to convert IBA to IAA is lost.

IBA is converted to IAA in a process similar to fatty acid beta oxidation within the peroxisome (see Chapter 1). Some of the catalytic enzymes function exclusively in IBA-to-IAA conversion, while others act on both IBA and fatty acid beta oxidation. Currently, the only enzyme known to act on both fatty acids and IBA is PED1 (Hayashi et al., 1998). Because IBA-to-IAA conversion takes place in the peroxisome and shares some steps with lipid breakdown, loss of IBA responsiveness can be caused by disruption of multiple biological processes.

Forward genetics screens in Arabidopsis for resistance to IBA have led to the discovery of mutants in four distinct classes: peroxisomal mutants (Zolman, 2002; Zolman and Bartel, 2004; Zolman et al., 2008; Zolman et al., 2005; Zolman et al., 2000), IBA-to-IAA conversion mutants (Zolman et al., 2007; Strader et al., 2011; Zolman et al., 2008), general auxin-resistant mutants (Monroe-Augustus et al., 2003), and IBA transporter mutants (Strader et al., 2008). These mutants have, in turn, informed researchers about the importance of all these processes. For example, it is difficult to track labeled auxin radioisotopes *in planta*, because auxin is catabolized or metabolized into different forms and conjugates (see Chapter 3.1). Therefore, the *ech2* and *ibr10* mutants, which disrupt IBA-to-IAA conversion, were instrumental to our understanding that many seedling auxin responses require IBA-derived-IAA, including lateral root formation, cell expansion, root hair and hypocotyl elongation, and smaller root meristems (Strader et al., 2010). In tomato, loss-of-function mutants only exist for general auxin resistance

in the form of RNAi lines against some *ARF* and *AUX/IAA* signaling components (Bassa et al., 2012; de Jong et al., 2009; Hao et al., 2015; Wang et al., 2005), and genes involved in IAA transport (Al-Hammadi et al., 2003; Ivanchenko et al., 2015; Mounet et al., 2012). Point mutations only exists for the general auxin perception mutants *polycot*, *diageotropica*, and *entire* (Al-Hammadi et al., 2003; Ivanchenko et al., 2015; Zhang et al., 2007). Currently, there are no point mutations known to affect tomato peroxisomes, IBA-specific transporters, or IBA-to-IAA conversion, so a tomato IBA-resistance screen has potential to isolate many mutants in unexplored biological processes.

4.1.1 IBA resistance as peroxisomal function marker

One common marker of peroxisomal function is sensitivity to IBA. Because IBA is converted to IAA in the peroxisome(Strader et al., 2010), and because IBA does not appear to act as an independent signaling molecule outside of its contribution to the IAA pool in a cell (Zolman et al., 2000; Zolman et al., 2007; Zolman et al., 2008; Strader et al., 2010; Strader and Bartel, 2011), changes in IBA sensitivity in Arabidopsis can be caused by increased or decreased peroxisomal biogenesis and function. These mutant screens and subsequent *pex* mutant identification are described in detail in Chapter 1.1.3.

4.1.2 IBA roles in stress responses

Beyond the clear developmental importance of IBA-derived-IAA, demonstrated by severe developmental problems in Arabidopsis seedlings that cannot convert IBA into IAA (Strader et al., 2010), numerous pieces of evidence suggest a central role for IBA-derived-IAA in plant stress responses as well. Overexpression of an IBA-glucose conjugating enzyme in Arabidopsis leads to increase salt tolerance, shoot branching, and drought tolerance (Tognetti et

al., 2010). Maize increases expression of IBA synthetase in response to drought and abscisic acid (ABA) treatment (Ludwig-Müller et al., 1995c), and maize seedlings that increase IBA levels in response to NaCl stress survived that stress better than seedlings with no IBA change (Zörb et al., 2013). However, the conditions in which IBA contributions to the auxin pool affect growth and stress responses, as well as the regulatory mechanisms that allow conversion of IBA into IAA are not yet understood. It also remains an open question whether IBA is capable of acting as a separate signaling molecule outside of conversion into IAA, although genetic data from Arabidopsis does not suggest another signaling mechanism for IBA (Strader and Bartel, 2011; Strader et al., 2010; Zolman et al., 2008; Zolman et al., 2007; Zolman et al., 2000). In both cases, the ability to study stress responses and auxin content in mutants that can no longer process IBA into IAA, or transport IBA through the plant, will greatly inform our understanding of the role of IBA in non-Arabidopsis species. For example, IBA-derived IAA is well-established in Arabidopsis as necessary for lateral root formation (Strader et al., 2011; De Rybel et al., 2012). Lateral root number, angle, and density are the major determinants of adult plants' ability to explore the soil and uptake nutrients, and change in response to drought, macronutrient depletion, and micronutrient depletion (Lynch, 2011). Plants may utilize IBA-to-IAA conversion under water or nutrient stress to stimulate lateral root development and enhance soil exploration.

4.2 IBA screen results

Based on the known importance of IBA in auxin homeostasis to Arabidopsis, its utility as an easy marker of peroxisomal function, evidence of IBA involvement in stress responses, and the paucity of IBA-specific mutants in *S. lycopersicum*, I undertook a forward genetics screen for IBA resistant mutants, hoping to find mutants in some or all of the classes listed in Chapter 4.1.

M_2 generation seeds from EMS-mutagenized *S. lycopersicum* cultivar M82 were screened for long primary roots on media supplemented with 600 µM IBA, then recovered on unsupplemented media prior to transplantation to soil, at which point they were named and numbered as *IBA-resistant1-19*. Of 19 isolated mutants, 8 survived to the flowering stage. Progeny of half of the surviving plants did not retest as IBA resistant, progeny from 3 retested as IBA resistant, and one individual, IR3, made all parthenocarpic fruit, a common auxin resistant phenotype in tomato (de Jong et al., 2009), and thus progeny could not be retested in the M_3 generation (Table 2).

	Auxin responsiveness compared to wild type M82							
Mutant	**IBA**	**IAA**	**NAA**	**2,4-DB**	**2,4-D**	**TIBA**	**Picloram**	**NPA**
IR3	Resistant	Resistant	No difference			Resistant	Resistant	No difference
IR5	Resistant	Sensitive	No difference		No difference			No difference
IR12	Resistant	No difference	No difference	Resistant	No difference	Sensitive	Sensitive	No difference
IR17	Resistant	No difference	No difference			Resistant	Sensitive	Resistant

Table 2: Summary of IR Mutant Hormone Responsiveness. "Resistant" indicates significantly longer roots than wild type when grown on the indicated hormone, "no difference" indicates statistically indistinguishable root elongation compared to wild type, and "sensitive" indicates significantly shorter roots than wild type. Fields left blank indicate that IR mutant/hormone combination has not yet been tested.

4.2.1 IR3 is a dominant, gain of function mutant

Although IR3 was parthenocarpic as an M_2 plant, its pollen was viable and IR3 was used as male in a backcross to wild type M82. IR3 was also used as the female parent in crosses with wild type pollen multiple times, but was unable to successfully fertilize and form seeds from these crosses. F_1 plants resultant from these crosses were allowed to self fertilize and made normal-sized fruit with viable seeds. These F_2 seeds were retested for IBA resistance and display strong resistance to IBA in about 75% of tested F_2 seedlings, a segregation ratio consistent with a

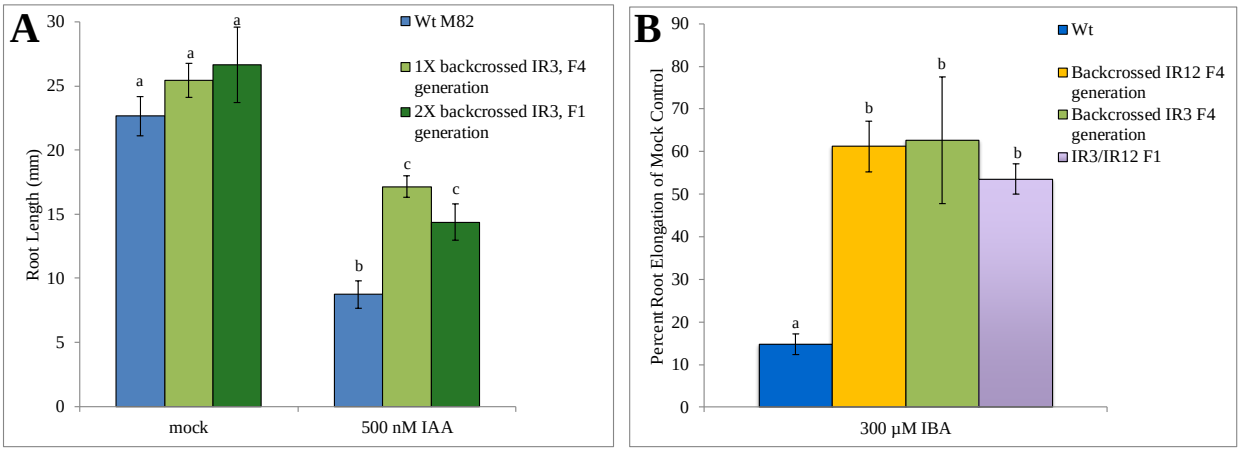

Figure 17: IR3 is a dominant mutant resistant to both active auxin and auxin precursors. **A)** Backcrossed IR3 F1 seeds look identical to IR3 lines homozygous for the lesion(s) causative of IBA resistance. All IR3 lines retain some sensitivity to auxin. **B)** Crosses between IR3 and recessive IR mutations, such as IR12 shown here, display identical auxin resistance as the IR3 parental line.

dominant mutation in IR3 causing resistance to IBA. To confirm this inheritance pattern, F_1 seeds for crosses between IR3 and wild type, as well as IR3 and other IR mutants were measured on both IBA and IAA. In all cases, F_1 generations of crosses with the IR3 mutant display auxin resistance, confirming that IR3 is a dominant mutant resistant to both active auxin and auxin precursors (Fig. 17).

In Arabidopsis, mutations in domain II of AUX/IAA proteins increase protein stability (Liscum and Reed, 2002) because they cannot be marked for degradation, and never release transcriptional activators of auxin signaling, the ARF proteins. Inability to mark the AUX/IAA

proteins for degradation therefore results in a dominant auxin resistance phenotype. (Fukaki et al., 2002; Tiwari et al., 2001). Additionally, other tomato *aux/iaa* mutants display parthenocarpy (Wang et al., 2005), consistent with the original M_2 phenotypes observed in IR3. Based on a similarity in segregation pattern, auxin resistance, and phenotypes between IR3 and known *aux/iaa* mutants in tomato and Arabidopsis, the instability region of domain II in all twenty-five annotated tomato *AUX/IAA* genes were sequenced from IR3. None of these contained any unique SNPs consistent with EMS mutagenesis (data not shown).

Although the causative mutation in IR3 is not yet known, these preliminary results suggest that an IBA resistance screening strategy in tomato is an effective way to isolate general auxin-resistant mutants, not only those affected in IBA-specific pathways. Other IR mutants demonstrate the efficacy of this screening approach in isolating IBA-resistant mutants in the other expected classes as well.

4.2.2 IR17 is an IBA-resistant mutant with transporter mutant-like phenotypes

The strongest resistance to IBA is exhibited by IR17. The M_2 plant was isolated as a long-root individual when grown on 600 µM IBA, then transferred to soil and backcrossed to wild type. IR17 contains a recessive mutation that confers resistance specifically to long-chain auxins, and is not resistant to short chain active auxins (Fig. 18A, B). In addition to these seedling phenotypes, IR17 displays earlier flower time (not pictured) and larger fruit size

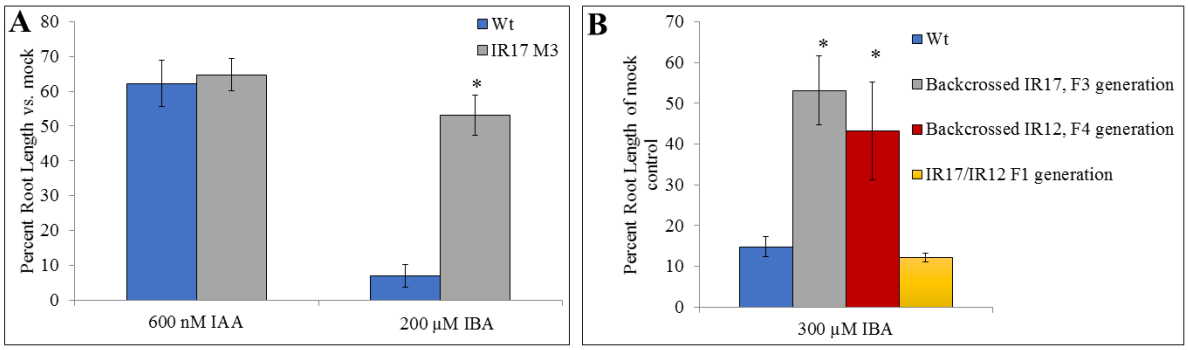

C

	M82 lab	M82 US	IR-5	IR-12	IR-17	x1510 F3- A3	x1510 F3- A4
Fruit weight (Mean ±SE)	12.56 (1.62)	17.24 (3.04)	17.24 (3.61)	21.27 (2.72)	28.97 (4.62)	14.037 (1.92)	13.98 (3.41)

Figure 18: IR17 is an IBA-resistant, recessive mutant. **A)** IR17 is strongly resistant to IBA, and sensitive to IAA. **B)** Backcrossed IR17 was crossed with IR12 for complementation testing. The F1 seedlings are indistinguishable from wild type in their auxin sensitivity, indicating that IR17 and IR12 are both recessive mutations. **C)** Fruit weight of biggest fruit from each plant of M82 and different mutants. 8 different fruit were picked from 8 different plants of M82 and IR mutants. M82 lab indicates the Israeli lab strain of M82, while M82 US is the line from which mutagenized populations were derived. Data in **C** were provided by Dr. Kamal Tyagi from the Yasuor Lab. **D)** Flowering time of 10 individuals of wt and 12 IR17 individuals age-matched and grown in a greenhouse with average daily temperatures of 26-29°C.

compared to wild type when grown under outdoor, desert conditions (Fig. 18C). This early flowering time was not observed in greenhouse conditions (Fig 18D).

As discussed in Chapter 3.4, IBA appears to be transported by a different set of transporters than those that carry IAA. In Arabidopsis, only two IBA transporters are currently

known, ABCG36 and ABCG37 (Strader and Bartel, 2009; Růžička et al., 2010). I examined the response of IR17 to artificial auxins which can facilitate the interaction between TIR1 and AUX/IAA proteins, including 1-naphthaleneacetic acid (NAA) (Kepinski and Leyser, 2005) and picloram (Calderón-Villalobos et al., 2012). IR17 is sensitive to both NAA and picloram (Fig. 19A,C), as expected, because IR17 is also sensitive to the active auxin IAA (Fig. 18A). However, when grown on the artificial auxins 2,3,5-triiodobenzoic acid (TIBA) and N-1-naphthylphthalamic acid (NPA), IR17 displays resistance (Fig. 19B,C,D). TIBA and NPA are both auxin transport inhibitors (Thomson et al., 1973); (Cande and Ray, 1976); (Delbarre et al., 1996), and loss-of-function mutants in the IBA transport mutant *pdr9* is hypersensitive to the effects of TIBA and NPA (Strader et al., 2008). Because of the hormone resistance and fruit

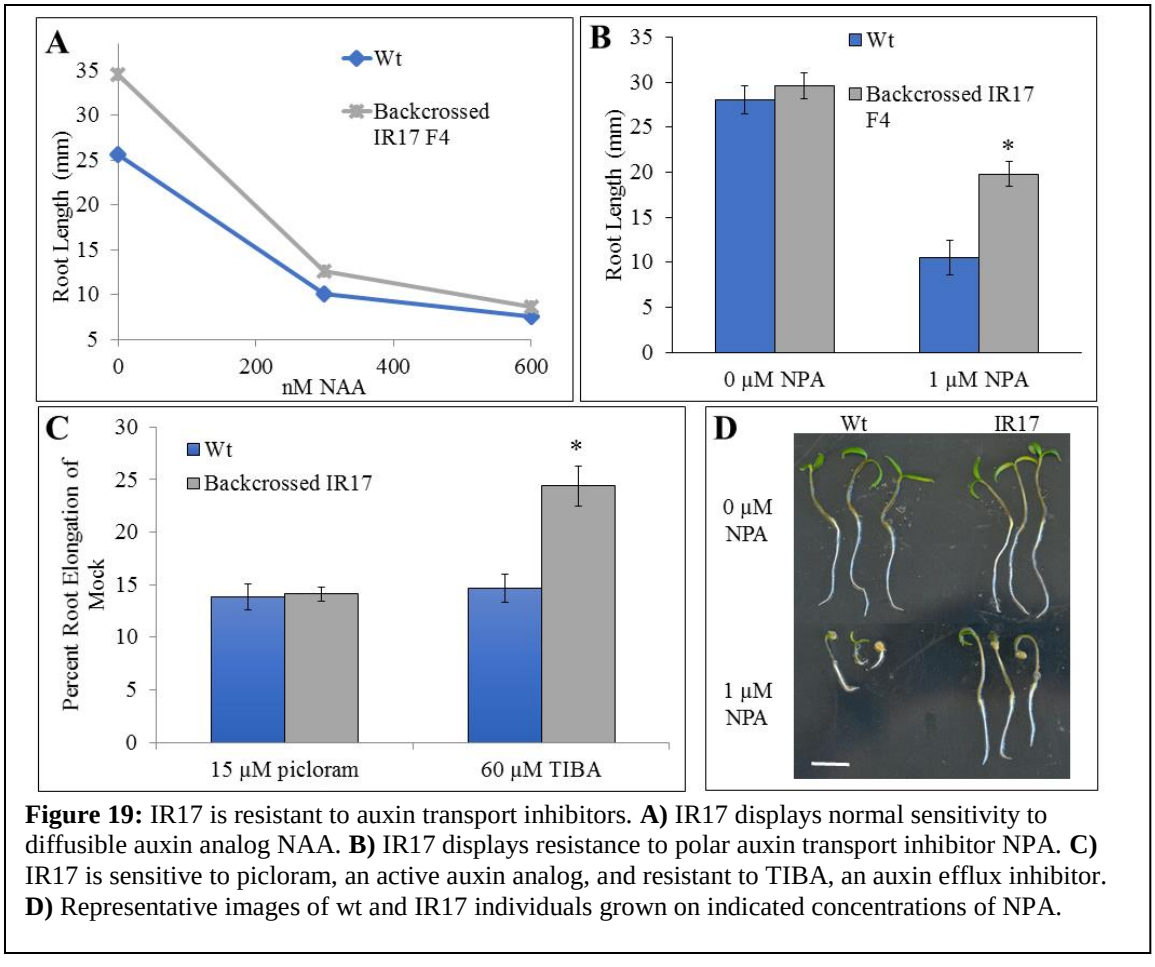

Figure 19: IR17 is resistant to auxin transport inhibitors. **A)** IR17 displays normal sensitivity to diffusible auxin analog NAA. **B)** IR17 displays resistance to polar auxin transport inhibitor NPA. **C)** IR17 is sensitive to picloram, an active auxin analog, and resistant to TIBA, an auxin efflux inhibitor. **D)** Representative images of wt and IR17 individuals grown on indicated concentrations of NPA.

phenotypes of IR17, this line was selected for a whole genome sequencing approach to determine causative mutations.

IR17 was backcrossed to wild type M82 as an M_2 plant, then F_1 plants were allowed to self fertilize. F_2 seedlings were screened on 300 µM IBA, of which approximately 25% show resistance, consistent with a recessive mutation. Eleven IBA-resistant F_2 seedlings were allowed to recover on unsupplemented media, transplanted to soil, and allowed to self-fertilize. F_3 progeny was screened for IBA resistance, and eight lines selected as germplasm for whole genome sequencing. Sequencing shows that IR17 has more than 850 genes with one or more SNPs indicative of EMS mutagenesis (Fig. 20). Because of the large number of mutations, a sequencing-assisted mapping approach was next employed to narrow down the list of candidate

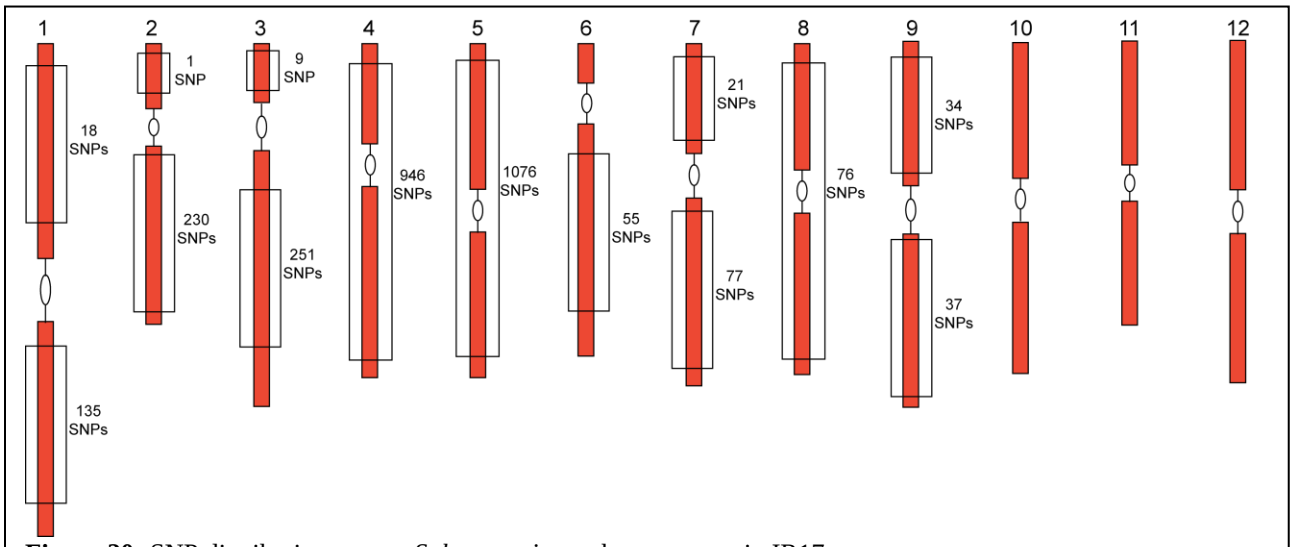

Figure 20: SNP distribution among *S. lycopersicum* chromosomes in IR17.

mutations (Table 3). Mapping showed that the IBA resistance locus was not linked to chromosomes 1, 8, or 9, nor the upper arms of chromosomes 4 or 7.

Genes with IR17 Unique SNPs	Gene Description	Sanger Sequencing Results
Solyc05g009440	Heavy metal transport/detoxification protein	
Solyc05g009500	Peptide transporter	silent mutation
Solyc05g009920	Anion-transporting ATPase	

Solyc05g018510	ABC transporter G family member 32	silent mutation
Solyc05g023970	Transport membrane protein	
Solyc05g050350	Cyclic nucleotide gated channel	
Solyc05g050380	Cyclic nucleotide-gated ion channel 1	
Solyc05g051920	Major facilitator superfamily transporter	silent mutation
Solyc05g052830	Proline transporter 2	

Table 3: Mutations in IR17 in genes with GO terms containing “transporter”.

Preliminary results from the IR17 mutant suggest that an IBA resistance screening strategy in tomato is an effective way to isolate mutants in IBA transport, and that mutations in IBA transport affect adult tomato plant auxin-related phenotypes. In addition to the strong IBA resistance resulting from both the likely transport mutation in IR17 and the general auxin resistance conferred by the lesion(s) in IR3, other mutants with weaker auxin resistance phenotypes were also isolated from this screen.

4.2.3 Other IR mutants

Two other mutants, IR5 and IR12, were also isolated in the IBA resistance screen. Both mutants are IBA-specific and display at least wild type sensitivity to active auxins (Fig. 21) and

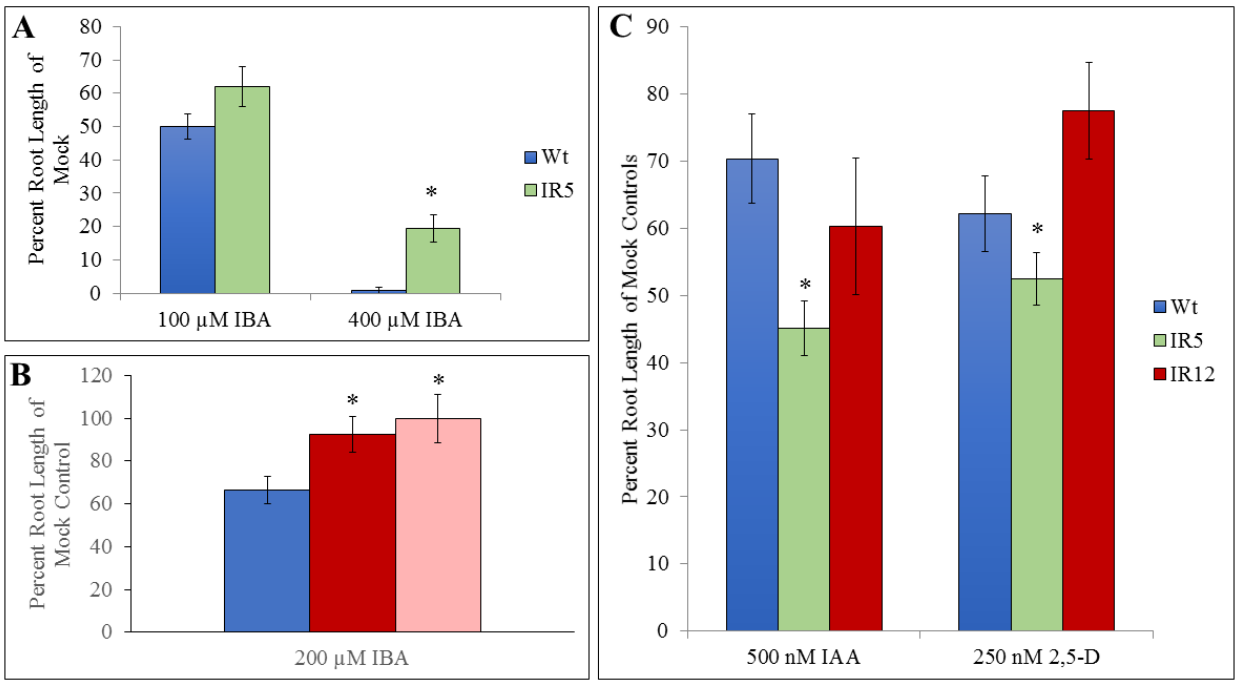

Figure 21: IR5 and IR12 are resistant to long-chain auxins. **A)** IR5 ^{M3} seeds were retested for IBA resistance. IR5 is significantly more resistant to IBA than wild type ($p<0.05$) in a root elongation assay **B)** IR12 M5 and backcrossed IR12 seeds were retested on IBA. Both the original IR12 and backcrossed lines had significantly longer roots than wild type ($p<0.05$). **C)** Neither IR5 nor IR12 display resistance to natural or artificial short chain active auxins. Both mutants were tested in the ^{M3} generation in a root elongation assay. IR5 roots grew significantly shorter than wild type, and IR12 did not display a statistically significant difference compared to wild type ($p<0.05$)

to auxin transport inhibitor NPA (Fig. 22A). IR12 is sensitive to the artificial active auxins NAA and picloram and to auxin transport inhibitor TIBA (Fig. 22B,C). Because IBA resistance in both of these mutants was lower than resistance displayed by IR17 and IR3, and because neither IR5 nor IR12 displayed noticeable adult plant phenotypes as M_2 plants, these mutants were not prepared for whole genome sequencing.

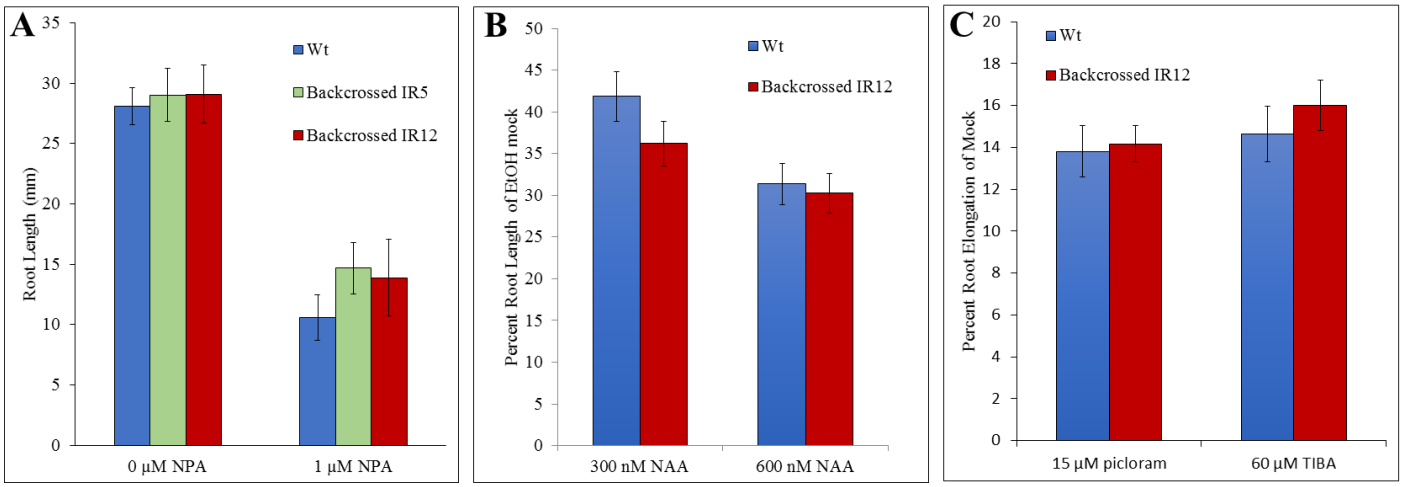

Figure 22: IR5 and IR12 display wild type sensitivity to all tested artificial auxins and auxin transport disruptors. **A)** Neither IR5 nor IR12 display significant differences compared to wild type when grown on auxin transport inhibitor NPA. **B)** IR12 does not display significant differences ($p<0.05$) compared to wild type on diffusible artificial auxin NAA **C)** IR12 does not display significant differences ($p<0.05$) compared to wild type on artificial active auxin picloram or auxin transport inhibitor TIBA.

Both were sent to collaborators in Yasuor lab, who reported no additional flowering or fruit phenotypes for IR12 (personal communication, Dr. Hagai Yasuor and Dr. Kamal Tyagi). However, they did find a striking fertility loss in IR5, with less than 2-5 seeds per fruit (Fig. 23A). Wild type typically contains 20-40 seeds per fruit. Loss of fertilization is likely a result of decreased pollen viability, with both IR5 and a backcrossed IR5 line showing a significant decrease in pollen viability (Fig. 23B,C).

Interestingly, this low fertility phenotype was not observed in St. Louis-grown plants. One explanation could be the temperature difference in growing conditions, as the St. Louis plants were grown in a temperature-controlled greenhouse with average daily temperatures of 26-29°, while the plants in Israel were grown in net houses with daytime temperatures between 30 and 40°C (Hagai Yasuor, personal communication).

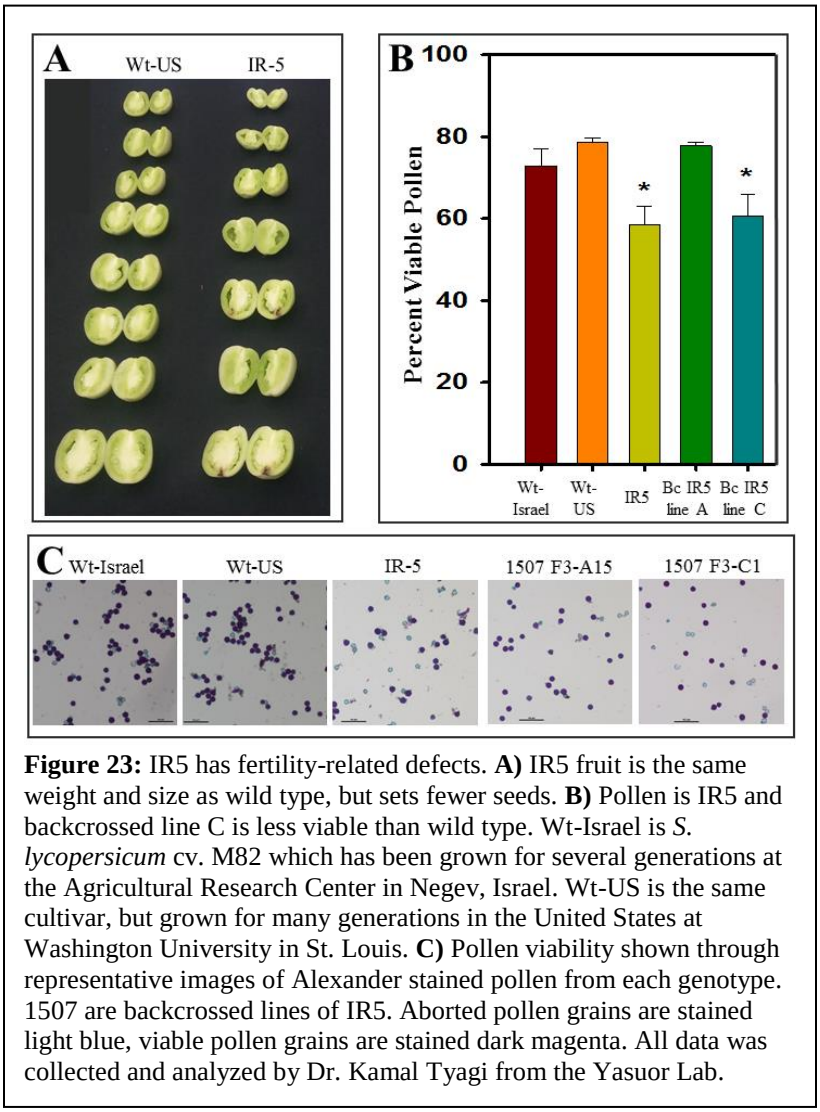

Figure 23: IR5 has fertility-related defects. **A)** IR5 fruit is the same weight and size as wild type, but sets fewer seeds. **B)** Pollen is IR5 and backcrossed line C is less viable than wild type. Wt-Israel is *S. lycopersicum* cv. M82 which has been grown for several generations at the Agricultural Research Center in Negev, Israel. Wt-US is the same cultivar, but grown for many generations in the United States at Washington University in St. Louis. **C)** Pollen viability shown through representative images of Alexander stained pollen from each genotype. 1507 are backcrossed lines of IR5. Aborted pollen grains are stained light blue, viable pollen grains are stained dark magenta. All data was collected and analyzed by Dr. Kamal Tyagi from the Yasuor Lab.

4.3 Discussion and Future Directions

Lack of stable, loss-of-function point mutations in non-model species has limited the study of auxin responses in agriculturally relevant species. Here, I present initial characterizations of four auxin-resistant mutants. These characterizations are consistent with

lesions in IR3 causing general auxin resistance, lesions in IR17 affecting an IBA transporter, and lesions in IR5 and IR12 causing resistance only to long-chain auxin precursors. However, much remains to be learned about these plants. Collaborators in the Iyer-Pascuzzi lab at Purdue University are currently investigating how auxin signaling affects the success of the tomato pathogen *Ralstonia solanacearum*, and are using these IR mutants to learn how loss of auxin responsiveness affects pathogen success in its native host. Work in the Yasuor lab continues on IR3, IR5, and IR17 to understand how auxin resistance affects floral morphology, pollen viability, and fruit production. Determining the basis of IBA resistance in IR17 will be particularly interesting, as yield is increased without sacrificing growing time or hardiness. In addition, these mutants could be used to provide additional insight into how hormones influence symbiotic relationships as well as pathogenic ones. Arabidopsis is one of the few land plants that does not associate with arbuscular mycorrhizal fungi (AMF) (Cameron et al., 2013), so there have been limited genetic resources available to study how perturbations in auxin and auxin precursors levels affects AMF associations. Interestingly, the Arabidopsis IBA effluxers *ABCG36* and *ABCG37* localize to the outer membrane of root tips, suggesting that IBA is effluxed into the soil (Strader et al., 2008); (Strader and Bartel, 2009). AMF associations with tomato roots decreases with increasing auxin resistance, and increases with increasing auxin sensitivity (Hanlon and Coenen, 2011),(Etemadi et al., 2014). Future work on determining whether auxin resistance in IR17 is due to a mutation in an IBA transporter, as its resistance to transport inhibitors suggests, and the localization of that transporter could provide valuable insight into IBA flux in tomato roots and their nearby soil environment.

Work is also ongoing looking at auxin-responsive transcription in each of these auxin-resistant mutants. All have been crossed to a DR5:Venus transcriptional reporter (Ben-Gera et

al., 2012) and will be examined in the presence and absence of auxin to determine the auxin-responsive transcriptional activation in these mutants. It will be particularly interesting to see whether auxin responsiveness during flower and early fruit development is altered in IR17, as auxin is well known to affect fruit development (de Jong et al., 2009; (Wang et al., 2005), although other auxin-resistant mutants have diminished seed and fruit set and IR17 has increased yield.

Together, these new IR mutants provide a valuable resource to understand how perturbations at different points within auxin homeostasis affect development, and particularly fruit development. Additionally, the method shows that seedling-stage auxin resistance screens can isolate mutants with fruiting defects. The ability to screen at two weeks instead of two months could accelerate the discovery and characterization of auxin-related fruiting mutants.

4.4 Materials and Methods

4.4.1 Generating mutant screening populations in *S. lycopersicum*

Approximately 1200 *S. lycopersicum* cv. M82 seeds were mutagenized with 0.5% ethylmethylsulfonate (EMS) for 12 hours, then neutralized with an equal volume of 1M NaOH. After 3 washes in sterile water, mutagenized seeds were pipetted onto moistened paper towels in Phytatrays (Sigma) and allowed to grow for about two weeks. Approximately 1000 seedlings were then transplanted into MetroMix soil and placed in a greenhouse with an 16 hours light/8 hours dark cycle in early May of 2015. Seedlings were allowed to grow for about one month, then hardened off by a combination of top watering and increasing outdoor exposure for until late June of 2015. After hardening off, seedlings were transplanted to field space owned and maintained by the University of Missouri-Columbia in Columbia, MO. Approximately 800

seedlings were transplanted in late June of 2015, divided into 5 rows, which were designated as separate pools. Seeds were harvested twice: once in early August, and again in mid September of 2015. Seeds from all plants bearing fruit were collected. Not all plants bore fruit. Seeds from the M1 fruits were harvested between August and December of 2015.

4.4.2 Screening mutagenized *S. lycopersicum* for IBA resistance

M_2 seeds were surface-sterilized with 20% bleach (Last and Fink, 1988)and plated on PN (Haughn and Somerville, 1986) supplemented with 600 µM IBA (Sigma) in DMSO (Sigma). Seedlings were placed under yellow-filtered light in a Percival incubator (22°C, 16 hours light and 8 hours dark) for 1-2 weeks, then visually inspected for long-root individuals. Long root individuals were then sterile-transferred to PN plates with no added hormones and allowed to recover for 2-7 days before transplanting into MetroMix soil. Seedlings were initially grown in 9x9cm pots and moved to 5 gallon pots when they outgrew the 9x9cm pots. All named mutants which survived to flowering and fruit set stage were crossed with wild type M82. All mutants that made viable seed were retested on 600 µM IBA and an equal amount of DMSO to confirm IBA resistance.

4.4.3 Auxin Assays

M_2 seeds were surface-sterilized with 20% bleach (Last and Fink, 1988) and plated on PN (Haughn and Somerville, 1986) supplemented with indicated hormone concentrations (Sigma) in DMSO (Sigma). Seedlings were placed under yellow-filtered light in a Percival incubator (22°C, 16 hours light and 8 hours dark) for 12-14 days, then root length was measured.

Chapter 5: *Double Root* is a Recessive, Low-penetrance Meristem Mutant in *Solanum lycopersicum*

Plants retain enormous developmental plasticity throughout their life cycle, critical to their ability to constantly adapt to environmental alterations which they cannot escape. Plants continuously generate new aerial tissue from two different meristems: the shoot apical meristem, and floral meristems (reviewed in Basile et al. 2017). Together, these meristems generate all visible plant organs past the embryonic cotyledon or cotyledons (reviewed in Basile et al. 2017). The process of meristem formation and maintenance is well-known to be dependent on the proper balance between the hormones auxin and cytokinin, and alterations in either endogenous or exogenous levels of these hormones can lead to altered meristematic activity and striking defects in plant growth patterning, such as altered organ number, spacing, or size (reviewed in Tognetti et al, 2017). Based on some of these phenotypes characteristic of disrupted meristem function, several mutants that appeared to be meristem mutants in *S. lycopersicum* were isolated during the IBA resistance screen described above. The following chapter describes their isolation and characterization.

5.1 *Double Root* phenotypes

During selection of long root individual in IBA screening, three seedlings were found that made two primary roots instead of the typical single root (Fig. 24A). All three were from the same pool of mutagenized seeds. These seedlings were named *Double root1-3* and transplanted to soil. Of the three, DR1 and DR3 made flowers, fruit, and seeds. DR2 produced a single true leaf, but not other adult organs, and died in soil (Fig. 24B).

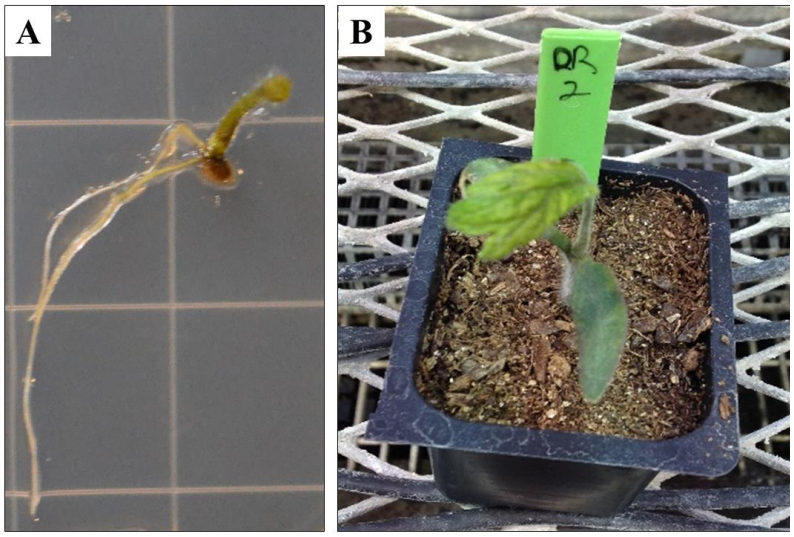

Figure 24: DR Mutant Isolation. **A)** Representative images of tomato mutant displaying the double root phenotype. Plant is DR3 ^{M3} generation, and had grown on PN plate for 2 weeks at time of photographing. **B)** DR2 M_2 final development stage. Plant was over two months old at time of photographing.

5.1.1 DR1 and DR3 are low penetrance mutations

M_3 seeds harvested from DR1 and DR3 were plated on plant nutrient plates to observe whether the double root phenotype was inheritable. At first, all M_3 seedlings appeared to be wild

type. However, upon closer examination of individuals, I found that a small percentage recapitulate the double root phenotype, as well as displaying numerous other defects never observed in wild type at low frequency (Fig. 24A, 25). Both plants displaying these aberrant phenotypes and individuals phenotypically indistinguishable from wild type seedlings were moved to soil, and the M_4 progeny was counted to determine the penetrance of this mutation. All M_4 progeny except those from DR3 F displayed some mutations at low rates ranging from <1% to 6.3% (Table 4).

Figure 25: DR M_3 henotypes. M_3 individuals display a variety of defects including the original double root phenotype, at a low frequency. Above, sibling seedlings of DR3, grown on the same plate for ~2 weeks. The far left seedling displays a headless phenotype in which the seedling makes no cotyledons, middle plant displays the original parental mutation of double root, and the far right seedling is representative of the majority of DR1 and DR3 seedlings and displays no obvious phenotypic differences compared to wild type .

Genotype and Generation	Phenotype	Number of Individuals	Percent of Individuals	Percent of Mutant Seedlings	Parent Plant Phenotype
M82, no gen	normal	148	96.10	0	normal
	lobed	6	3.90		
	Total seedlings	154			
DR1 A M_4	normal	368	97.61	1.59	
	very small and pale green	6	1.59		
	lobed	3	0.80		
	Total seedlings	377			
DR1 B M_4	normal	277	93.90	4.75	
	lobed	4	1.36		
	root off of a cotyledon	1	0.34		
	small and pale green	8	2.71		
	headless	5	1.69		
	Total seedlings	295			
DR3 A M_4	normal	576	97.46	0.04	normal
	lobed	14	2.37		
	double root	1	0.04		
	Total seedlings	591			
DR3 B M_4	normal	101	94.39	0.93	normal
	lobed	5	4.67		
	small and pale green	1	0.93		
	Total seedlings	107			
DR3 C M_4	normal	129	90.85	6.34	normal
	lobed	4	2.82		
	tricot	1	0.70		
	double root	1	0.70		
	headless	6	4.23		
	monocot	1	0.70		
	Total seedlings	142			
DR3 D M_4	normal	134	89.93	4.70	normal
	lobed	8	5.37		
	tricot	3	2.01		
	single cotlydeon	1	0.67		
	Unequal sized cotyledons	1	0.67		
	small and pale green	1	0.67		
	headless	1	0.67		
	Total seedlings	149			

DR3 E M_4	normal	117	92.86	3.17	normal
	lobed	5	3.97		
	tricot	1	0.79		
	four cotyledons	1	0.79		
	rootless	2	1.59		
	Total seedlings	4			
DR3 F M_4	normal	233		0.00	normal
	Total seedlings	233			
DR3 G M_4	normal	198	88.79	3.15	
	lobed	18	8.07		
	small and pale green	3	1.35		
	root off cotyledon	1	0.45		
	monocot	1	0.45		
	headless	2	0.90		
	Total seedlings	223			
DR 3 H M_4	normal	292	92.41	2.53	tricot
	lobed	16	5.06		
	small and pale green	5	1.58		
	short root and small cotyledons	1	0.32		
	headless	2	0.63		
	Total seedlings	316			
DR3 J M_4	normal	136	97.84	0.72	2 shoots and a root from a cotyledon
	lobed	2	1.44		
	tricot	1	0.72		
	Total seedlings	139			
DR3 K M_4	normal	411	94.92	1.16	tricot
	lobed	17	3.93		
	headless	1	0.23		
	tricot	1	0.23		
	small and pale green	1	0.23		
	root growing off cotyledon	1	0.23		
	monocot	1	0.23		
	Total seedlings	433			
DR3 M M_4	normal	203	97.13		normal
	lobed	3	1.44	1.44	
	headless	2	0.96		

	small and pale green	1	0.48		
	Total seedlings	209			

Table 4: Mutant frequency in DR1 and DR3 M4 lines.

5.1.2 Inheritance and Complementation Groups

Because DR1 and DR3 are low penetrance mutations, many separate backcrosses to wild type M82 were performed in order to examine inheritance. Of thirty-eight F_1 individuals, none displayed any aberrant phenotypes, suggesting the lesion causing DR1 and DR3 is recessive. The recessive nature of the lesion(s) in DR1 and DR3 makes complementation testing by crossing possible.

Because DR1 and DR3 were isolated from the same mutant pool and displayed the same phenotype, I expected they were siblings and contained the same lesion. If DR1 and DR3 were siblings, plants would be expected to display aberrant phenotypes at similar ratios to DR1 and

DR1/DR3 F1 Phenotypes		
Phenotype	Number of seedlings	Percent of seedlings
normal	83	89.25%
lobed	7	7.53%
root off cotyledon	1	1.08%
rootless	1	1.08%
tricot	1	1.08%
total:	**93**	

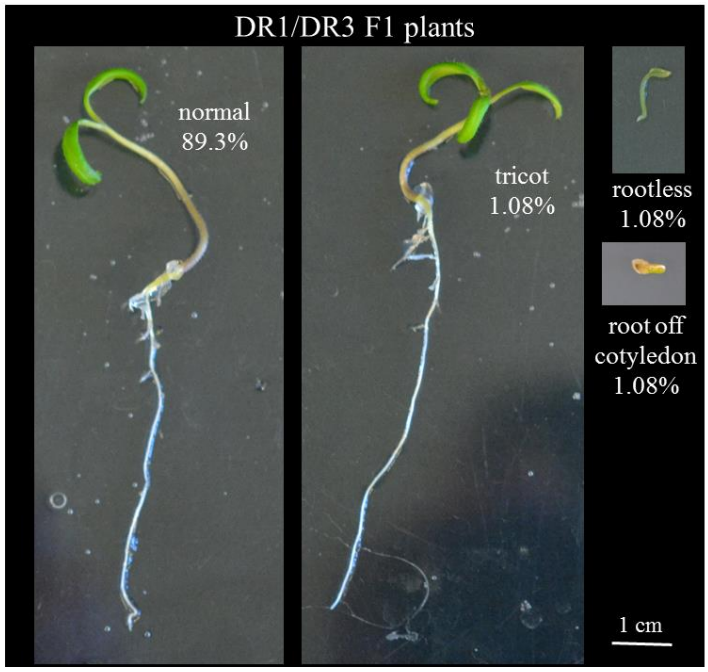

Figure 26: DR1/DR3 complementation testing. F_1 individual of DR1/DR3 cross displays aberrant phenotype consistent with parental mutations. Table on the left shows the prevalence of mutant phenotypes, which are pictured on the right. All pictured plants were 2 weeks old.

DR3 parental lines in the F_1 generation, as they would be homozygous at the mutant allele. If DR1 and DR3 contain lesions in two different genes, the F_1 plants would not show any aberrant phenotypes, because they would be heterozygous at both loci. To determine whether DR1 and DR3 contained the same lesion causing the double root phenotype, multiple DR1 and DR3 crosses were undertaken, and the phenotypes of all the F_1 progeny tallied (Fig. 26). Because F_1 individuals display a clearly aberrant morphology never observed in wild type seedlings, DR1 and DR3 likely contain the same causative lesion (Fig. 26).

The low penetrance of the mutant phenotypes in DR1 and DR3 complicates interpretation of results in determining both inheritance and complementation. Ideally, around 200 F_1 seedlings of both backcrossed DR1 and DR3 would need to be examined and display no aberrant phenotypes for certainty about the inheritance of both lesions. However, the data are consistent with recessive inheritance, and the isolation of these mutants is likewise consistent with sibling plants which contain the same lesion.

5.2 Whole Genome Sequencing of DR1

Both DR1 and DR3 were backcrossed to wild type M82 plants as M_2 individuals. Because the mutant phenotype was low penetrance and recessive, seven F_1 individuals from backcrossed DR1 and six F_1 individuals from backcrossed DR3 were transplanted to soil. All appeared wild type. Because mutant phenotypes were low penetrance, I expected around 5% of one-quarter of the F_2 progeny to display any mutant phenotype, so I screened for mutants in the F_3 generation. To screen for the DR1/3 mutation, more than one hundred F_3 seeds of each line were plated on PN and allowed to grow for two to three weeks, at which time any mutant phenotypes were clearly observable. Because DR1 and DR3 mutants and backcrossed F_3 lines

displayed many variations in mutant phenotypes, only plants displaying the original M_2 phenotype, double primary root, were selected as germplasm for whole genome sequencing. Based on the results in 5.1.1 showing that DR1 and DR3 were in the same complementation group, and the happenstance that DR1 backcrossed F3 lines had a larger percentage of double root individuals than F_3 lines deriving from DR3, whole genome sequencing was performed on DR1 germplasm only. Genomic DNA was prepared from all double root F3 adult plants and sent for whole genome sequencing through the Genome Technology Access Center (GTAC) at Washington University in St. Louis. GTAC returned data on all exonic mutations.

5.2.1 Whole genome sequencing results

Whole genome sequencing determined that eight mutations in exonic regions indicative of EMS mutagenesis were present in DR1 and absent in wild type (Table 4).

Mutated Gene	GO Annotation	Described Function
Solyc01g008471	Histone-lysine N-methyltransferase SUVR5	Arabidopsis homolog reported to recruit chromatin modifying-enzymes for gene silencing. *suvr5* mutant also reported to be late flowering (Li Jikun, Master's Thesis for University of Singapore, unpublished, 2013)
Solyc01g008550	phenylacetaldehyde reductase 2, *par2*	Catalyzes conversion of 2-phenylacetaldehyde into 2-phenylethanol, no mutant phenotype for *par2* described in tomato (Tieman et al., 2007)
Solyc01g074040	Beta-glucosidase 01	
Solyc02g065085	2,3-bisphosphoglycerate-dependent phosphoglycerate mutase	
Solyc04g017800	Unknown Protein	
Solyc04g017950	Unknown Protein	
Solyc04g039670	ATP-citrate lyase A-2	Knocking down homologous gene in Arabidopsis yields range of aberrant phenotypes including smaller plants, sterile plants, plants with no roots, dark green plants (Fatland et al., 2005)
Solyc04g039760	Ycf2	Essential nuclear-encoded chloroplast protein of undetermined function (Bryant et al., 2011)
Solyc06g050455	No gene annotated	

Table 5: Genes from DRI whole genome sequencing with SNP changes consistent with EMS mutagenesis.

5.2.2 SNP verification

To confirm whether SNPs listed in Table 5 could be the cause of the aberrant phenotypes seen in both DR1 and DR3 lines, I amplified the regions containing SNPs from wild type germplasm not used for whole genome sequencing, and from DR3 backcrossed F_4 lines displaying the double root mutant phenotype. Regions containing putative SNPs were Sanger sequenced (Genewiz) to confirm whole genome sequencing results and ensure these SNPs were not present in wild type (Table 6).

Gene	Sanger Sequencing SNP Verification
Solyc01g008471	
Solyc01g008550	SNPs did not correlate with mutant phenotypes in all DR1 and DR3 lines
Solyc01g074040	WGS called the SNPs wrong; not present in any DR1 or DR3 lines
Solyc02g065085	Wild type has same SNPs and DR1 and DR3
Solyc04g017800	
Solyc04g017950	
Solyc04g039670	Wild type has same SNPs and DR1 and DR3
Solyc04g039760	Wild type has same SNPs and DR1 and DR3
Solyc06g050455	

Table 6: Additional sequencing of other wild type germplasm and DR3 lines eliminated many mutations suggested by WGS to be causative.

Additionally, given the phenotypic, inheritance, and penetrance similarity between the DR mutants and mutations in the Arabidopsis *TOPLESS* genes (Szemenyei et al., 2008), I also sequenced the entirety of *TOPLESS3*, the most highly expressed *TOPLESS* gene in *S. lycopersicum*. *TPL3* had no unique mutations in DR1 or DR3, and no other *TPL* genes had unique mutations in whole genome sequencing (data not shown).

5.3 Discussion and Future Directions

In this work, I describe a novel meristem mutant isolated in tomato. Although there are a number of tomato loss-of-function mutations affecting meristem development, including

defective embryos and meristem (dem) (Keddie et al., 1998) , *goblet (gob)* (Brand et al., 2007), *clausa (clau)* (Avivi et al., 2000), *expelled shoot1&2 (exp1/2)* (Brand et al., 2007), *short pedicle1&2 (spl1/2)* (Brand et al., 2007), *multidrop (mud)* (Brand et al., 2007), and *trifoliate (tf)* (Naz et al., 2013), none are low penetrance phenotypes and are all recessive, Mendelian inheritance. Thus, these siblings likely encode a novel component of meristematic fate or patterning in tomato. Future work should continue verifying whether SNPs identified by WGS are truly unique to DR1/3, and which may be causative for the altered phenotypes. Even if the whole genome sequencing approach ultimately proves unsuccessful in identifying a causative mutation, more work should be done to determine whether DR1/3 affects meristem size, patterning, or maintenance. Determining size and maintenance can be accomplished with scanning electron microscopy or by crossing these plants with a reporter highly expressed in tomato meristems, such as DR5:Venus {Ben-Gera, 2012 #2874}. Patterning would be best examined through *in situ* hybridization probing expression of genes with localized meristem expression, such as the *KNOX* genes (Janssen et al., 1998).

5.4 Materials and Methods

Isolation and characterization of DR Mutants

DR1-3 were found during IBA resistance screen (see Chapter 4). All three seedlings came from the same pool, and appear to be siblings based on complementation testing. After the initial isolation on the IBA plate, the M_3 and beyond generations were tracked by plating at least 100 seeds on PN plates and grown for two to three weeks. Between two and three weeks, each seedling was visually inspected for deviations from wild type morphology. Starting with the M_4 seedlings, only mutant seedlings were carried forward to the next generation.

Seedling Selection for WGS

DR1 and DR3 M_2 plants were backcrossed to wild type M82. All F_1 seeds were plated on unsupplemented media and inspected for any deviations from the wild type phenotype, which none displayed. F_2 seedlings were not scored for phenotype, but instead moved directly to soil. F_3 seedlings were scored, and mutants displaying double root phenotypes from individual F_3 lines moved to soil for tissue collection. Genomic DNA was prepared as described in (Thole and Strader, 2015).

Chapter 6: Conclusions and Future Directions

6.1 New Methods of Regulating Peroxisomes in Arabidopsis

In this thesis, I demonstrate a novel function for Arabidopsis MPK17 in regulating peroxisome and mitochondrial division. Regulation by MPK17 depends on PMD1, a peroxisome and mitochondrial division factor. Although Arabidopsis MPK17 is less-studied than its well-documented relatives MPK3 and MPK6 (reviewed in Mishra et al., 2006), studies on MPK17 homologs from other plants suggest it plays roles in stress response. For example, expression of cotton *GhMPK17* is upregulated during NaCl, mannitol, and ABA treatment, and overexpression of *GhMPK17* in Arabidopsis led to increased tolerance of both salinity and ABA (Zhang et al., 2014). Similarly, in *Setaria italica*, *SiMPK17* transcript is upregulated in response to dehydration stress (Lata et al., 2010). Transcript of the maize homolog, *ZmMPK17*, increases upon cold, ROS, or osmotic stresses and during treatments with abscisic acid, salicylic acid, jasmonic acid, and ethylene (Pan et al., 2012). Further, the two closest rice *MPK17* homologs, *OsMPK13* and *OsMPK14*, are induced upon inoculation with a rice fungal pathogen (Reyna and Yang, 2006). Clearly, MPK17 and its homologs respond to stress transcriptionally and, at least in some cases, mediates tolerance to various stress conditions.

Disruption of either *MPK17* or *PMD1* results in decreased salt-induced peroxisome proliferation, thus both MPK17 and PMD1 are necessary for this dynamic salt response. Because the peroxisome numbers in non salt-stressed *mpk17-1* are not as high as wild type grown on NaCl, the *MPK17-PMD1* proliferation pathway cannot be the only salt-responsive pathway regulating peroxisome proliferation on NaCl. Losing the ability to divide peroxisomes in

response to NaCl does not substantially impact survival or growth of these mutants under high-NaCl conditions (Fig. 8, Chapter 2), which suggests that peroxisome proliferation may not enhance the fitness of NaCl- stressed plants. This result contrasts with recent results by Fahy et al. (2017), who observed that the salt-hypersensitive mutants *fry1* and *sos1* did not proliferate peroxisomes in response to NaCl, and have very poor survival on high NaCl. Both *mpk17* and *pmd1* display the same nonproliferation molecular phenotype, but no whole plant NaCl phenotype. It remains unclear whether peroxisome proliferation in response to NaCl may provide salt tolerance to the plant under specific conditions, or whether peroxisome proliferation is a side effect caused by regulation of a different pathway.

In this thesis, I have also discovered a novel function for PMD1 as an actin-binding protein (Fig. 13B, Chapter 2). PMD1 may act as a mechanical input to the peroxisome (and mitochondrial) division process, an idea that is supported by the peroxisome clustering phenotype seen in *PMD1* overexpression lines (Aung and Hu, 2011). The increased fraction of *mpk17-1* peroxisomes moving in a linear versus Brownian pattern is also consistent with the hypothesis that connections between PMD1 and the actin cytoskeleton contribute to peroxisome distribution *in planta*, as PMD1 appears to be genetically downstream of MPK17 and repressed by MPK17, and *mpk17-1* peroxisomes show an increased ability to move around the cell than in wild type or *pmd1-1* (Fig. 13, Chapter 2). Peroxisomes in cells treated with latrunculin B still undergo Brownian movement (Mathur et al., 2002), further supporting the hypothesis by Aung and Hu (2011) that PMD1 might act in peroxisome distribution within the plant cell. Recently, the distribution, not just the number, of peroxisomes was shown to be vital for proper cell division in mice skin cells (Asare et al., 2017). Knocking down Pex11b retained peroxisome attachment to the microtubule cytoskeleton, but peroxisomes were mislocalized. This

mislocalization led to improper positioning of the peroxisomes during cell division and mitotic delay, as well as aberrant angles of the mitotic plane of division (Asare et al., 2017). Other findings suggest the ability of plants to traffic actin-dependent contents is important for ordinary growth and development, not just organelle distribution during stress. The speed of myosins was shown to directly affect plant size, with expression of a faster myosin leading to larger plant size, and slower myosin causing smaller plant size (Tominaga et al., 2013). The findings, along with the data presented in this thesis, further support a role for localization, not just number, in peroxisome function.

6.2 Peroxisome-derived Products in *S. lycopersicum*

One of the most developmentally important processes that takes place in plant peroxisomes is the conversion of IBA into the active hormone IAA. Disruption of this process leads to profound defects in seedling development ((Strader et al., 2011), Chapter 3). Discovering the importance of IBA-derived-IAA in Arabidopsis, and the dependence of this process on functioning peroxisomes, would have been difficult without the collection of mutants isolated through many IBA-resistance screens (Zolman, 2002); (Zolman et al., 2000). Insights from these screens have advanced our understanding of both peroxisome biology and auxin homeostasis in Arabidopsis, but have not yet been widely translated into organisms with other lifecycle stages and stress responses which Arabidopsis does not experiences. Most obviously, Arabidopsis does not form fleshy fruits, a process which is highly dependent on auxin regulation in non-climacteric fruits ((Given et al., 1988); (Davies et al., 1997; Jones et al., 2002); (Epstein et al., 2001). The successful isolation of IR mutants with adult fruit and flower phenotypes by a seedling forward genetic screen demonstrates that this screening method is an efficient way to

isolate and study tomato mutants with altered auxin homeostasis. Additionally, this forward genetics screen isolated mutants generally defective in auxin responses, mutants with an apparent IBA transport defect, and mutants with IBA-specific response defects. This demonstrates that this method is robust at uncovering a wide range of interesting mutations. Similar screens in Arabidopsis uncovered mutants in four classes: peroxisomal mutants (Zolman, 2002); (Zolman and Bartel, 2004); (Zolman et al., 2008); (Zolman et al., 2005; Zolman et al., 2000), IBA-to-IAA conversion mutants (Zolman et al., 2007), general auxin-resistant mutants (Monroe-Augustus et al., 2003), and IBA transporter mutants (Strader et al., 2008). So far, the *S. lycopersicum* screen seems an efficient way to isolate mutants in three of those four classes. Only peroxisomal mutants were not discovered by this screening method, which is far from saturation. Future work will determine whether seedling IBA resistance is also a hallmark of tomato *pex* mutants as it is for most Arabidopsis *pex* mutants. Even without isolating any apparent *pex* mutants, the new IR mutants provide many avenues for future study.

6.4 Future Directions

These findings expand the importance of the actin cytoskeleton in not just peroxisome distribution, but in division as well. Lack of an actin cytoskeleton abolishes the ability of peroxisomes divide, even under stressful conditions that ordinarily enhance division. However, they do not resolve the question of what adaptive effect this peroxisome proliferation on salt might confer to plants, or whether upregulating division is a side effect of other salt-induced cellular responses. It will also be interesting to see whether other peroxisome division factors associate with actin, or if PMD1 is noncanonical in this function. In summary, many questions about how, why, and when plants regulate peroxisome numbers remain.

6.5.1 Peroxisome stress responses and interactions with the cytoskeleton

The utility and adaptive benefit of peroxisome proliferation in response to stress in plants remains a mystery. Neither artificially increasing peroxisome number by Pex11 overexpression, decreasing division by gene knockout in *pmd1-1*, nor maintaining higher baseline numbers of peroxisomes as in *mpk17-1* impairs or enhances the ability of a plant to tolerate or survive salt stress. To demonstrate true protective effects of increased peroxisome number against salinity stress, a division factor like *Pex11* should be overexpressed in mutants like *fry1-6* and *sos1*. These mutants do not proliferate peroxisomes on NaCl and are salt hypersensitive due to loss of a stress-responsive signaling component (FRY1, (Xiong et al., 2001), and a proton/Na^+ antiporter (SOS1, (Shi et al., 2000), neither of which appear to be related to peroxisome number. If artificially increasing peroxisome number in mutants with peroxisome-independent causes of hypersensitivity could increase salt tolerance, it would be strong evidence for a protective effect of peroxisomes. While the protective benefits of peroxisome division are still unclear, this thesis supports a model in which different signaling pathways are used to respond to a variety of division-inducing stresses, as evidenced by the normal responses of *mpk17-1* and *pmd1-1* to respond to a variety of stresses other than NaCl (Chapter 2.4). Going forward, placing MPK17 into a signaling cascade more extensive than MKK9/10 will likely shed light on how the salt-responsive pathway and peroxisome division pathways are interrelated. Similarly, determining whether PMD1 interacts with any myosins known to transport peroxisomes in plants may refine our understanding of its functions as both a peroxisome division factor and actin-binding protein, and provide new insight to how the cytoskeleton affects division.

6.5.2 New auxin-resistant tomato mutants

Arabidopsis is also an oilseed plant in which germination is highly dependent on the ability to mobilize lipid stores. Lipid mobilization requires fatty acid beta-oxidation within the peroxisome (see Chapter 1.1.2). It is unknown whether non-oilseed plants are equally dependent on peroxisomes for these earliest stages of development. From a basic biology perspective, if early seedling development in non-oilseeds is not entirely dependent on functioning peroxisomes, *pex* mutants which are embryo lethal in Arabidopsis may not be lethal in non-oilseeds and could provide a better avenue to study the function of certain PEX proteins than Arabidopsis does. From an applied biology perspective, only one of the major crops grown in the United States (soybean) is an oilseed (Walls, 2017), so findings from an oilseed model organism may not translate to the majority of our agronomically important plant species. This was a pilot study, and the screen is far from saturated, so the lack of any tomato *pex* mutants should not yet be interpreted as evidence that IBA resistance screening is not effective for isolating peroxisome mutants in non-oilseed plants. However, if IBA resistance is not a marker of decreased peroxisome function in tomato, the screen has already yielded several interesting mutants.

With the isolation of IR3, IR5, IR12, and IR17, the number of auxin-resistant point mutants has more than doubled. Previously, only three auxin point mutants, *diageotropica* (Oh et al., 2006), *entire* (Zhang et al., 2007), and *polycotyledon* (Al-Hammadi et al., 2003) have been described. We have already received interest from several lab groups about using these lines to study various auxin-dependent pathways. As described in Chapter 4, the Yasuor lab is currently characterizing flower and fruit phenotypes in IR3, IR5, and IR17. In addition, the Iyer-Pascuzzi lab is using all four IR mutants to examine how altered auxin responsiveness affects

pathogenesis of *Ralstonia solanacearum*. Another direction worth exploring is the ability of these mutants to form associations with arbuscular mycorrhizal fungi, a process which is dependent on auxin signaling in tomatoes (Hanlon and Coenen, 2011). These broader exploratory studies benefit from having four mutants will varied degrees of auxin sensitivity, so that auxin sensitivity and response to the stimuli can be place on a spectrum. More specific follow-ups for each mutant could also elucidate the genetic reason for differences in auxin sensitivity between the IR mutants.

Most pressing will be determining whether IR17 is truly an IBA transport mutant. Before knowing the causative lesion, transport assays with radiolabeled auxin could determine whether transport of IBA differs between wild type and IR17 (Al-Hammadi et al., 2003; Strader and Bartel, 2011). Continued genotyping of possible causative lesions in genes encoding transporters, combined with the creation of rescue lines and additional mutant alleles will be needed to definitively say whether IR17 is an auxin transport mutant.

IR3 is a dominant, gain of function mutant resistant to most auxins. These phenotypes are highly suggestive of mutations in the instability region of an AUX/IAA protein; yet sequencing determined that all the AUX/IAAs are unaffected in IR3. A second backcross to wild type M82 has already been made, and selection of IAA-resistant lines should yield enough lines for whole genome sequencing. Work is also continuing in the Yasuor lab to determine whether the parthenocarpic phenotype only observed in St. Louis once, in the IR3 M_2, is separable or linked to the auxin resistance of IR3. Although phenotypes of IR3 strongly suggested an *AUX/IAA* mutant, this does not appear to be the case, indicating that IR3 could be a novel regulator of auxin signaling, or that mutant phenotypes for known auxin response elements differ in tomato

compared to what is observed in Arabidopsis. Thus, the isolation of IR3 demonstrates the continued utility of forward genetic screens to discover novel regulators of even well-studied processes. This stands in contrast to the insight gleaned from *mpk17*, in which the auxin resistance phenotypes suggested a peroxisome mutant, which does appear to be the primary defect in *mpk17-1* (see Chapter 2). Comparison to characterized mutants provides a good starting point, but cannot be expected to correctly identify all lesion sites, particularly in species like tomato which have much smaller mutant collections than Arabidopsis.

Both IR5 and IR12 display weaker IBA resistance compared to either IR3 or IR17 (Figs. 15,16, and 19). Weaker resistance presents a challenge when selecting a good population for whole genome sequencing. If small fruit and low seed set phenotypes observed in Israel could be replicated through high heat in St. Louis, or remain consistent under various growth conditions in Israel, this could provide a way to select a population for sequencing. Finding and verifying the causative mutation would be particularly helpful for comparison with IR17. Both IR5 and IR17 are auxin-resistant mutants, yet display opposite fruit phenotypes. IR17 makes larger fruit with more seeds, IR5 makes smaller fruit with fewer seeds. Determining how disrupting different aspects of auxin biology leads opposite developmental outcomes will be vital to our understanding of how auxin biology can be modified to enhance plant yield without compromising hardiness.

In the future, work on peroxisome responses to salt stress should focus on determining whether increasing peroxisome number confers any adaptive benefits during salt stress. Mutants in peroxisome-independent parts of NaCl response, such as *sos1*, could be transformed with an inducible *Pex11b* gene. Increased peroxisome division could then be induced concurrently with salt stress to see if increasing peroxisome number can mitigate the effects of NaCl stress to a

hypersensitive mutant. The discovery in this thesis that PMD1 is an actin-binding protein raises several questions about the interaction between peroxisome division and the cytoskeleton. First, is PMD1 the only division factor that directly associates with actin? If division factors like Pex11b, DRP3a, and FIS1a can be heterologously expressed, actin cosedimentation assays might determine if PMD1 is unique among plant division factors, or whether direct association with actin is common. Another question pertaining to the cytoskeleton is whether PMD1 interacts with some or all of the four myosins that transport peroxisomes (Peremyslov et al., 2010). Answering these will enhance our understanding of how the cytoskeleton influences peroxisome division.

Appendix

Glycerol Number	Plasmid	Host	Resistance	Name	Date	Comments
1809	pFL61: Athaliana library pool		Amp	EMF	10/17/2012	T-1, from Bartel lab. Unsure of host
1810	pFL61: Athaliana library pool		Amp	EMF	10/17/2012	T-2, from Bartel lab. Unsure of host
1811	pFL61: Athaliana library pool		Amp	EMF	10/17/2012	T-3, from Bartel lab. Unsure of host
1812	pFL61: Athaliana library pool		Amp	EMF	10/17/2012	T-4, from Bartel lab. Unsure of host
1813	pFL61: Athaliana library pool		Amp	EMF	10/17/2012	T-5, from Bartel lab. Unsure of host
1814	pFL61: Athaliana library pool		Amp	EMF	10/17/2012	T-6, from Bartel lab. Unsure of host
1815	pFL61: Athaliana library pool		Amp	EMF	10/17/2012	T-7, from Bartel lab. Unsure of host
1816	pFL61: Athaliana library pool		Amp	EMF	10/17/2012	T-8, from Bartel lab. Unsure of host
1833	At5g41890 cDNA in pCR4	Top10	kan	EMF	10/28/2012	not yet sequenced colony 6
1834	At5g41890 cDNA in pCR4	Top10	kan	EMF	10/28/2012	not yet sequenced colony 7
1835	At5g41890 cDNA in pCR4	Top10	kan	EMF	10/28/2012	not yet sequenced colony 13

1836	At5g41890 cDNA in pCR4	Top10	kan	EMF	10/28/2012	
2179	pCR4:CRF6	NEB5a	kan	EMF	5/21/2013	
2180	pCR4:GL2	NEB5a	kan	EMF	5/21/2013	
2230	pZL1:118N2	DH10B	amp	EMF	6/12/2013	bacterial host containing Arabidopsis EST of Pex1, from ABRC
2231	pZL1:192D14	DH10B	amp	EMF	6/12/2013	bacterial host containing Arabidopsis EST of UBQ10, from ABRC
2232	pUNI51:U09878	PIR1	kan	EMF	6/12/2013	bacterial host containing Arabidopsis cDNA of DRP3A, from ABRC
2233	pUNI51:U83915	PIR1	kan	EMF	6/12/2013	bacterial host containing Arabidopsis cDNA of PMD1, from ABRC
2234	pUNI51:U13324	PIR1	kan	EMF	6/12/2013	bacterial host containing Arabidopsis cDNA of FIS1A, from ABRC
2235	pUNI51:U15712	PIR1	kan	EMF	6/12/2013	bacterial host containing Arabidopsis cDNA of Pex11b, from ABRC
2339	pADH1:GW	DB3.1	kan	EMF	8/17/2013	colony #4, sequenced and correct
2,457.	promCOBL1:GW	DB3.1	kan	EMF	9/6/2013	colony #2- sequenced and correct

2457	pCOBL1:GW	DB3.1	kan	EMF	9/6/2013	colony #2- sequenced and correct
2,458.	promCOBL1:GW	DB3.1	kan	EMF	9/6/2013	colony #3- sequenced and correct
2,478.	pDEST-GBKT		kan	EMF	9/10/2013	yeast expression vector from Bonnie Bartel
2,479.	pDEST-GADT7		AMP	EMF	9/10/2013	yeast expression vector from Bonnie Bartel
2,480.	promUBQ10-GW	DB3.1	kan	EMF	9/12/2013	colony 7, sequenced and correct
2,491.	pBI770-MPK17	Neb5a	amp	EMF	9/17/2013	colony 1, sequenced and correct
2,492.	pBI770-MPK17	NEB5a	amp	EMF	9/17/2013	colony 11, sequenced and correct
2,527.	GL2-GW	DB3.1	kan	EMF	10.2.13	colony number 2, sequenced and correct. Glycerol #2527-2589 are all promoters of indicated genes
2,528.	LBD16-GW	DB3.1	kan	EMF	10.3.13	colony number 8, sequenced and correct
2,548.	SCR-GW	DB3.1	kan	EMF	10/28/2013	colony 10, sequenced and correct on 10/24
2,565.	CAB1-GW	DB3.1	kan	EMF	11/5/2013	colony 15, sequenced and correct
2,574.	AGL42-GW	DB3.1	kan	EMF	11/14/2013	colony 23, sequenced and correct

2,589.	CFR6-GW	DB3.1	kan	EMF	11/15/2013	colony 10, sequenced and correct on 11/13
2,629.	pENTR-At2g23450-A2	NEB5a	kan	EMF	12/2/2013	first half of At2g23540 cDNA, colony 2
2,630.	pENTR-At2g23450-A10	NEB5a	kan	EMF	12/2/2013	first half of At2g23540 cDNA, colony 10
3,095.	pMDC32-MPK17 T178D	Top10	kan	EMF	7/1/2014	colony 1, sequenced and correct on 7/1/2014. Untagged plant expression vector for transformation into pmd1-1 background plants
3,096.	pMDC43-MPK17 T178D	Top10	kan	EMF	7/1/2014	colony 1, sequenced and correct on 7/1/2014. YFP tagged plant expression vector for transformation into pmd1-1 background plants
3,108.	pEXP7-GW	DB3.1	kan	EMF	7/7/2014	colony 1, sequenced and correct on 7/3/14. This is the EXP7 promoter region.
3,117.	pMDC32-MPK17 T178D	GV3101	kan gent	EMF	7/9/2014	phosphomimic MPK17 cDNA for hygromycin resistant transformation into plants. from E.coli colony #1 (gly #3095)

3,118.	pMDC43-MPK17 T178D	GV3101	kan gent	EMF	7/9/2014	phosphomimic MPK17 cDNA for hygromycin resistant transformation into plants. from E.coli colony #1 (gly #3096)
3,166.	pUBQ10: MPK17	NEB5a	kan	EMF	8/8/2014	colony 7, not yet sequenced
3,167.	pUBQ10: YFP-MPK17	NEB5a	kan	EMF	8/8/2014	colony 1
3,168.	pUBQ10: MPK17DDD	NEB5a	kan	EMF	8/8/2014	colony 1, Sequenced and correct on 8/12/14
3,169.	pUBQ10: YFP-MPK17DDD	NEB5a	kan	EMF	8/8/2014	colony 1, sequenced and correct on 8/12/14
3,172.	pUBQ10: YFP-MPK17	GV3101	kan gent	EMF	8/13/2014	wild type cDNA, colony 1, from DNA in glycerol #3167. used for dipping
3,173.	pUBQ10: YFP-MPK17	GV3101	kan gent	EMF	8/13/2014	wild type cDNA, colony 2, from DNA in glycerol #3167
3,174.	pUBQ10: MPK17DDD	GV3101	kan gent	EMF	8/13/2014	phosphomimic cDNA, colony 1, from DNA in glycerol #3168. Used for dipping
3,175.	pUBQ10: MPK17DDD	GV3101	kan gent	EMF	8/13/2014	phosphomimic cDNA, colony 2, from DNA in glycerol #3168

3,176.	pUBQ10: YFP-MPK17DDD	GV3,101	kan gent	EMF	8/13/2014	phosphomimic cDNA with YFP tag, colony1, from DNA in glycerol #3169. Used for dipping
3,177.	pUBQ10: YFP-MPK17DDD	GV3,101	kan gent	EMF	8/13/2014	phosphomimic cDNA with YFP tag, colony 2, from DNA in glycerol #3169
3,189.	pENTR-MIR390 b/c	DB3.1	kan	EMF	8/14/2014	From Jim Carrington's lab, for amiRNA construction
3,190.	pMDC32-MIR390 b/c	DB3.1	kan	EMF	8/14/2014	amiRNA plant expression vector from Alberto Carbonell in Jim Carrington's lab. Sequenced and correct
3,191.	pMDC123-MIR90 b/c	DB3.1	kan	EMF	8/14/2014	amiRNA plant expression vector from Alberto Carbonell in Jim Carrington's lab. Sequenced and correct
3,217.	pENTR-MPK17 T178A Y180A	NEB5	spec	EMF	8/22/2014	cDNA, colony 4, sequenced and correct (had ADA) on 8/22
3,218.	pENTR-MPK17 T178A Y180A	NEB5	spec	EMF	8/22/2014	cDNA, colony 44, sequenced and correct (had ADA) on 8/22

3,231.	UBQ10-MPK17 T178A Y180A	NEB5a	kan	EMF	8/29/2014	cDNA, colony 1, sequenced and correct on 8/29
3,232.	UBQ10-YFP-MPK17 T178A Y180A	NEB5a	kan	EMF	8/29/2014	cDNA, colony 1, sequenced and correct at 8/29/14
3,233.	Bluescript-RIA1 cDNA	NEB5a	amp	EMF	8/29/2014	colony 1, sequenced and correct on 8/29/14, with NdeI and NotI sites for pET28a cloning
3,241.	UBQ10-MPK17 T178A Y180A	GV3101	kan gent	EMF	9/4/2014	colony 1, DNA from #3231, used for dipping
3,242.	UBQ10-MPK17 T178A Y180A	GV3,101	kan gent	EMF	9/4/2014	colony 2, DNA from #3231
3,243.	UBQ10-YFP-MPK17 T178A Y180A	GV3101	kan gent	EMF	9/4/2014	colony 1, DNA from #3232, used for dipping
3,244.	UBQ10-YFP-MPK17 T178A Y180A	GV3,101	kan gent	EMF	9/4/2014	colony 1, DNA from #3232
3,252.	pMDC32-Mir390a-amiMPK17	GV3101	kan gent	EMF	9/5/2014	colony 1, used for dipping, DNA sequenced and correct on 8/11/14
3,253.	pBI770-MPK17 T178AY 180A	NEB5a	amp	EMF	9/8/2014	colony 13, sequenced and correct 9/8/14
3,254.	pBI770-MPK17 T178AY 180A	NEB5a	amp	EMF	9/8/2014	colony 14, sequenced and correct on 9/8/14

3,264.	pET28a-RIA1 cDNA	NEB5a	kan	EMF	9/25/2014	colony 28, not yet sequenced
3,265.	pET28a-RIA1 cDNA	NEB5a	kan	EMF	9/25/2014	colony 31, not yet sequenced
3,266.	pET28a-RIA1 cDNA	NEB5a	kan	EMF	9/25/2014	colony 32, not yet sequenced
3,267.	U60912	TOP10	kan	EMF	9/26/2014	MKK9 cDNA in pUNI vector, from ABRC. sequenced and correct, contains stop
3,268.	DQ652874	TOP10	kan	EMF	9/26/2014	MKK10 cDNA in pDONR221, sequenced and correct but no stop codon
3,269.	pET28a:RIA1	Rosetta	kan	EMF	10/1/2014	colony 1
3,270.	pET28a:RIA1	Rosetta	kan	EMF	10/1/2014	colony 2
3,271.	pET28a:RIA1	Rosetta	kan	EMF	10/1/2014	colony 3
3288	pCR4-MKK9 cDNA	NEB5a	kan	EMF	10/8/2014	colony 12, with RE sites for cloning into pBI770,sequenced and correct on 10/16
3289	pCR4-MKK9 cDNA	NEB5a	kan	EMF	10/8/2014	colony 14, with RE sites for cloning into pBI770, sequenced and correct on 10/16
3356	pCR4-MKK10 cDNA	NEB5a	kan	EMF	10/17/2014	colony 7, sequneced and correct 10/17/14

3357	pCR4-MKK10 cDNA	NEB5a	kan	EMF	10/17/2014	colony 14, sequenced and correct 10/17/14
3358	pCR4-MKK10 cDNA	NEB5a	kan	EMF	10/17/2014	colony 16, sequenced and correct 10/17
3362	pBI771-MKK9	NEB5a	amp	EMF	10/20/2014	colony 4, sequenced and correct 10/21/14
3363	pBI771-MKK9	NEB5a	amp	EMF	10/20/2014	colony 9, not sequenced
3368	pBI770-MKK10	NEB5a	amp	EMF	10/21/2014	colony 2, sequenced and correct on 10/22
3369	pBI770-MKK10	NEB5a	amp	EMF	10/21/2014	colony 6, sequenced and not correct! Don't use!
3370	pBI770-MPK17 T178AY180A	YPB2	-L	EMF	10/22/2014	colony 13C, confirmed by Western to express protein, used in Y2H screen and directed Y2H with MKK9
3383	pCR4-MPK17 T178A Y180A	NEB5a	kan	EMF	10/31/2014	colony 7, sequencing and correct 10/31
3400	pBI771-MPK17 T178A Y180A	NEB5a	amp	EMF	11/11/2004	colony 6, sequenced and correct on 11/10/14
3405	pENTR-MPK17	NEB5a	kan	EMF	11/21/2014	colony 11, with stop codon for Co-IP cloning. sequenced and correct 11/20/14
3406	pENTR-MPK17 T178A Y180A	NEB5a	kan	EMF	11/21/2014	colony 7, with stop codon and phosphodead mutation for Co-IP

						cloning. sequenced and correct 11/20/14
3407	pENTR-MPK17 T178A Y180A no stop	NEB5a	kan	EMF	11/21/2014	colony 2, with mutated stop codon and phosphodead for Co-IP cloning. sequenced and correct 11/20/14
3411	pBI771	NEB5a	amp	EMF	12/3/2014	original glycerol was growing poorly for me
3441	pBI771-MKK10	TOP10	amp	EMF	12/9/2014	colony 13, sequenced and correct on 12/10/14
3442	pBI771-MKK10	TOP10	amp	EMF	12/9/2014	colony 14, sequenced and correct on 12/10/14
3495	pBI770:MPK17 / empty pBI771	YPB2	-L-W	EMF	1/22/2015	wild type MPK17 cDNA
3496	pBI770:MPK17 / pBI117:MKK9	YPB2	-L-W	EMF	1/22/2015	wild type MPK17 cDNA and MKK9 cDNA
3497	pBI770:MPK17 / pBI117:MKK10	YPB2	-L-W	EMF	1/22/2015	wild type MPK17 cDNA and MKK10 cDNA
3554	pUNI51-PMD1	PIR1	kan	EMF	2/27/2015	PMD1 cDNA from ABRC
3560	pCR4-MPK17 NdeI/XhoI	TOP10	kan	EMF	3/13/2015	colony 4, sequenced and correct on 3/16. Contains sites for pET28 cloning
3561	pCR4-MPK17 NdeI/XhoI	TOP10	kan	EMF	3/13/2015	colony 6,sequenced and correct on 3/16. Contains sites for pET28 cloning

3570	pCR4-PMD1 SalI/NotI	TOP10	kan	EMF	3/19/2015	colony 5, sequenced and correct on 3/18
3604	pBI770-PMD1	NEB5	amp	EMF	4/10/2015	colony 2, lacks the TM domain and unordered region, not yet sequenced
3605	pBI770-PMD1	NEB5	amp	EMF	4/10/2015	colony 9, lacks the TM domain and unordered region, not yet sequenced
3623	pDEST24	DB3.1	amp	EMF	5/6/2015	Gateway destination vector for GST-tagged protein expression from Invitrogen
3628	pBI770-PMD1	NEB5a	amp	EMF	5/15/2015	colony 7, sequenced and correct 5/13/15
3632	pDEST24-MPK17	NEB5a	amp	EMF	5/19/2015	colony 3, wild type MPK17 cDNA in GST protein expression vector. Sequenced on 5/15/15
3633	pDEST24-MPK17 DDD	NEB5a	amp	EMF	5/20/2015	colony 2, constituitively active MPK17 cDNA in GST protein expression vector. Sequenced on 5/15/15
3634	pDEST24-MPK17 ADA	NEB5a	amp	EMF	5/21/2015	colony 3, phosphodead MPK17 cDNA in GST protein expression vector. Sequenced on 5/15/15

3667	pCR4-PMD1	TOP10	kan	EMF	6/12/2015	colony 5, with NdeI and XhoI sites, sequenced and correct 6/12
3668	pCR4-PMD1	TOP10	kan	EMF	6/12/2015	colony 20, with NdeI and XhoI sites, sequenced and correct 6/13
3672	pEG100-YFP-PTS1	TOP10	kan	EMF	6/15/2015	colony 6, sequenced and correct on 6/12/15
3673	pEG100-YFP-PTS1	TOP10	kan	EMF	6/16/2015	colony 17, sequenced and correct on 6/12/15
3692	pEG100:YFP-PTS1	GV3101	kan gent	EMF	6/22/2015	DNA from colony 6, correct
3693	pEG100:YFP-PTS1	GV3101	kan gent	EMF	6/22/2015	DNA from colony 17, correct
3720	pET28a-PMD1	Top10	kan	EMF	7/6/2015	colony 3, sequenced and correct on 7/2/15
3721	pET28a-PMD1	TOP10	kan	EMF	7/6/2015	colony 7, sequenced and correct on 7/2/15
3722	pET28a-PMD1	rosetta	kan	emf	7/6/2015	DNA from glycerol 3720, colony A
3723	pET28a-PMD1	rosetta	kan	emf	7/6/2015	DNA from glycerol 3720, colony B
3724	pET28a-PMD1	rosetta	kan	emf	7/6/2015	DNA from glycerol 3721, colony A
3725	pET28a-PMD1	rosetta	kan	emf	7/6/2015	DNA from glycerol 3721, colony B
3735	pDEST24-MPK17	Rosetta	amp	EMF	7/9/2015	colony 3A

3736	pDEST24-MPK17	Rosetta	amp	EMF	7/9/2015	colony 3B
3737	pDEST24-MPK17 DDD	Rosetta	amp	EMF	7/9/2015	colony 2A
3738	pDEST24-MPK17 DDD	Rosetta	amp	EMF	7/9/2015	colony 2B
3739	pDEST24-MPK17 ADA	Rosetta	amp	EMF	7/9/2015	colony 5A
3740	pDEST24-MPK17 ADA	Rosetta	amp	EMF	7/9/2015	colony 5B
3871	pCR4:MPK17 SalIgg#1		Kan	EMF	8/6/2015	colony 1
3872	pCR4:MPK17 SalIgg#12		Kan	EMF	8/6/2015	colony 12
3887	pCR4-MPK17 DDD	NEB5a	kan	EMF	8/11/2015	colony 6, sequenced and correct on 8/10/15. With SalIgg for pGEX cloning
3916	pCR4-PMD1 salIgg	NEB5a	kan	EMF	8/19/2015	colony 5, sequenced and correct 8/18/15. With RE sites for pGEX4T1 cloning
3921	pGEX4T1-MPK17	NEB5a	amp	EMF	8/23/2015	colony 22, sequenced and in frame
3929	pGEX4T1-MPK17	Rosetta	amp	EMF	8/27/2015	DNA from glycerol 3921
3940	pCR4-MPK17 ADA	Neb5a	kan	EMF	9/3/2015	colony 10, with SalI and NotI sites for pGEX cloning, sequenced and correct 9/2/15

3941	pEG100-At3g51560	Neb5a	kan	EMF	9/3/2015	colony 2, sequenced and correct 9/4/15
3942	pEG100-At3g51561	Neb5a	kan	EMF	9/3/2015	colony 11, sequenced and correct 9/4/15
3943	pGEX4T1-MPK17 DDD	Neb5a	amp	EMF	9/4/2015	colony 24, not yet sequenced
3966	pGEX4T1-PMD1	top10	amp	EMF	9/23/2015	colony 8, sequenced and in frame 9/18/15
3967	pGEX4T1-PMD1	top11	amp	EMF	9/23/2015	colony 21, sequenced and in frame 9/18/15
3971	pENTR-MPK17 gene+prom	Top10	kam	EMF	9/29/2015	colony 3, sequenced and correct on 9/25/15
4014	pMDC123:MPK17 gene and promoter	NEB5A	kan	EMF	10/9/2015	colony 15, sequenced and correct 10/9
4015	pMDC123:MPK17 gene and promoter	NEB5A	kan	EMF	10/9/2015	colony 16, sequenced and correct 10/9
4016	pMDC123:MPK17 gene and promoter	GV3101	kan, gent	EMF	10/14/2015	colony 15A, DNA from glycerol 4014, used for dipping
4017	pMDC123:MPK17 gene and promoter	GV3101	kan, gent	EMF	10/14/2015	colony 16A, DNA from glycerol 4015
4024	pENTR-PMD1	NEB5A	kan	EMF	10/27/2015	colony 3, sequenced and correct 10/27. Contains transmembrane domain for a plant overexpression line

4030	UBQ10-YFP-PMD1	NEB5A	kan	EMF	11/5/2015	colony 2, sequenced and correct on 11/3/15
4031	pEG104-PMD1	NEB5A	kan	EMF	11/5/2015	colony 1, sequenced and correct 11/5/15
4032	pEG104-PMD1	NEB5A	kan	EMF	11/6/2015	colony 3, sequenced and correct 11/5/16
4036	pEG104-PMD1	GV3101	kan gent	EMF	11/10/2015	colony 1A, DNA from #4031, used for dipping
4037	pEG104-PMD1	GV3101	kan gent	EMF	11/10/2015	colony 3A, DNA from #4032
4038	UBQ10-YFP-PMD1	GV301	kan gent	EMF	11/10/2015	colony 2A, DNA from #4030, used for dipping
4120	LucTrap3	DB3.1	kan	EMF	3/8/2016	Gateway-compatible EV for driving Luciferase expression. From Claus Schwechheimer,not yet sequenced
4121	LucTrap	NEB5a	kan	EMF	3/8/2016	promoterless empty vector for driving luciferase expression behind your promoter of choice. From Claus Schwechheimer, not yet sequenced
4136	pEG100-YFP-PTS1	NEB5a	kan	EMF	4/19/2016	colony 7, sequenced and correct

4137	pEG100-YFP-PTS1	GV3101	kan gent	emf	4/19/2016	from glycerol 4136
4144	U50007		kan	EMF	4/22/2016	MYA2 cDNA from ABRC. single colony streaked out from stab. Does not contain the entire MYA2 region, do not use
4173	pOO2-TOB1 D457A	NEB5a	amp	EMF	6/17/2016	colony 2, sequenced and correct
4184	promTOB1-CFP-TOB1 EEAA	NEB5a	kan	EMF	7/27/2016	colony 2 sequenced and correct
4185	promTOB1-CFP-TOB1 EEAA	NEB5a	kan	EMF	7/27/2016	colony 21 sequenced and correct
4186	promTOB1-CFP-TOB1 D453A	NEB5a	kan	EMF	7/27/2016	colony 18, sequenced and correct
4187	promTOB1-CFP-TOB1 D453A	NEB5a	kan	EMF	7/27/2016	colony 22, sequenced and correct
4188	promTOB1-CFP-TOB1-P473L	NEB5a	KAN	EMF	7/27/2016	colony 8, sequenced and correct
4189	promTOB1-CFP-TOB1-P473L	NEB5a	KAN	EMF	7/27/2016	colony 10, sequenced and correct
4440	pCambia2301	DH5	kan	EMF	1/5/2017	from University of Missouri Columbia plant transformation center

4441	pCR4-YFP-PTS1 AhdI/BstEII	NEB5a	kan	EMF	1/13/2017	colony 12, sequenced and correct, for pCAMBIA cloning
4466	pCAMBIA-YFP-PTS1	NEB5a	kan	EMF	1/24/2017	colony 7, not yet sequenced
4467	pCAMBIA-YFP-PTS1	NEB5a	kan	EMF	1/24/2017	colony 15, not yet sequenced
4506	pCR4-YFP-PTS1 AhdI/BstEII	NEB5a	kan	EMF	2/21/2017	colony 2, sequenced and correct
4507	pCR4-YFP-PTS1 AhdI/BstEII	NEB5a	kan	EMF	2/21/2017	colony 3, sequenced and correct
4508	pCAMBIA-YFP-PTS1	NEB5a	kan	EMF	2/21/2017	from glycerol 4506, colony 9, not yet sequenced
4509	pCAMBIA-YFP-PTS1	NEB5a	kan	EMF	2/21/2017	from glycerol 4507, colony 9, not yet sequenced
4510	pCAMBIA-YFP-PTS1	NEB5a	kan	EMF	2/21/2017	from glycerol 4507, colony 10, not yet sequenced
4511	pCAMBIA-YFP-PTS1	NEB5a	kan	EMF	2/21/2017	from glycerol 4507, colony 12, not yet sequenced

Table S1: List of all correct bacterial cultures made during the thesis research.

Seed Stock Number	Genotype	Ecotype	Inheritance	Gene	Source	Encodes
652	mpk17-1 GFP-PTS1	Col				x1045, F2 #21, homozygous line
657	x1508 F1	M82		IR12		first generation backcrossed IR12 (female)
658	x1510 F1	M82		IR3		first generation backcrossed IR3 (fertility defect, no IR3 M3 seed)
659	IR5 M3	M82		IR5		M3 seed of IBA-resistant IR5 isolate
660	IR12 M3	M82		IR12		M3 seed of IBA-resistant IR12 isolate
661	IR17 M3	M82		IR17		M3 seed of IBA-resistant IR17 isolate
662	DR3 M3	M82	recessive/low penetrance	DR3		M3 seed of doubleroot3, see notes from spring 2016 for phenotypes
663	DR1 M3	M82	recessive/low penetrance	DR1		M3 of doubleroot1, see notes from spring 2016 for phenotypes
664	wild type M82	M82				wild type parent of X1506-X1511
665	x1514 F1	M82	recessive	DR3		F1 seed of backcrossed DR3
911	*mpk17-1 promoterMPK17:MPK17 T5-6A bulk*	Col	recessive			untagged wild type MPK17 gene driven by native promoter in the *mpk17-1* background
912	*mpk17-1 promoterMPK17:MPK17 T5-20B bulk*	Col	recessive			untagged wild type MPK17 gene driven by native promoter in the *mpk17-1* background

Table S2: List of seed lines used in thesis research in publications and for ongoing projects. All seed lines used in manuscripts or for ongoing projects were cleaned and stored at 4°.

References

Abe, I., and Fujiki, Y. (1998). cDNA Cloning and Characterization of a Constitutively Expressed Isoform of the Human Peroxin Pex11p. Biochem Biophys Res Commun *252*, 529-533.

Agrawal, G., Fassas, S.N., Xia, Z.J., and Subramani, S. (2016). Distinct requirements for intra-ER sorting and budding of peroxisomal membrane proteins from the ER. The Journal of cell biology *212*, 335-348.

Al-Hammadi, A.S., Sreelakshmi, Y., Negi, S., Siddiqi, I., and Sharma, R. (2003). The polycotyledon mutant of tomato shows enhanced polar auxin transport. Plant physiology *133*, 113-125.

Asare, A., Levorse, J., and Fuchs, E. (2017). Coupling organelle inheritance with mitosis to balance growth and differentiation. Science *355*.

Aung, K., and Hu, J. (2011). The Arabidopsis tail-anchored protein PEROXISOMAL AND MITOCHONDRIAL DIVISION FACTOR1 is involved in the morphogenesis and proliferation of peroxisomes and mitochondria. The Plant cell *23*, 4446-4461.

Avivi, Y., Lev-Yadun, S., Morozova, N., Libs, L., Williams, L., Zhao, J., Varghese, G., and Grafi, G. (2000). Clausa, a tomato mutant with a wide range of phenotypic perturbations, displays a cell type-dependent expression of the homeobox gene LeT6/TKn2. Plant physiology *124*, 541-552.

Bajguz, A., and Piotrowska, A. (2009). Conjugates of auxin and cytokinin. Phytochemistry *70*, 957-969.

Basile A, Fambrini M, and Pugliesi C. (2017). The vascular plants: open system of growth. Development, Genes, and Evolution *227*, 129-157.

Bassa, C., Mila, I., Bouzayen, M., and Audran-Delalande, C. (2012). Phenotypes associated with down-regulation of Sl-IAA27 support functional diversity among Aux/IAA family members in tomato. Plant & cell physiology *53*, 1583-1595.

Bellini, C., Pacurar, D.I., and Perrone, I. (2014). Adventitious roots and lateral roots: similarities and differences. Annual Review of Plant Biology *65*, 639-666.

Ben-Gera, H., Shwartz, I., Shao, M.R., Shani, E., Estelle, M., and Ori, N. (2012). ENTIRE and GOBLET promote leaflet development in tomato by modulating auxin response. The Plant journal : for cell and molecular biology *70*, 903-915.

Boisson-Dernier, A., Frietsch, S., Kim, T.H., Dizon, M.B., and Schroeder, J.I. (2008). The peroxin loss-of-function mutation abstinence by mutual consent disrupts male-female gametophyte recognition. Current biology : CB *18*, 63-68.

Brand, A., Shirding, N., Shleizer, S., and Ori, N. (2007). Meristem maintenance and compound-leaf patterning utilize common genetic mechanisms in tomato. Planta *226*, 941-951.

Bryant, N., Lloyd, J., Sweeney, C., Myouga, F., and Meinke, D. (2011). Identification of nuclear genes encoding chloroplast-localized proteins required for embryo development in Arabidopsis. Plant physiology *155*, 1678-1689.

Calderón-Villalobos, L.I., Lee, S., De Oliveira, C., Ivetac, A., Brandt, W., Armitage, L., Sheard, L.B., Tan, X., Parry, G., Mao, H., *et al.* (2012). A combinatorial TIR1/AFB-Aux/IAA co-receptor system for differential sensing of auxin. Nat Chem Biol *8*, 477-485.

Cameron, D.D., Neal, A.L., van Wees, S.C., and Ton, J. (2013). Mycorrhiza-induced resistance: more than the sum of its parts? Trends in plant science *18*, 539-545.

Campanella, J.J., Olajide, A.F., Magnus, V., and Ludwig-Müller, J. (2004). A novel auxin conjugate hydrolase from wheat with substrate specificity for longer side-chain auxin amide conjugates. Plant Physiol *135*, 2230-2240.
Cande, W.Z., and Ray, P.M. (1976). Nature of cell-to-cell transfer of auxin in polar transport. Planta *129*, 43-52.
Charlton, W.L., Johnson, B., Graham, I.A., and Baker, A. (2005a). Non-coordinate expression of peroxisome biogenesis, beta-oxidation and glyoxylate cycle genes in mature Arabidopsis plants. Plant cell reports *23*, 647-653.
Charlton, W.L., K., M., Johnson, B., Graham, I.A., M., O.-T., and Baker, A. (2005b). Salt-induced expression of peroxisome associated genes requires components of the ethylene, jasmonate, and abscisic acid signalling pathways. Plant, Cell, and Environment *28*, 11.
Chhun, T., Taketa, S., Ichii, M., and Tsurumi, S. (2005). Involvement of ARM2 in the uptake of indole-3-butyric acid in rice (*Oryza sativa* L.) roots. Plant Cell Physiology *46*, 1161-1164.
Chhun, T., Taketa, S., Tsurumi, S., and Ichii, M. (2003). The effects of auxin on lateral root initiation and root gravitropism in a lateral rootless mutant *Lrt1* of rice (*Oryza sativa* L.). Plant Growth Reg *39*, 161-170.
Clough, S.J., and Bent, A.F. (1998). Floral dip: a simplified method for *Agrobacterium*-mediated transformation of *Arabidopsis thaliana*. Plant J *16*, 735-743.
Curtis, M.D., and Grossniklaus, U. (2003). A gateway cloning vector set for high-throughput functional analysis of genes *in planta*. Plant physiology *133*, 462-469.
Davies, C., Boss, P.K., and Robinson, S.P. (1997). Treatment of Grape Berries, a Nonclimacteric Fruit with a Synthetic Auxin, Retards Ripening and Alters the Expression of Developmentally Regulated Genes. Plant physiology *115*, 1155-1161.
de Jong, M., Wolters-Arts, M., Feron, R., Mariani, C., and Vriezen, W.H. (2009). The Solanum lycopersicum auxin response factor 7 (SlARF7) regulates auxin signaling during tomato fruit set and development. The Plant journal : for cell and molecular biology *57*, 160-170.
De Rybel, B., Audenaert, D., Xuan, W., Overvoorde, P., Strader, L.C., Kepinski, S., Hoye, R., Brisbois, R., Parizot, B., Vanneste, S., *et al.* (2012). A role for the root cap in root branching revealed by the non-auxin probe naxillin. Nat Chem Biol *8*, 798-805.
Delbarre, A., Muller, P., Imhoff, V., and Guern, J. (1996). Comparison of mechanisms controlling uptake and accumulation of 2,4-dichlorophenoxy acetic acid, naphthalene-1-acetic acid, and indole-3-acetic acid in suspension-cultured tobacco cells. Planta *198*, 532-541.
Delfosse, K., Wozny, M.R., Jaipargas, E.A., Barton, K.A., Anderson, C., and Mathur, J. (2015). Fluorescent Protein Aided Insights on Plastids and their Extensions: A Critical Appraisal. Frontiers in plant science *6*, 1253.
Desai, M., and Hu, J. (2008). Light induces peroxisome proliferation in Arabidopsis seedlings through the photoreceptor phytochrome A, the transcription factor HY5 HOMOLOG, and the peroxisomal protein PEROXIN11b. Plant physiology *146*, 1117-1127.
Enders, T.A., and Strader, L.C. (2015). Auxin activity: Past, present, and future. American journal of botany *102*, 180-196.
Epstein, E., Chen, K.-H., and Cohen, J.D. (1989). Identification of indole-3-butyric acid as an endogenous constituent of maize kernels and leaves. Plant Growth Regul *8*, 215-223.
Epstein, E., Cohen, J.D., and Slovin, J.P. (2001). Studies of IAA biosynthesis in tomato fruit using stable isotope labeled anthranilic acid, indole and tryptophan. Plant Growth Regul *to be submitted*.

Epstein, E., and Ludwig-Müller, J. (1993). Indole-3-butyric acid in plants: Occurrence, synthesis, metabolism, and transport. Physiol Plant *88*, 382-389.
Epstein, E., and Sagee, O. (1992). Effect of ethylene treatment on transport and metabolism of indole-3-butyric acid in citrus leaf midribs. Plant Growth Regul *11*.
Etemadi, M., Gutjahr, C., Couzigou, J.M., Zouine, M., Lauressergues, D., Timmers, A., Audran, C., Bouzayen, M., Becard, G., and Combier, J.P. (2014). Auxin perception is required for arbuscule development in arbuscular mycorrhizal symbiosis. Plant physiology *166*, 281-292.
Fahy, D., Sanad, M.N., Duscha, K., Lyons, M., Liu, F., Bozhkov, P., Kunz, H.H., Hu, J., Neuhaus, H.E., Steel, P.G., *et al.* (2017). Impact of salt stress, cell death, and autophagy on peroxisomes: quantitative and morphological analyses using small fluorescent probe N-BODIPY. Sci Rep *7*, 39069.
Fakhry, C., Qualliotine, J.R., Zhang, Z., Agrawal, N., Gaykalova, D.A., Bishop, J.A., Subramaniam, R.M., Koch, W.M., Chung, C.H., Eisele, D.W., *et al.* (2016). Serum Antibodies to HPV16 Early Proteins Warrant Investigation as Potential Biomarkers for Risk Stratification and Recurrence of HPV-Associated Oropharyngeal Cancer. Cancer prevention research *9*, 135-141.
Fan, J., Quan, S., Orth, T., Awai, C., Chory, J., and Hu, J. (2005). The Arabidopsis *PEX12* gene is required for peroxisome biogenesis and is essential for development. Plant Physiol *139*, 231-239.
Fatland, B.L., Nikolau, B.J., and Wurtele, E.S. (2005). Reverse genetic characterization of cytosolic acetyl-CoA generation by ATP-citrate lyase in Arabidopsis. The Plant cell *17*, 182-203.
Fourcroy, P., Sisó-Terraza, P., Sudre, D., Savirón, M., Reyt, G., Gaymard, F., Abadía, A., Abadia, J., Álvarez-Fernández, A., and Briat, J.F. (2014). Involvement of the ABCG37 transporter in secretion of scopoletin and derivatives by Arabidopsis roots in response to iron deficiency. The New phytologist *201*, 155-167.
Fukaki, H., Tameda, S., Masuda, H., and Tasaka, M. (2002). Lateral root formation is blocked by a gain-of-function mutation in the *SOLITARY-ROOT/IAA14* gene of *Arabidopsis*. Plant J *29*, 153-168.
Given, N.K., Venis, M.A., and Gierson, D. (1988). Hormonal regulation of ripening in the strawberry, a non-climacteric fruit. Planta *174*, 402-406.
Hanlon, M.T., and Coenen, C. (2011). Genetic evidence for auxin involvement in arbuscular mycorrhiza initiation. The New phytologist *189*, 701-709.
Hans Thordal-Christensen; Ziguo Zhang; Yangdou Wei, D.B.C. (1997). Subcellular localization of H2o2 in plants. H2O2 accumulation in papillae and hypersensitive response during barley-powdery mildew interaction. The Plant Journal *11*, 1187-1194.
Hao, Y., Hu, G., Breitel, D., Liu, M., Mila, I., Frasse, P., Fu, Y., Aharoni, A., Bouzayen, M., and Zouine, M. (2015). Auxin Response Factor SlARF2 Is an Essential Component of the Regulatory Mechanism Controlling Fruit Ripening in Tomato. PLoS genetics *11*, e1005649.
Haughn, G.W., and Somerville, C. (1986). Sulfonylurea-resistant mutants of *Arabidopsis thaliana*. Mol Gen Genet *204*, 430-434.
Hayashi, M., Toriyama, K., Kondo, M., and Nishimura, M. (1998). 2,4-dichlorophenoxybutyric acid-resistant mutants of Arabidopsis have defects in glyoxysomal fatty acid β-oxidation. The Plant cell *10*, 183-195.
Hess, R., Staubli, W., and Riess, W. (1965). Nature of the hepatomegalic effect produced by ethyl-chlorophenoxy-isobutyrate in the rat. Nature *208*, 856-858.

Hoepfner, D., van den Berg, M., Philippsen, P., Tabak, H.F., and Hettema, E.H. (2001). A role for Vps1p, actin, and the Myo2p motor in peroxisome abundance and inheritance in Saccharomyces cerevisiae. The Journal of cell biology *155*, 979-990.
Honkanen, S., and Dolan, L. (2016). Growth regulation in tip-growing cells that develop on the epidermis. Current Opinion in Plant Biology *34*, 77-83.
Hu, J., Aguirre, M., Peto, C., Alonso, J., Ecker, J., and Chory, J. (2002). A role for peroxisomes in photomorphogenesis and development of *Arabidopsis*. Science *297*, 405-409.
Hu, J., Baker, A., Bartel, B., Linka, N., Mullen, R.T., Reumann, S., and Zolman, B.K. (2012). Plant peroxisomes: biogenesis and function. Plant Cell *24*, 2279-2303.
Islinger, M., Abdolzade-Bavil, A., Liebler, S., Weber, G., and Volkl, A. (2012a). Assessing heterogeneity of peroxisomes: isolation of two subpopulations from rat liver. Methods in molecular biology *909*, 83-96.
Islinger, M., Grille, S., Fahimi, H.D., and Schrader, M. (2012b). The peroxisome: an update on mysteries. Histochemistry and cell biology *137*, 547-574.
Ito, H., and Gray, W.M. (2006). A gain-of-function mutation in the Arabidopsis pleiotropic drug resistance transporter PDR9 confers resistance to auxinic herbicides. Plant Physiol *142*, 63-74.
Ivanchenko, M.G., Zhu, J., Wang, B., Medvecka, E., Du, Y., Azzarello, E., Mancuso, S., Megraw, M., Filichkin, S., Dubrovsky, J.G., *et al.* (2015). The cyclophilin A DIAGEOTROPICA gene affects auxin transport in both root and shoot to control lateral root formation. Development *142*, 712-721.
Iyer-Pascuzzi, A.S., and Benfey, P.N. (2009). Transcriptional networks in root cell fate specification. Biochimica et biophysica acta *1789*, 315-325.
Janssen, B.J., Lund, L., and Sinha, N. (1998). Overexpression of a homeobox gene, LeT6, reveals indeterminate features in the tomato compound leaf. Plant physiology *117*, 771-786.
Jones, B., Frasse, P., Olmos, E., Zegzouti, H., Li, Z.G., Latche, A., Pech, J.C., and Bouzayen, M. (2002). Down-regulation of DR12, an auxin-response-factor homolog, in the tomato results in a pleiotropic phenotype including dark green and blotchy ripening fruit. The Plant journal : for cell and molecular biology *32*, 603-613.
Karnik, S.K., and Trelease, R.N. (2005). Arabidopsis Peroxin 16 coexists at steady state in peroxisomes and endoplasmic reticulum. Plant Physiol *138*, 1967-1981.
Karnik, S.K., and Trelease, R.N. (2007). Arabidopsis peroxin 16 trafficks through the ER and an intermediate compartment to pre-existing peroxisomes via overlapping molecular targeting signals. Journal of experimental botany *58*, 1677-1693.
Katano, M., Takahashi, K., Hirano, T., Kazama, Y., Abe, T., Tsukaya, H., and Ferjani, A. (2016). Suppressor Screen and Phenotype Analyses Revealed an Emerging Role of the Monofunctional Peroxisomal Enoyl-CoA Hydratase 2 in Compensated Cell Enlargement. Frontiers in Plant Science *7*, 132.
Kaur, N., and Hu, J. (2009). Dynamics of peroxisome abundance: a tale of division and proliferation. Current opinion in plant biology *12*, 781-788.
Keddie, J.S., Carroll, B.J., Thomas, C.M., Reyes, M.E., Klimyuk, V., Holtan, H., Gruissem, W., and Jones, J.D. (1998). Transposon tagging of the Defective embryo and meristems gene of tomato. The Plant cell *10*, 877-888.
Kepinski, S., and Leyser, O. (2005). The *Arabidopsis* F-box protein TIR1 is an auxin receptor. Nature *435*, 446-451.
Kim, D.Y., Bovet, L., Maeshima, M., Martinoia, E., and Lee, Y. (2007). The ABC transporter AtPDR8 is a cadmium extrusion pump conferring heavy metal resistance. Plant J *50*, 207-218.

Kim, P.K., Mullen, R.T., Schumann, U., and Lippincott-Schwartz, J. (2006). The origin and maintenance of mammalian peroxisomes involves a de novo PEX16-dependent pathway from the ER. The Journal of cell biology *173*, 521-532.
Koch, J., Pranjic, K., Huber, A., Ellinger, A., Hartig, A., Kragler, F., and Brocard, C. (2010). PEX11 family members are membrane elongation factors that coordinate peroxisome proliferation and maintenance. Journal of cell science *123*, 3389-3400.
Koh, S., Andre, A., Edwards, H., Ehrhardt, D., and Somerville, S. (2005). Arabidopsis thaliana subcellular responses to compatible Erysiphe cichoracearum infections. The Plant journal : for cell and molecular biology *44*, 516-529.
Korasick, D.A., Enders, T.A., and Strader, L.C. (2013). Auxin biosynthesis and storage forms. Journal of experimental botany *64*, 2541-2555.
Kreiser, M., Giblin, C., Murphy, R., Fiesel, P., Braun, L., Johnson, G., Wyse, D., and Cohen, J.D. (2016). Conversion of indole-3-butyric acid to indole-3-acetic acid in shoot tissue of hazelnut (*Corylus*) and elm (*Ulmus*). Journal of Plant Growth Regulation *35*, 710.
Landrum, M., Smertenko, A., Edwards, R., Hussey, P.J., and Steel, P.G. (2010). BODIPY probes to study peroxisome dynamics *in vivo*. The Plant journal : for cell and molecular biology *62*, 529-538.
Laskowski, M., and Ten Tusscher, K.H. (2017). Periodic Lateral Root Priming: What Makes It Tick? Plant Cell *29*, 432-444.
Last, R.L., and Fink, G.R. (1988). Tryptophan-requiring mutants of the plant *Arabidopsis thaliana*. Science *240*, 305-310.
Lata, C., Sahu, P.P., and Prasad, M. (2010). Comparative transcriptome analysis of differentially expressed genes in foxtail millet (Setaria italica L.) during dehydration stress. Biochemical and biophysical research communications *393*, 720-727.
LeClere, S., Tellez, R., Rampey, R.A., Matsuda, S.P.T., and Bartel, B. (2002). Characterization of a family of IAA-amino acid conjugate hydrolases from *Arabidopsis*. J Biol Chem *277*, 20446-20452.
Lee, J.R., Park, S.C., Kim, M.H., Jung, J.H., Shin, M.R., Lee, D.H., Cheon, M.G., Park, Y., Hahm, K.S., and Lee, S.Y. (2007). Antifungal activity of rice Pex5p, a receptor for peroxisomal matrix proteins. Biochemical and biophysical research communications *359*, 941-946.
Li, X., and Gould, S.J. (2002). PEX11 promotes peroxisome division independently of peroxisome metabolism. Journal of Cell Biology *156*, 643-651.
Li, X.R., Li, H.J., Yuan, L., Liu, M., Shi, D.Q., Liu, J., and Yang, W.C. (2014). Arabidopsis DAYU/ABERRANT PEROXISOME MORPHOLOGY9 is a key regulator of peroxisome biogenesis and plays critical roles during pollen maturation and germination in planta. The Plant cell *26*, 619-635.
Lin, Y., Cluette-Brown, J.E., and Goodman, H.M. (2004). The peroxisome deficient Arabidopsis mutant *sse1* exhibits impaired fatty acid synthesis. Plant Physiol *135*, 814-827.
Lin, Y., Sun, L., Nguyen, L.V., Rachubinski, R.A., and Goodman, H.M. (1999). The Pex16p homolog SSE1 and storage organelle formation in *Arabidopsis* seeds. Science *284*, 328-330.
Lingard, M.J., and Trelease, R.N. (2006). Five Arabidopsis peroxin 11 homologs individually promote peroxisome elongation, duplication or aggregation. Journal of cell science *119*, 1961-1972.
Lipka, V., Dittgen, J., Bednarek, P., Bhat, R., Wiermer, M., Stein, M., Landtag, J., Brandt, W., Rosahl, S., Scheel, D., *et al.* (2005). Pre- and postinvasion defenses both contribute to nonhost resistance in Arabidopsis. Science *310*, 1180-1183.

Liscum, E., and Reed, J.W. (2002). Genetics of Aux/IAA and ARF action in plant growth and development. Plant Mol Biol *49*, 387-400.
Lisenbee, C.S., Heinze, M., and Trelease, R.N. (2003). Peroxisomal ascorbate peroxidase resides within a subdomain of rough endoplasmic reticulum in wild-type Arabidopsis cells. Plant Physiol *132*, 870-882.
Liu, X., Barkawi, L., Gardner, G., and Cohen, J.D. (2012a). Transport of indole-3-butyric acid and indole-3-acetic acid in Arabidopsis hypocotyls using stable isotope labeling. Plant physiology *158*, 1988-2000.
Liu, X., Hegeman, A.D., Gardner, G., and Cohen, J.D. (2012b). Protocol: High-throughput and quantitative assays of auxin and auxin precursors from minute tissue samples. Plant Methods *8*, 31.
Lopez-Huertas, E., Charlton, W.L., Johnson, B., Graham, I.A., and Baker, A. (2000). Stress induces peroxisome biogenesis genes. EMBO J *19*, 6770-6777.
Lu, X., Dittgen, J., Piślewska-Bednarek, M., Molina, A., Schneider, B., Svatoš, A., Doubsky, J., Schneeberger, K., Weigel, D., Bednarek, P., *et al.* (2015). Mutant Allele-Specific Uncoupling of PENETRATION3 Functions Reveals Engagement of the ATP-Binding Cassette Transporter in Distinct Tryptophan Metabolic Pathways. Plant Physiology *168*, 814-827.
Ludwig-Müller, J. (2000). Indole-3-butyric acid in plant growth and development. Plant Growth Regul *32*, 219-230.
Ludwig-Müller, J. (2007). Indole-3-butyric acid synthesis in ecotypes and mutants of *Arabidopsis thaliana* under different growth conditions. Journal of Plant Physiology *164*, 47-59.
Ludwig-Müller, J. (2011). Auxin conjugates: their role for plant development and in the evolution of land plants. Journal of experimental botany *62*, 1757-1773.
Ludwig-Müller, J., Hilgenberg, W., and Epstein, E. (1995a). The *in vitro* biosynthesis of indole-3-butyric acid in maize. Phytochem *40*, 61-68.
Ludwig-Müller, J., Kaldorf, M., Sutter, E.G., and Epstein, E. (1997). Indole-3-butyric acid (IBA) is enhanced in young maize (*Zea mays* L.) roots colonized with the arbuscular mycorrhizal fungus *Glomus intraradices*. Plant Science *125*, 153-162.
Ludwig-Müller, J., Raisig, A., and Hilgenberg, W. (1995b). Uptake and transport of indole-3-butyric acid in *Arabidopsis thaliana*: Comparison with other natural and synthetic auxins. J Plant Physiol *147*, 351-354.
Ludwig-Müller, J., Sass, S., Sutter, E.G., Wodner, M., and Epstein, E. (1993). Indole-3-butyric acid in *Arabidopsis thaliana*. I. Identification and quantification. Plant Growth Regul *13*, 179-187.
Ludwig-Müller, J., Schubert, B., and Pieper, K. (1995c). Regulation of IBA synthetase from maize (*Zea mays* L.) by drought stress and ABA. J Exp Bot *46*, 423-432.
Lynch, J.P. (2011). Root phenes for enhanced soil exploration and phosphorus acquisition: tools for future crops. Plant physiology *156*, 1041-1049.
Mano, S., Nakamori, C., Kondo, M., Hayashi, M., and Nishimura, M. (2004). An *Arabidopsis* dynamin-related protein, DRP3A, controls both peroxisomal and mitochondrial division. Plant J *38*, 487-498.
Martínez-de la Cruz, E., García-Ramírez, E., Vázquez-Ramos, J.M., Reyes de la Cruz, H., and López-Bucio, J. (2015). Auxins differentially regulate root system architecture and cell cycle protein levels in maize seedlings. Journal of Plant Physiology *176*, 147-156.
Mashiguchi, K., Tanaka, K., Sakai, T., Sugawara, S., Kawaide, H., Natsume, M., Hanada, A., Yaeno, T., Shirasu, K., Yao, H., *et al.* (2011). The main auxin biosynthesis pathway in

Arabidopsis. Proceedings of the National Academy of Sciences of the United States of America *108*, 18512-18517.
Mathur, J., Mathur, N., and Hülskamp, M. (2002). Simultaneous visualization of peroxisomes and cytoskeletal elements reveals actin and not microtubule-based peroxisome motility in plants. Plant Physiol *128*, 1031-1045.
McDonnell, M.M., Burkhart, S.E., Stoddard, J.M., Wright, Z.J., Strader, L.C., and Bartel, B. (2016). The Early-Acting Peroxin PEX19 Is Redundantly Encoded, Farnesylated, and Essential for Viability in Arabidopsis thaliana. PloS one *11*, e0148335.
Michniewicz, M., Powers, S.K., and Strader, L.C. (2014). IBA transport by PDR proteins. In Plant ABC Transporters, M. Geisler, ed. (Switzerland: Springer International Publishing), pp. 313-331.
Mishra, N.S., Tuteja, R., and Tuteja, N. (2006). Signaling through MAP kinase networks in plants. Archives of Biochemistry and Biophysics *452*, 55-68.
Mitsuya, S., El-Shami, M., Sparkes, I.A., Charlton, W.L., Lousa Cde, M., Johnson, B., and Baker, A. (2010). Salt stress causes peroxisome proliferation, but inducing peroxisome proliferation does not improve NaCl tolerance in Arabidopsis thaliana. PloS one *5*, e9408.
Monroe-Augustus, M., Ramon, N.M., Ratzel, S.E., Lingard, M.J., Christensen, S.E., Murali, C., and Bartel, B. (2011). Matrix proteins are inefficiently imported into Arabidopsis peroxisomes lacking the receptor-docking peroxin PEX14. Plant molecular biology *77*, 1-15.
Monroe-Augustus, M., Zolman, B.K., and Bartel, B. (2003). IBR5, a dual-specificity phosphatase-like protein modulating auxin and abscisic acid responsiveness in Arabidopsis. The Plant cell *15*, 2979-2991.
Motley, A.M., and Hettema, E.H. (2007). Yeast peroxisomes multiply by growth and division. The Journal of cell biology *178*, 399-410.
Mounet, F., Moing, A., Kowalczyk, M., Rohrmann, J., Petit, J., Garcia, V., Maucourt, M., Yano, K., Deborde, C., Aoki, K., *et al.* (2012). Down-regulation of a single auxin efflux transport protein in tomato induces precocious fruit development. Journal of experimental botany *63*, 4901-4917.
Naz, A.A., Raman, S., Martinez, C.C., Sinha, N.R., Schmitz, G., and Theres, K. (2013). Trifoliate encodes an MYB transcription factor that modulates leaf and shoot architecture in tomato. Proceedings of the National Academy of Sciences of the United States of America *110*, 2401-2406.
Nelson, B.K., Cai, X., and Nebenführ, A. (2007). A multicolored set of in vivo organelle markers for co-localization studies in Arabidopsis and other plants. The Plant journal : for cell and molecular biology *51*, 1126-1136.
Nito, K., Kamigaki, A., Kondo, M., Hayashi, M., and Nishimura, M. (2007). Functional classification of Arabidopsis peroxisome biogenesis factors proposed from analyses of knockdown mutants. Plant & cell physiology *48*, 763-774.
Nordström, A.-C., Jacobs, F.A., and Eliasson, L. (1991). Effect of exogenous indole-3-acetic acid and indole-3-butyric acid on internal levels of the respective auxins and their conjugation with aspartic acid during adventitious root formation in pea cuttings. Plant Physiol *96*, 856-861.
Novák, O., Hényková, E., Sairanen, I., Kowalczyk, M., Pospíšil, T., and Ljung, K. (2012). Tissue-specific profiling of the *Arabidopsis thaliana* auxin metabolome. The Plant journal : for cell and molecular biology *72*, 523-536.
Oh, K., Ivanchenko, M.G., White, T.J., and Lomax, T.L. (2006). The diageotropica gene of tomato encodes a cyclophilin: a novel player in auxin signaling. Planta *224*, 133-144.

Orth, T., Reumann, S., Zhang, X., Fan, J., Wenzel, D., Quan, S., and Hu, J. (2007). The PEROXIN11 protein family controls peroxisome proliferation in Arabidopsis. The Plant cell.
Pan, J., Zhang, M., Kong, X., Xing, X., Liu, Y., Zhou, Y., Liu, Y., Sun, L., and Li, D. (2012). ZmMPK17, a novel maize group D MAP kinase gene, is involved in multiple stress responses. Planta *235*, 661-676.
Pan, X., Chen, J., and Yang, Z. (2015). Auxin regulation of cell polarity in plants. Current Opinion in Plant Biology *28*, 144-153.
Pastori, G.M., and Del Rio, L.A. (1997). Natural Senescence of Pea Leaves (An Activated Oxygen-Mediated Function for Peroxisomes). Plant physiology *113*, 411-418.
Peer, W.A., Cheng, Y., and Murphy, A.S. (2013). Evidence of oxidative attenuation of auxin signalling. Journal of Experimental Botany *64*, 2629-2639.
Peremyslov, V.V., Prokhnevsky, A.I., and Dolja, V.V. (2010). Class XI myosins are required for development, cell expansion, and F-Actin organization in Arabidopsis. The Plant cell *22*, 1883-1897.
Poupart, J., Rashotte, A.M., Muday, G.K., and Waddell, C.S. (2005). The *rib1* mutant of Arabidopsis has alterations in indole-3-butyric acid transport, hypocotyl elongation, and root architecture. Plant Physiol *139*, 1460-1471.
Poupart, J., and Waddell, C.S. (2000). The *rib1* mutant is resistant to indole-3-butyric acid, an endogenous auxin in Arabidopsis. Plant Physiol *124*, 1739-1751.
Preece, J.D. (2003). A century of progress with vegetative plant propogation. HortScience *38*, 1015-1025.
Prestele, J., Hierl, G., Scherling, C., Hetkamp, S., Schwechheimer, C., Isono, E., Weckwerth, W., Wanner, G., and Gietl, C. (2010). Different functions of the C3HC4 zinc RING finger peroxins PEX10, PEX2, and PEX12 in peroxisome formation and matrix protein import. Proceedings of the National Academy of Sciences of the United States of America *107*, 14915-14920.
Ramón, N.M., and Bartel, B. (2010). Interdependence of the peroxisome-targeting receptors in *Arabidopsis thaliana*: PEX7 facilitates PEX5 accumulation and import of PTS1 cargo into peroxisomes. Mol Biol Cell *21*, 1263-1271.
Rapp, S., Saffrich, R., Anton, M., Jäkle, U., Ansorge, W., Gorgas, K., and Just, W.W. (1996). Microtubule-based peroxisome movement. Journal of Cell Science *109*, 837-849.
Rashotte, A.M., Poupart, J., Waddell, C.S., and Muday, G.K. (2003). Transport of the two natural auxins, indole-3-butyric acid and indole-3-acetic acid, in Arabidopsis. Plant Physiol *133*, 761-772.
Rellán-Álvarez, R., Lobet, G., and Dinneny, J.R. (2016). Environmental Control of Root System Biology. Annu Rev Plant Biol.
Reyna, N.S., and Yang, Y. (2006). Molecular analysis of the rice MAP kinase gene family in relation to Magnaporthe grisea infection. Molecular plant-microbe interactions : MPMI *19*, 530-540.
Rodriguez-Serrano, M., Romero-Puertas, M.C., Sanz-Fernandez, M., Hu, J., and Sandalio, L.M. (2016). Peroxisomes Extend Peroxules in a Fast Response to Stress via a Reactive Oxygen Species-Mediated Induction of the Peroxin PEX11a. Plant physiology *171*, 1665-1674.
Rodríguez-Serrano, M., Romero-Puertas, M.C., Sanz-Fernández, M., Hu, J., and Sandalio, L.M. (2016). Peroxisomes Extend Peroxules in a Fast Response to Stress via a Reactive Oxygen Species-Mediated Induction of the Peroxin PEX11a. Plant Physiology *171*, 1665-1674.

Rodriguez-Serrano, M., Romero-Puertas, M.C., Sparkes, I., Hawes, C., del Rio, L.A., and Sandalio, L.M. (2009). Peroxisome dynamics in Arabidopsis plants under oxidative stress induced by cadmium. Free radical biology & medicine *47*, 1632-1639.
Růžička, K., Strader, L.C., Bailly, A., Yang, H., Blakeslee, J., Łangowski, Ł., Nejedlá, E., Fujita, H., Itoh, H., Syōno, K.*, et al.* (2010). Arabidopsis *PIS1* encodes the ABCG37 transporter of auxinic compounds including the auxin precursor indole-3-butyric acid. Proc Natl Acad Sci U S A *107*, 10749-10753.
Rylott, E.L., Rogers, C.A., Gilday, A.D., Edgell, T., Larson, T.R., and Graham, I.A. (2003). *Arabidopsis* mutants in short- and medium-chain acyl-CoA oxidase activities accumulate acyl-CoAs and reveal that fatty acid β-oxidation is essential for embryo development. J Biol Chem *278*, 21370-21377.
Sandalio, L.M., Dalurzo, H.C., Gomez, M., Romero-Puertas, M.C., and del Rio, L.A. (2001). Cadmium-induced changes in the growth and oxidative metabolism of pea plants. Journal of experimental botany *52*, 2115-2126.
Savić, B., Tomić, S., Magnus, V., Gruden, K., Barle, K., Grenković, R., Ludwig-Müller, J., and Salopek-Sondi, B. (2009). Auxin amidohydrolases from *Brassica rapa* cleave the alanine conjugate of indolepropionic acid as a preferable substrate: a biochemical and modeling approach. Plant & cell physiology *50*, 1587-1599.
Schafer, D.A., Jennings, P.B., and Cooper, J.A. (1998). Rapid and efficient purification of actin from nonmuscle sources. Cell motility and the cytoskeleton *39*, 166-171.
Schlicht, M., Ludwig-Müller, J., Burbach, C., Volkmann, D., and Baluska, F. (2013). Indole-3-butyric acid induces lateral root formation via peroxisome-derived indole-3-acetic acid and nitric oxide. The New phytologist *in press*.
Schmid, M., Davison, T.S., Henz, S.R., Pape, U.J., Demar, M., Vingron, M., Schölkopf, B., Weigel, D., and Lohmann, J.U. (2005). A gene expression map of *Arabidopsis thaliana* development. Nature Genetics *37*, 501-506.
Schrader, M. (2006). Shared components of mitochondrial and peroxisomal division. Biochimica et biophysica acta *1763*, 531-541.
Schrader, M., Burkhardt, J.K., Baumgart, E., Lüers, G., Spring, H., Völkl, A., and Fahimi, H.D. (1996). Interaction of microtubules with peroxisomes. Tubular and spherical peroxisomes in HepG2 cells and their alterations induced by microtubule-active drugs. European Journal of Cell Biology *69*, 24-35.
Shi, H., Ishitani, M., Kim, C., and Zhu, J.K. (2000). The Arabidopsis thaliana salt tolerance gene SOS1 encodes a putative Na+/H+ antiporter. Proceedings of the National Academy of Sciences of the United States of America *97*, 6896-6901.
Sparkes, I.A., Brandizzi, F., Slocombe, S.P., El-Shami, M., Hawes, C., and Baker, A. (2003). An Arabidopsis *pex10* null mutant is embryo lethal, implicating peroxisomes in an essential role during plant embryogenesis. Plant Physiol *133*, 1809-1819.
Stasinopoulos, T.C., and Hangarter, R.P. (1990). Preventing photochemistry in culture media by long-pass light filters alters growth of cultured tissues. Plant Physiol *93*, 1365-1369.
Staswick, P.E., Serban, B., Rowe, M., Tiryaki, I., Maldonado, M.T., Maldonado, M.C., and Suza, W. (2005). Characterization of an Arabidopsis enzyme family that conjugates amino acids to indole-3-acetic acid. The Plant cell *17*, 616-627.
Steinberg, S.J., Raymond, G.V., Braverman, N.E., and Moser, A.B. (1993). Peroxisome Biogenesis Disorders, Zellweger Syndrome Spectrum. In GeneReviews(R), R.A. Pagon, M.P.

Adam, H.H. Ardinger, S.E. Wallace, A. Amemiya, L.J.H. Bean, T.D. Bird, N. Ledbetter, H.C. Mefford, R.J.H. Smith, *et al.*, eds. (Seattle (WA)).
Stepanova, A.N., Robertson-Hoyt, J., Yun, J., Benavente, L.M., Xie, D.Y., Dolezal, K., Schlereth, A., Jurgens, G., and Alonso, J.M. (2008). TAA1-mediated auxin biosynthesis is essential for hormone crosstalk and plant development. Cell *133*, 177-191.
Strader, L.C., and Bartel, B. (2009). The Arabidopsis PLEIOTROPIC DRUG RESISTANCE8/ABCG36 ATP binding cassette transporter modulates sensitivity to the auxin precursor indole-3-butyric acid. The Plant cell *21*, 1992-2007.
Strader, L.C., and Bartel, B. (2011). Transport and metabolism of the endogenous auxin precursor indole-3-butyric acid. Molecular plant *4*, 477-486.
Strader, L.C., Hendrickson Culler, A., Cohen, J.D., and Bartel, B. (2010). Conversion of endogenous indole-3-butyric acid to indole-3-acetic acid drives cell expansion in Arabidopsis seedlings. Plant Physiol *153*, 1577-1586.
Strader, L.C., Monroe-Augustus, M., Rogers, K.C., Lin, G.L., and Bartel, B. (2008). Arabidopsis *iba response5* (*ibr5*) suppressors separate responses to various hormones. Genetics *180*, 2019-2031.
Strader, L.C., Wheeler, D.L., Christensen, S.E., Berens, J.C., Cohen, J.D., Rampey, R.A., and Bartel, B. (2011). Multiple facets of *Arabidopsis* seedling development require indole-3-butyric acid-derived auxin. The Plant cell *23*, 984-999.
Sutter, E.G., and Cohen, J.D. (1992). Measurement of indolebutyric acid in plant tissues by isotope dilution gas chromatography-mass spectrometry analysis. Plant Physiol *99*, 1719-1722.
Szemenyei, H., Hannon, M., and Long, J.A. (2008). TOPLESS mediates auxin-dependent transcriptional repression during Arabidopsis embryogenesis. Science *319*, 1384-1386.
Tao, Y., Ferrer, J.L., Ljung, K., Pojer, F., Hong, F., Long, J.A., Li, L., Moreno, J.E., Bowman, M.E., Ivans, L.J., *et al.* (2008). Rapid synthesis of auxin via a new tryptophan-dependent pathway is required for shade avoidance in plants. Cell *133*, 164-176.
Thole, J.M., and Strader, L.C. (2015). Next-generation sequencing as a tool to quickly identify causative EMS-generated mutations. Plant signaling & behavior *10*, e1000167.
Thomson, K.-S., Hertel, R., and Müller, S. (1973). 1-N-Naphthylphthalamic acid and 2,3,4-triiodobenzoic acid. Planta *109*, 337-352.
Tieman, D.M., Loucas, H.M., Kim, J.Y., Clark, D.G., and Klee, H.J. (2007). Tomato phenylacetaldehyde reductases catalyze the last step in the synthesis of the aroma volatile 2-phenylethanol. Phytochemistry *68*, 2660-2669.
Tiwari, S.B., Wang, X.-J., Hagen, G., and Guilfoyle, T.J. (2001). Aux/IAA proteins are active repressors, and their stability and activity are modulated by auxin. The Plant cell *13*, 2809-2822.
Tognetti, V.B., Bielach A, and Hrytan M. (2017). Redox regulation at the site of primary growth: auxin, cytokinin, and ROS crosstalk. Plant, Cell, & Environment *epub ahead of print*, September 11th, 2017, doi:10.1111/pce.13021.ch
Tognetti, V.B., Van Aken, O., Morreel, K., Vandenbroucke, K., van de Cotte, B., De Clercq, I., Chiwocha, S., Fenske, R., Prinsen, E., Boerjan, W., *et al.* (2010). Perturbation of indole-3-butyric acid homeostasis by the UDP-glucosyltransferase *UGT74E2* modulates Arabidopsis architecture and water stress tolerance. The Plant cell *22*, 2660-2679.
Tominaga, M., Kimura, A., Yokota, E., Haraguchi, T., Shimmen, T., Yamamoto, K., Nakano, A., and Ito, K. (2013). Cytoplasmic streaming velocity as a plant size determinant. Developmental cell *27*, 345-352.

Uzunova, V.V., Quareshy, M., Del Genio, C.I., and Napier, R.M. (2016). Tomographic docking suggests the mechanism of auxin receptor TIR1 selectivity. Open Biol *6*.
Veloccia, A., Fattorini, L., Della Rovere, F., Sofo, A., D'Angeli, S., Betti, C., Falasca, G., and Altamura, M.M. (2016). Ethylene and auxin interaction in the control of adventitious rooting in *Arabidopsis thaliana*. Journal of Experimental Botany *67*, 6445-6458.
Walls, C. (2017). Power of 10: Top 10 Produce Crops in the U.S. In AgAmerica (AgAmerica.com: AgAmerica Lending).
Wang, H., Jones, B., Li, Z., Frasse, P., Delalande, C., Regad, F., Chaabouni, S., Latche, A., Pech, J.C., and Bouzayen, M. (2005). The tomato Aux/IAA transcription factor IAA9 is involved in fruit development and leaf morphogenesis. The Plant cell *17*, 2676-2692.
Wiemer, E.A., Wenzel, T., Deerinck, T.J., Ellisman, M.H., and Subramani, S. (1997). Visualization of the peroxisomal compartment in living mammalian cells: dynamic behavior and association with microtubules. The Journal of cell biology *136*, 71-80.
Williams, C., Opalinski, L., Landgraf, C., Costello, J., Schrader, M., Krikken, A.M., Knoops, K., Kram, A.M., Volkmer, R., and van der Klei, I.J. (2015). The membrane remodeling protein Pex11p activates the GTPase Dnm1p during peroxisomal fission. Proceedings of the National Academy of Sciences of the United States of America *112*, 6377-6382.
Winter, D., Vinegar, B., Nahal, H., Ammar, R., Wilson, G.V., and Provart, N.J. (2007). An "Electronic Fluorescent Pictograph" browser for exploring and analyzing large-scale biological data sets. PloS one *2*, e718.
Woodward, A.W., and Bartel, B. (2005a). The *Arabidopsis* peroxisomal targeting signal type 2 receptor PEX7 is necessary for peroxisome function and dependent on PEX5. Mol Biol Cell *16*, 573-583.
Woodward, A.W., and Bartel, B. (2005b). Auxin: regulation, action, and interaction. Ann Bot *95*, 707-735.
Xiong, L., Lee, B., Ishitani, M., Lee, H., Zhang, C., and Zhu, J.K. (2001). FIERY1 encoding an inositol polyphosphate 1-phosphatase is a negative regulator of abscisic acid and stress signaling in Arabidopsis. Genes & development *15*, 1971-1984.
Xuan, W., Audenaert, D., Parizot, B., Möller, B.K., Njo, M.F., De Rybel, B., De Rop, G., Van Isterdael, G., Mahonen, A.P., Vanneste, S., *et al.* (2015). Root Cap-Derived Auxin Pre-patterns the Longitudinal Axis of the Arabidopsis Root. Current biology : CB *25*, 1381-1388.
Yamada, M., Greenham, K., Prigge, M.J., Jensen, P.J., and Estelle, M. (2009). The *TRANSPORT INHIBITOR RESPONSE2* gene is required for auxin synthesis and diverse aspects of plant development. Plant physiology *151*, 168-179.
Yoshida, Y., Niwa, H., Honsho, M., Itoyama, A., and Fujiki, Y. (2015). Pex11mediates peroxisomal proliferation by promoting deformation of the lipid membrane. Biology open *4*, 710-721.
Yu, X., and Cai, M. (2004). The yeast dynamin-related GTPase Vps1p functions in the organization of the actin cytoskeleton via interaction with Sla1p. Journal of cell science *117*, 3839-3853.
Zažímalová, E., Murphy, A.S., Yang, H., Hoyerová, K., and Hošek, P. (2010). Auxin transporters--why so many? Cold Spring Harbor Perspectives in Biology *2*, a001552.
Zhang, G.Z., Jin, S.H., Jiang, X.Y., Dong, R.R., Li, P., Li, Y.J., and Hou, B.K. (2016). Ectopic expression of UGT75D1, a glycosyltransferase preferring indole-3-butyric acid, modulates cotyledon development and stress tolerance in seed germination of *Arabidopsis thaliana*. Plant Molecular Biology *90*, 77-93.

Zhang, J., Chen, R., Xiao, J., Qian, C., Wang, T., Li, H., Ouyang, B., and Ye, Z. (2007). A single-base deletion mutation in SlIAA9 gene causes tomato (Solanum lycopersicum) entire mutant. Journal of plant research *120*, 671-678.
Zhang, J., Zou, D., Li, Y., Sun, X., Wang, N.N., Gong, S.Y., Zheng, Y., and Li, X.B. (2014). GhMPK17, a cotton mitogen-activated protein kinase, is involved in plant response to high salinity and osmotic stresses and ABA signaling. PloS one *9*, e95642.
Zhang, X.C., and Hu, J.P. (2008). FISSION1A and FISSION1B proteins mediate the fission of peroxisomes and mitochondria in Arabidopsis. Molecular plant *1*, 1036-1047.
Zhao, Y. (2010). Auxin biosynthesis and its role in plant development. Annu Rev Plant Biol *61*, 49-64.
Zhao, Y. (2012). Auxin biosynthesis: a simple two-step pathway converts tryptophan to indole-3-acetic acid in plants. Molecular plant *5*, 334-338.
Zimmerman, P.W., and Wilcoxon, F. (1935). Several chemical growth substances which cause initiation of roots and other responses in plants. Contrib Boyce Thompson Inst *7*, 209-229.
Zolman, B.K. (2002). Genetic analysis of indole-3-butyric acid response mutants in *Arabidopsis thaliana*. In Biochemistry and Cell Biology (Houston: Rice University), pp. 240.
Zolman, B.K., and Bartel, B. (2004). An *Arabidopsis* indole-3-butyric acid-response mutant defective in PEROXIN6, an apparent ATPase implicated in peroxisomal function. Proc Natl Acad Sci USA *101*, 1786-1791.
Zolman, B.K., Martinez, N., Millius, A., Adham, A.R., and Bartel, B. (2008). Identification and characterization of *Arabidopsis* indole-3-butyric acid response mutants defective in novel peroxisomal enzymes. Genetics *180*, 237-251.
Zolman, B.K., Monroe-Augustus, M., Silva, I.D., and Bartel, B. (2005). Identification and functional characterization of *Arabidopsis* PEROXIN4 and the interacting protein PEROXIN22. The Plant cell *17*, 3422-3435.
Zolman, B.K., Nyberg, M., and Bartel, B. (2007). IBR3, a novel peroxisomal acyl-CoA dehydrogenase-like protein required for indole-3-butyric acid response. Plant Mol Biol *64*, 59-72.
Zolman, B.K., Yoder, A., and Bartel, B. (2000). Genetic analysis of indole-3-butyric acid responses in *Arabidopsis thaliana* reveals four mutant classes. Genetics *156*, 1323-1337.
Zörb, C., Geilfus, C.M., Mühling, K.H., and Ludwig-Müller, J. (2013). The influence of salt stress on ABA and auxin concentrations in two maize cultivars differing in salt resistance. J Plant Physiol *170*, 220-224.